Quantum and Classical Methods to Improve the Efficiency of Infocom Systems

DsC Thesis

Sándor IMRE

Budapest University of Technology and Economics

Department of Telecommunications

To may father who taught me the way of thinking and to my mother who showed me how to endure to the end.

Sandor Imre

P.S. And of course to my children Sanyus, Marci, Orsi, Andris and their mother Adel.

Acknowledgments

The author gratefully acknowledges the comments, helpful advices and permanent encouragement of Prof. László Pap. Pressure and interest of colleagues and students of Mobile Communication and Computing Laboratory were very motivating.

Contents

List of Figures

Acronyms

BSi	Base Station in cell i
BER	Bit Error Ratio
BPSK	Binary Phase Shift Keying
CAC	Call Admission Control
CDMA	Code Division Multiple Access
DES	Data Encryption Standard
DCT	Discrete Cosine Transform
DFT	Discrete Fourier Transform
DS-CDMA	Direct Sequence-Code Division Multiple Access
FDMA	Frequency Division Multiple Access
FFT	Fast Fourier Transform
HLR	Home Location Register
GC	Guard Channel
GSM	Global System for Mobile communications
GUT	Great Unified Theory
IQFT	Inverse Quantum Fourier Transform
LMGF	Logarithmic Moment Generator Function
LSB	Least Significant Bit
MSB	Most Significant Bit

MAC	Medium Access Control
MAI	Multiple Access Interference
MAP	Maximum A Posteriori
ML	Maximum Likelihood
MLS	Maximum Likelihood Sequence
MUD	Multiuser Detection
NMR	Nuclear Magnetic Resonance
pdf	probability density function
PLMN	Public Land Mobile Networks
PG	Processing Gain
QC	Quantum Computation/Quantum Computing
QFT	Quantum Fourier Transform
QoS	Quality of Service
QMUD	Quantum based Multiuser Detection
r.v.	random variable
SDM	Space Division Multiplexing
SDMA	Space Division Multiple Access
SIM	Subscriber Identity Module
SIR	Signal to Interference Ratio
SNR	Signal to Noise Ratio
SIDR	Signal to Interference Density Ratio
SRM	Square-Root Measurement
SS	Spread Spectrum
TDM	Time Division Multiplexing
TDMA	Time Division Multiple Access
UMTS	Universal Mobile Telecommunication System
URL	Uniform Resource Locator
UTC	User Traffic Control
WCDMA	Wideband Code Division Multiple Access
WLAN	Wireless Local Area Network
WWW	World Wide Web

Notations

$\tilde{a}$	Measured/estimated value of variable a
$\breve{a}$	Technical constrain/demand for variable a, e.g. a must be less than $\breve{a}$
$\forall$	for all
j	$\sqrt{-1}$
$\|\cdot\rangle$	Vector representing a quantum state, its coordinates are probability amplitudes
$\mathbf{x}$	Traditional vector, e.g. $\mathbf{x} \in \{0,1\}^n$ refers to the vector representation of n-bit binary numbers
$\|\cdot\rangle_N$	State of an N-dimensional quantum register, i.e. the qregister contains $n = \mathrm{ld}(N)$ qubits
$\|\mathbf{0}\rangle$	Special notion for the more than one-qbit zero computational basis vector to distinguish it from the single qbit $\|0\rangle$
U	Operator
$U^{\otimes n}$	n-qbit (2^n-dimensional) operator
$\mathbf{U}$	Matrix of operator U
$P(\alpha)$	Phase gate with matrix $\begin{bmatrix} 1 & 0 \\ 1 & e^{j\alpha} \end{bmatrix}$
H	Hadamard gate with matrix $\frac{1}{\sqrt{2}} \begin{bmatrix} 1 & 1 \\ 1 & -1 \end{bmatrix}$
X	Pauli-X (bit-flip) gate with matrix $\begin{bmatrix} 0 & 1 \\ 1 & 0 \end{bmatrix}$
Y	Pauli-Y gate with matrix $\begin{bmatrix} 0 & -j \\ j & 0 \end{bmatrix}$

Z	Pauli-Z (phase-flip) gate with matrix $\begin{bmatrix} 1 & 0 \\ 0 & -1 \end{bmatrix}$
$\otimes$	Tensor product, this notation is often omitted, it is used only if the tensor product operation has to be emphasized
$\oplus$	Modulo 2 addition
$(\cdot)^*$	Complex conjugate
$\langle\cdot\|\cdot\rangle$	Inner product
$\|\cdot\rangle\langle\cdot\|$	Outer product
$\dagger$	Adjoint
$(\cdot)^T$	Transpose
$*$	Convolution
$\triangleq$	Definition
$\equiv$	Equivalence
$\wedge$	Logical AND operator
$\vee$	Logical OR operator
$\|$	Logical IF operator
$\mathbb{Z}$	Set of integer numbers
$\mathbb{Z}_2 \equiv \{0, 1\}$	Set of binary numbers
$(\mathbb{Z}_2)^n$	Set of n-bit binary numbers
$\mathbb{Z}_N$	Set of positive integer numbers between 0 and $(N-1)$, i.e. set belonging to the modulo N additive group
$\mathbb{Z}^+$	Set of natural numbers i.e. positive integer numbers
$\mathbb{Z}^-$	Set of negative integer numbers
$\mathbb{Z}_p^*$	Set of positive integers belonging to the modulo N multiplicative group
$\mathbb{C}$	Set of complex numbers
$\mathrm{ld}(\cdot)$	Logarithmus dualis, $\log_2(\cdot)$
$\lceil\cdot\rceil$	Smallest integer greater than or equal to a number
$\lfloor\cdot\rfloor$	Greatest integer less than or equal to a number
$\lfloor\cdot\rceil$	Rounds to the nearest integer
$\gcd(a, b)$	Greatest common divisor of a and b
$f_Q(q)$	Probability density function of r. v. Q
$f(x)$	Function continuous in x
$f[x]$	Function discrete in x

$\Re(x)$	Real part of complex number x
$\Im(x)$	Imaginary part of complex number x
$\#(\cdot)$	Number of, counts the occurrence of its argument
Thin line	Quantum channel
Thick line	Classical channel

Special indices applied in chapters devoted to WCDMA

Remark: Generally in case of any variable with indexes ij is written only with index j means that it represents one variable from class j and this variable is the same for all terminals in the given class.

$k^{\#} = 1...K$:sequence number of base stations (cells) in the interference region.

$k = 1..K_{k^{\#}}$:cell IDs of CAC region of base station $k^{\#}$.

$j = 1..J$: traffic classes.

h: auxiliary variable of j.

$i = 1..N_{jk^{\#}}$:refers to terminal i from class j located in cell and $k^{\#}$.

l: auxiliary variable of i.

$t = 1..\infty$: sequence number of actual call event (arrival or termination).

Motto

"It takes a thousand men to invent a telegraph, or a steam engine, or a phonograph, or a photograph, or a telephone, or any other Important thing – and the last man gets the credit and we forget the others. He added his little mite – that is all he did."

Mark Twain

1
Motivations

"Navigare necesse est!"[1]

Ancient Romans

If one compares wired and wireless/mobile communications several differences can be recognized in such fields as security, power consumption, medium access, channel behavior etc. However, the most differently handled resource is bandwidth. In case of wired networks link capacity can overcome almost any limitations by deploying optical fibres. In contrast wireless bandwidth is strongly restricted thanks to on one hand regulation and on the other hand to enormously large licence prices. Therefore, spectral efficiency is one of the most significant key parameters of every mobile system. Spectrally efficient wireless solutions are fairly complex, they consist of techniques applied in physical and data link layers. Call Admission Control (CAC) methods are very important since they ensure Quality of Service (QoS) while increasing spectral efficiency so they provide tradeoff between two competing aspects. Quantum computing and communications just appeared in infocom systems. They offer completely new principles and techniques which are not available in classical computing and communications. Therefore, it is worth attacking wide range of computationally complex problems of infocom systems from data base searching to useful signal detection in multiuser environment.

[1] *"Shipping is a must!"*

1.1 QUANTUM COMPUTERS AND COMPUTING

"Man is the best computer we can put aboard a spacecraft... and the only one that can be mass-produced with unskilled labor.

Wernher von Braun

In order to understand the importance of quantum computing and communications let us focus shortly on the history of computers, computing and communications. The most important steps towards an electronic computer were done during World War II when the large number of calculations in the Manhattan project required an elementary new equipment which is fast enough and adaptive (programmable). Many clever scientist were engaged with this problem. We mention here among them the polymath Neumann because he played important role in quantum mechanics as well but at this moment we say thank to him for the invention of the 'control by stored program' principle[2]. This principle combined with the vacuum tube hardware formed the basis of the first successful computers[3]. Unfortunately the tubes strongly limited the possibilities of miniaturization hence first computers filled up a whole room, which strongly restricted their wide applications. Therefore scientists paid distinguished attention to the small-scale behavior of matter. Fortunately the invention of semiconductors and the appearance of the transistor in 1948 by Bardeen, Brattain and Schockley open the way to personal computers and other handhold equipment.

One day in 1965 when Gordon Moore from Intel was preparing his talk and started to draw a plot about the performance of memory chips suddenly he observed an interesting rule called Moore's Law. As it is depicted in Fig. 1.1 he concluded that since the invention of the transistor the number of transistors per chip roughly doubled every 18-24 months, which means an exponential increase in the computing power of computers. Although it was an empirical observation without theoretical proof the Law seems to be still valid nowadays. However, similarly to the case of steam engine farseeing experts tried to determine the future of this technology. They estimate serious problems around 2015. What reasons may stand behind this prophecy?

No matter how surprisingly it sounds this trend can be traced back simply to drawing lines. The growth in processors' performance is due to the fact that we put more and more transistors on the same size chip. This requires smaller and smaller transistors, which can be achieved if we are able to draw thinner and thinner – even much thinner than a hair – lines onto the surface of a semiconductor disc. Next the current technology enables to remove

[2]The third area where he is counted among the founding father is called game theory.
[3]As an interesting story we mention here that Neumann was talented in mental arithmetic, too. The correct operation of the computer under construction was tested by multiplying two 8-digit numbers. Typically Neumann was the faster...

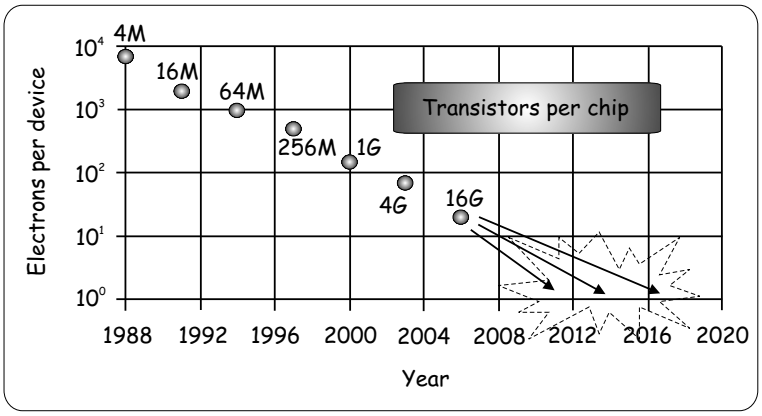

Fig. 1.1 Moore's Law

or retain parts of the disk according to the line structure evolving to transistors, diodes, contacts, etc. Apart from the technical problem of drawing such thin lines one day our lines will leave our well-known natural environment with well-known rules revealed step by step during the evolution of human race and enter into a new world where the traveller must obey new and strange rules if he/she would like to pass this land. The new world is called nano-world, the new rules are explained by quantum mechanics and the border between the worlds lies around nanometer (10^{-9}m) thickness. Fortunately scientists have already performed many reconnaissance missions in the nano-scale region thus we have not only theoretical but technology-related knowledge in our hands called nanotechnology.

From a computer scientist point of view who has algorithms and programs in his/her mind the growth in the capabilities of the underlying hardware is vital. If we have an algorithm which is not efficient enough often Time alone solves the problem due to the faster new hardware. We can say that we got used to Moore's Law during the last decades and forgot to follow what is happening and what will happen with the hardware. For decades, this attitude was irrelevant but the deadline to change it is near to its expiration. Fortunately experts called our attention to the fact that we will have to face serious problems if this trend can not be maintained. One thing is sure, however, the closer we are to the one-electron transistor (see Fig. 1.1) disturbing quantum effects will appear more often and stronger. Hence either we manage to find a new way of miniaturization or we have to learn how to exploit the difficulties and strangeness of quantum mechanics. Independently from the chosen way we must do something because *Computing is a must* or as ancient Romans said *"Navigare necesse est!"*

In compliance with the latter concept Feynman suggested a new straightforward approach. Instead of regarding computers as devices working under the laws of classical Physics – which is common sense – let us consider their operation as a special case of a more general theory governed by quantum mechanics. Thus the way becomes open from

hardware point of view. On the other hand hardware and software always influence each other. Since new hardware concepts require and enables new software concepts we have to study quantum mechanics from computer science point of view. Moreover it is worth seeking for algorithms which are more efficient than their best classical counterparts thanks to the exploited possibilities available only in the quantum world. These software related efforts are comprehended by *quantum computing*. Once we familiarized ourselves with quantum-faced computing why keep away communications from the new chances. Maybe the capacity of a quantum channel could exceed that of a nowadays used classical cable or we can design more secure protocols than currently applied ones. *Quantum communications* or *Quantum information theory* tries to answer these questions.

Concerning the subject of this Thesis – which is the application of quantum computing in solving classical infocom problems – quantum computing and communications have passed several important milestones. Top experts have experimentally validated algorithms which overcome the classical competitors. For instance we are able to find an item in an unsorted database or factorize large numbers very quickly. Quantum principles allow solving easily a long discussed problem, namely random number generators e.g. [8]. Furthermore as we mentioned before implementation of certain algorithms reached such a stage that one can buy a corresponding equipment in the appropriate shop. Fortunately many questions are waiting to be answered thus the reader will find not only solutions but open questions in this book. Nothing shores up more convincing the spreading of the new paradigm than the fact that more and more publications appear in popular-science magazines and journals [15, 9, 67, 69].

1.2 CALL ADMISSION CONTROL IN WCDMA ENVIRONMENT

Wireless communication systems and networks are spreading all over the World as last mile/feet access solutions to global infocom networks. Mobile terminals allow resilience connectivity for users while providing near wired-magnitude transmission rates. However, merging wired and wireless networks require subtle interconnection because different QoS provisioning capabilities may cause serious problems at the interfaces. In order to avoid dramatic packet loss at the bottlenecks QoS parameter (e.g. packet loss probability, average packet delay, packet delay variation) matching has to be performed. Fortunately several network management control mechanisms have already been introduced in wired networks to guarantee QoS contracts, e.g.: Call Admission Control (CAC) decides whether a new incoming call (service) request can be accepted without violating QoS contracts with already active subscribers? User Traffic Control (UTC) supervises whether a given user keeps the QoS contract with the network or not (e.g. his/her peak or mean transmission rate remains

under the agreed limits)? Congestion Control acts when packet collision occurs somewhere in the network. It decides which packet should be dropped and which ones should be kept because of their high priority? When combining wired networks with wireless access points (so called base stations) mobile equivalents of the above listed functions must be involved under Radio Resource Management [70].

Spread spectrum systems conquered the wireless/mobile world recently and there is no doubt they will dominate during the next decades. They offer better spectral efficiency, they tolerate wide range of demands claimed by multimedia applications and they are able to adapt to time-varying resource requirements of customers. The price we pay for that resilience is increased computational complexity. This is the situation in case of CAC as well. The optimal solution exists only theoretically thanks to its complexity, hence efficient suboptimal solutions are requested.

1.3 STRUCTURE OF THIS THESIS

This Thesis is organized as follows:

Part I is devoted to quantum assisted solutions of problems arising in infocom systems. It has the following structure: Chapter 2 contains the state of the art literature survey for Chapter 3, 4 and 5. Chapter 3 introduces the generalization problem of the Grover algorithm and proposes a general solution. Quantum existence testing and its application for finding extreme values of a function/data base are discussed in Chapter 4. Finally Chapter 5 demonstrates how to apply quantum computing to solve a computationally complex telecom problem.

Part II is related to Call Admission Control in WCDMA environment. WCDMA-CAC related literature is summarized in Chapter 6. The uplink CAC problem is formulated in Chapter 7. Chapter 8 provides abstract formulation of CAC problem and effective bandwidth based CAC is explained with its shortcomings. The new dynamic CAC method is introduced in Chapter 9. In Chapter 10 we show how to apply dynamic CAC in spread spectrum WCDMA environment assuming general multiplicative fading and traffic conditions. Furthermore as practical results lognormal and Rayleigh fading and ON/OFF sources are considered. Important extensions in terms of downlink and soft handover are discussed in Chapter 11. Chapter 12 contains simulation results which shore up the efficiency of the proposed solution.

Chapter 13 concludes the Thesis and summarizes open problems for future research.

Appendices contain summary of theses, definitions, detailed derivations and proofs of theorems.

Part I

Quantum Assisted Solutions of Infocom Problems

2

Introduction to Quantum Based Searching and its Applications

L. K. Grover published his fast database searching algorithm first in [45] and [43] using the diffusion matrix approach to illustrate the effect of the Grover operator, that took $\mathcal{O}(\sqrt{N})$ iterations to carry out the search, which is the optimal solution, as it was proved in [103]. Boyer, Brassard, Hoyer and Tapp [63] enhanced the original algorithm for more than one marked entry in the database and introduced upper bounds for the required number of evaluations.

After a short debate Bennett, Bernstein, Brassard and Vazirani gave the first poof of the optimality of Grover's algorithm in [14]. The proof was refined by Zalka in [103] and [102].

Later the rotation in a 2-dimensional state space (with the bases of separately superpositioned marked and unmarked states) SU(2) approach were introduced by Boyer et al in [63]. Within this book we followed this representation form according to its popularity in the literature.

During the above mentioned evolution of the Grover algorithm a new quest started to formulate the building blocks of the algorithm as generally as possible. The motivations for putting so much effort into this direction were on one hand to get a much deeper insight into the heart of the algorithm and on the other hand to overcome the main shortcoming of the algorithm, namely the sure success of finding a marked state can not be guaranteed. In [44] the authors replaced the Hadamard transformation with an arbitrary unitary one. The next step was the introduction of arbitrary phase rotations in the Oracle and in the phase shifter instead of π in [40]. To provide sure success at the final measurement Brassard et all [36] run the original Grover algorithm, but for the final turn a special Grover operator with smaller step was applied. Hoyer et al. [49] gave another ingenious solution of the problem. They modified the original Grover algorithm and the initial distribution.

To give another viewpoint Long et al. introduced the 3-dimensional SO(3) picture in the description of Grover operator in [38]. The achievements were summarized and extended by Long [61] and an exact matching condition was derived for multiple marked states in [39]. Unfortunately the SO(3) picture is less picturesque and it misses the global phase factor before the measurement. In normal cases it does not cause any difficulty because measurement results are immune of it. However, if it is planed (we plan) to reuse the final state of the index register without measurement as the input of a further algorithm (operator), it is crucial to deal with the global phase. Therefore, Hsieh and Li [56] returned to the traditional 2-dimensional SU(2) formulation and derived the same matching condition for one marked element as Long achieved but they saved the final global phase factor. One important part of these solutions, however, was missing. Namely, they required that the initial sate should fit into the 2-dimensional state space defined by the marked and unmarked states with uniform probability amplitudes. This gives large freedom for designers but encumber the application of the generalized Grover algorithm as a building block of a larger quantum system.

Therefore another very important question within this topic proved to be the analysis of the evolution of the basic Grover algorithm when it is started from an arbitrary initial state, i.e. the amplitudes are either real or complex and follow any arbitrary distribution. In this case sure success can not be guaranteed, but the probability of success can be maximized. Biham and his team first gave the analysis of the original Grover algorithm in [21] and [27]. In [28] the analysis was extended to the generalized Grover algorithm with arbitrary unitary transformation and phase rotations.

I have combined and enhanced the results for generalized Grover searching algorithm in terms of arbitrary initial distribution, arbitrary unitary transformation, arbitrary phase rotations and arbitrary number of marked items to construct an unsorted database search algorithm which can be included inside a quantum computing system in [82, 81]. Because its constructive nature this algorithm is capable to get any amplitude distribution at its input, provides sure success in case of measurement and allows connecting its output to another algorithm if no measurement is performed. Of course, this approach assumes that the initial distribution is given and it determines all the other parameters according to the construction rules. However, readers who are interested in applying a predefined unitary transformation as the fixed parameter should settle for a restricted set of initial states and suggested to take a look at [56].

Grover´s database search algorithm assumes the knowledge of the number of marked states, but it is typical that we do not have this information in advance. Brassard et al. [35] gave the first valuable idea how to estimate the missing number of marked states, which was enhanced in [36] and traced back to a phase estimation of the Grover operator.

A rather useful extension of the Grover algorithm when we decided to find minimum/maximum point of a cost function. Dürr and Hoyer suggested the first statistical method and bound to solve the problem in [13]. Later based on this result Ahuya and Kapoor improved the bounds in [2]. Both paper exploits the estimation of the expected number of iterations introduced in [63]. Unfortunately all these algorithms provide the extreme value efficiently in terms of expected value thus no reasonable upper bound for the number of required elementary steps can be given. This fact strongly restricts the usage of such solutions in real applications. Therefore I introduced another approach based on quantum existence testing [82, 53].

Recently Grover emphasized in [46] that the number of elementary unitary operations can be reduced which lunched a new quest for the most effective Grover structure in terms of number of basic operations.

The Grover algorithm has been verified first experimentally in a liquid-state NMR system [52] and [57] with a few qbits. Bhattacharya and his colleagues reported the implementation of the quantum search algorithm using classical Fourier optics in [68].

Subscribers of the next generation wireless systems will communicate simultaneously, sharing the same frequency band. All around the world 3G mobile systems apply DS-CDMA because of its high capacity and inherent resistance to interference, hence it comes into the limelight in many communication systems. Nevertheless due to the hostile property of the channel, in case of CDMA communication the orthogonality between user codes at the receiver is lost, which leads to performance degradation in multi-user environment. A good overview of wireless channel models can be found in [71, 20] while state of the art mobile systems such as GSM, IS-95, cdma2000, UMTS, W-CDMA, etc. are surveyed in [48, 62, 89].

Single-user detectors were overtaxed and showed rather poor performance even in multi-path environment [91]. To overcome this problem, in recent years multi-user detection has received considerable attention and become one of the most important signal processing task in wireless communication.

Verdu [91] has proved that the optimal solution is an *NP*-hard problem as the number of users grows, which causes significant limitation in practical applications. Many authors proposed suboptimal linear and nonlinear solutions such as Decorrelating Detector, MMSE (Minimum Mean Square Error) detector, Recurrent and Hoppfield Neural Network based detectors, Multi-stage detector [10, 65, 91, 4], and the references therein. One can find a comparison of the performance of the above mentioned algorithms in [37].

The unwanted effects of the radio channel can be compensated by means of channel equalization [3, 75, 5]. The most conventional method for channel equalization employs training sequences of known data. However, such a scheme requires more bandwidth to

transmit the some amount of payload. Furthermore, in multi-user CDMA systems the co-ordination of users is practically hard task. Consequently, there is a tremendous interest in blind detection schemes for multi-user systems, where no training sequences are needed. Our quantum based MUD proposal belongs to this latter group because it does not requires any information about the channel. The basic idea which traces back MUD to set separation was published in [77, 78] and analyzed [80, 79]. This chapter introduces a refined version which extends (deterministic) set separation to (probabilistic) hypothesis testing published first in [82, 32].

3

Searching in an Unsorted Database

"Man - a being in search of meaning."

Plato

Searching was born together with the human race. In order to survive from day to day in a very hostile and dangerous environment prehistoric men spent most of their time on seeking for such resources as food, fresh water, suitable stone for tools, etc. The world around us was nothing else than a large *unsorted database*. Efficiency of the originally applied two basic methods, namely random and exhaustive search proved to be rather poor. The only way to achieve some improvement was the involvement of more people (*parallel processing*). The first breakthrough in this field can be connected to the first settlements and the appearance of agriculture which brought along the intention to make and keep order in the world[1]. A field of wheat or a vegetable-garden compared to a meadow embodied the order which increased the probability of successful searching almost up to 1. Therefore our ancestors were balancing during the last 10 thousand years between the resource requirement of making order and seeking for a requested thing. However, at the dawn of third millennium our dreams seem to become true due to quantum computing. Grover's database search algorithm enables dramatic reduction in computational complexity of seeking in an unsorted database. The change is tremendous, the classically required $O(N)$ database queries in case we have N different entries has been replaced by $O(\sqrt{N})$ steps using quantum computers.

[1] Ancient Greeks referred this change as the born of cosmos ($\kappa o \sigma \mu o \sigma$=order) from chaos ($\chi \alpha o \sigma$=disorder). So to use cosmos as a synonym of universe is not unintentional.

This chapter is organized as follows: Section 3.1 provides a short introduction to the original Grover algorithm explaining the related architecture. Finally Section 3.2 focuses on the generalization of the basic algorithm providing sure success measurements and enabling arbitrary initial state of the algorithm which can be quite useful when deploying the searching circuit within a larger quantum network. First Subsection 3.2.1 explains the new parameters enabling the generalization. Next the number of iterations is derived in Subsection 3.2.2. Finally design considerations and various scenarios are discussed in Subsection 3.2.3.

3.1 SUMMARY OF BASIC GROVER ALGORITHM

In order to give a solid reference for the generalized searching algorithm, first the original Grover algorithm is introduced and evaluated. The object of the Grover algorithm is to find the index of a requested item in an unsorted database of size N. The multiple occurrence M of the searched entry is allowed. Classically one needs N database queries to find one of the marked states[2] with certainty. However, with the Grover algorithm, this task can be carried out in $O(\sqrt{N/M})$ steps.

The algorithm has to be launched from the state

$$|\gamma\rangle|q\rangle = \frac{1}{\sqrt{N}} \sum_{x=0}^{N-1} |x\rangle|q\rangle, \tag{3.1}$$

where $|\gamma\rangle$ refers to the fact that we prepare a quantum register containing all the possible indices, and $|q\rangle = \frac{|0\rangle - |1\rangle}{\sqrt{2}}$ stands for the auxiliary qbit required for the proper operation of the algorithm. During the search the algorithm repeats the so-called Grover operator G depicted in Fig. 3.1 and defined as

$$G \triangleq HPHO, \tag{3.2}$$

where

$$O = I - 2 \sum_{x \in S} |x\rangle\langle x| \tag{3.3}$$

represents the so-called Oracle which inverts (multiplies with -1) the probability amplitudes of the marked states, where the set S stands for the set of the marked entries. H denotes the n-qbit Hadamard gate defined as

$$H|x\rangle = \frac{1}{\sqrt{2^n}} \sum_{z \in \{0,1\}^n} (-1)^{xz} |z\rangle,$$

[2]Entries, which are solutions of the search problem are called *marked* states according to the literature and the ones which do not lead to a solution are referred to as *unmarked* ones.

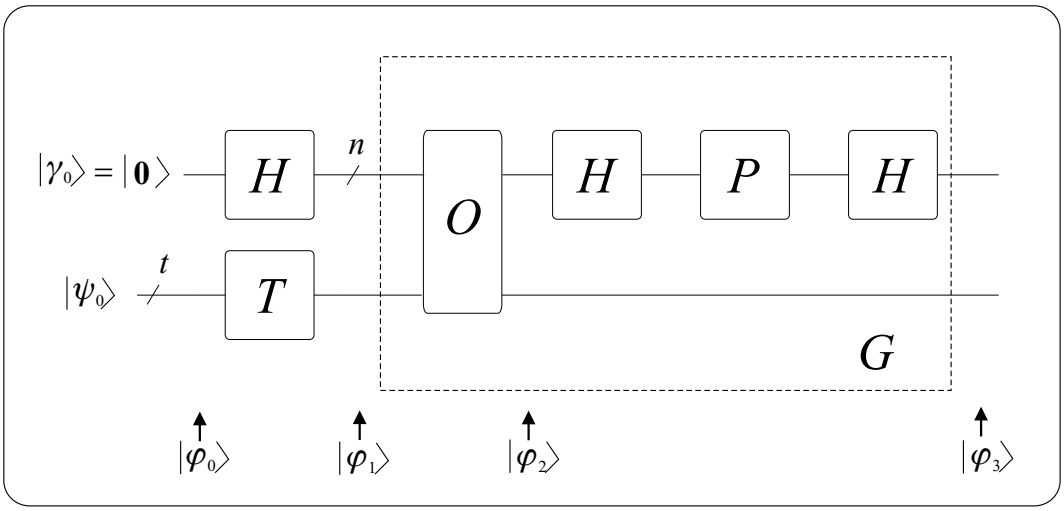

Fig. 3.1 Circuit implementing the Grover operator

where xz refers to the binary scalar product of the two n-bit integer numbers considering them as binary vectors (sum of bitwise products modulo 2). The phase shifter gate P performs a similar operation to O in (3.3) but it flips only the probability amplitude belonging to $|\mathbf{0}\rangle$

$$P \triangleq (2|\mathbf{0}\rangle\langle\mathbf{0}| - I)\,. \tag{3.4}$$

In order to determine the optimal number of Grover gates, i.e. the least number which minimizes the probability of failed search P_ε, we introduce a two-dimensional geometrical representation of the search. First we divide the indices into two sets, one (S) for the marked and another ($\overline{S}$) for the unmarked ones i.e. we build two superpositions comprising uniformly distributed computational basis states

$$|\alpha\rangle \triangleq \frac{1}{\sqrt{N-M}} \sum_{x\in\overline{S}} |x\rangle, \tag{3.5}$$

$$|\beta\rangle \triangleq \frac{1}{\sqrt{M}} \sum_{x\in S} |x\rangle, \tag{3.6}$$

where $|\alpha\rangle$ and $|\beta\rangle$ form an orthonormal basis of a two-dimensional Hilbert space as depicted in Fig. 3.2.

Now let us follow the effect of G on $|\gamma\rangle$ in Fig. 3.2. Since the Oracle flips the probability amplitudes of all the marked indices forming $|\beta\rangle$, thus because of the Oracle $|\gamma\rangle$ will be reflected at an axis $|\alpha\rangle$. The two Hadamard gates H together with P in the middle perform the so-called *inversion about the average* transformation which is nothing else than a reflection onto $|\gamma\rangle$. Therefore provided $|\gamma\rangle$ is angular to $|\alpha\rangle$ with an angle of $\frac{\Omega_\gamma}{2}$ then the two reflections together produce a single rotation towards $|\beta\rangle$ by an angle of Ω_γ.

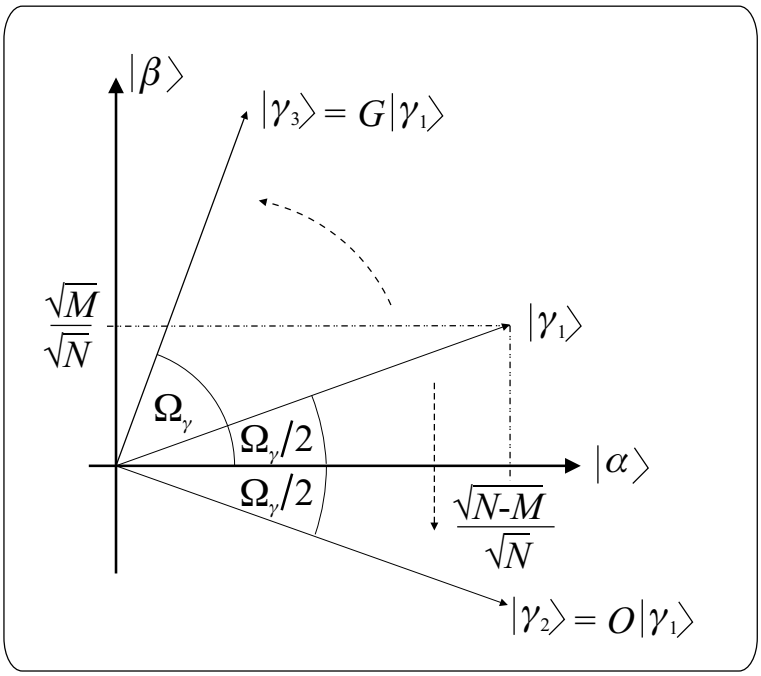

Fig. 3.2 Geometrical interpretation of the Grover operator

Sure success search requires in this approach an index register rotated from $|\gamma\rangle$ to $|\beta\rangle$ since a measurement on $|\beta\rangle$ always provides one of its basis vectors (indices). Thus the number of rotations ensuring absolute success can be easily calculated in the following way

$$\hat{l}_j = \frac{\frac{\pi}{2} + j\pi - \frac{\Omega_\gamma}{2}}{\Omega_\gamma}, \tag{3.7}$$

which is minimal if $j = 0$. Typically $l_{opt} = \hat{l}_0$ must be an integer thus

$$L_{opt} = \lfloor \hat{l}_0 \rceil = \left\lfloor \frac{\frac{\pi}{2} - \frac{\Omega_\gamma}{2}}{\Omega_\gamma} \right\rceil, \tag{3.8}$$

where $\lfloor \cdot \rceil$ denotes the rounding function to the nearest integer.

Because of this correction $G^{L_{opt}}|\gamma\rangle$ will be angular to $|\beta\rangle$, hence the measurement may answer with a wrong (unmarked) index. The probability of error can be computed as the squared absolute value of the projection of $G^{L_{opt}}|\gamma\rangle$ onto axis $|\alpha\rangle$

$$P_\varepsilon = \langle\alpha|G^{L_{opt}}|\gamma\rangle = \cos^2\left((2L_{opt}+1)\frac{\Omega_\gamma}{2}\right), \tag{3.9}$$

where the only missing parameter Ω_γ can be obtained as

$$\Omega_\gamma = 2\arcsin\left(\sqrt{\frac{M}{N}}\right). \tag{3.10}$$

Combining these results a quite surprising fact can be reached, namely $L_{opt} = O\left(\sqrt{\frac{N}{M}}\right)$ compared to the classical case $O\left(\frac{N}{M}\right)$.

If M is not given as an input parameter then phase estimation based *quantum counting* can be applied with the help of which M can be found in a computationally efficient way.

In possession of all the required results regarding the basic Grover algorithm. We can now focus our attention on its generalization.

3.2 THE GENERALIZED GROVER ALGORITHM

During the previous analysis of the basic Grover algorithm we aspired to find a suitable trade off between computational complexity (number of rotations or more precisely number of database queries l) and uncertainty (probability of error P_ε). We tried to use as few iterations as possible meanwhile ensuring as high probability of success as achievable. Moreover we have some limitations that may prevent the application of our clever quantum searching algorithm in many practical cases.

- Unfortunately sure success can not be guaranteed merely in exchange of increased number of rotations in the basic Grover algorithm. We have proposed some techniques (e.g. extended database with 'dummy' entries) a in [82] which provides sure success asymptotically but they require $O(N)$ rotations to achieve this. However, there are technical problems where we are not permitted to exceed a given $\breve{P}_\varepsilon$ while the number of Grover operators has also to be upperbounded.
- According to the potential applications of Grover's database search algorithm in practice, larger quantum systems should be taken into account where the input index register of the algorithm is given as an arbitrary output state of a former circuit and the output of the algorithm can feed another circuit without any measurement. Therefore we need a modified Grover algorithm which allows arbitrary initial state instead of the original $H|\mathbf{0}\rangle$.

In order to tame the above listed problems the original Grover algorithm will be generalized and discussed in the next subsections.

3.2.1 Generalization of the basic Grover database search algorithm

Before investigating the possibilities how to introduce some freedom into the Grover algorithm enabling its generalization let us summarize our knowledge about the Grover operator

$$G \triangleq HPHO,$$

where

$$P \triangleq 2|\mathbf{0}\rangle\langle\mathbf{0}| - I,$$

$$O \triangleq I - 2\sum_{x\in S} |x\rangle\langle x|.$$

These definitions were motivated by considerations emerging during the design of the searching algorithm. Furthermore it is known that the Hadamard transform is nothing else than a special QFT. Therefore it seems to be reasonable to replace the original operators with more general ones. New parameters can be involved in this way which could be the base of a more efficient solution.

1. We allow an arbitrary unitary gate U instead of the Hadamard gate H.

2. We let the Oracle to rotate the probability amplitudes of the marked items in the index register with angle ϕ in lieu of π (the original setup), where $\phi \in [-\pi, \pi]$. Thus (3.3) is altered to
$$O \rightarrow I_\beta \triangleq I + \left(e^{j\phi} - 1\right)\sum_{x\in S} |x\rangle\langle x|, \tag{3.11}$$
where subscript β refers to the fact that the Oracle modifies the probability amplitudes of the computational basis states forming $|\beta\rangle$. The matrix of I_β is a modified identity matrix with diagonal elements $I_{\beta_{xx}} = e^{j\phi}$ if $x \in S$.

3. Analogously to the Oracle above, the controlled phase gate P which was working originally on state $|\mathbf{0}\rangle$ should be based on an arbitrary basis state $|\eta\rangle$ resulting in a multiplication by $e^{j\theta}$ instead of -1, where $\theta \in [-\pi, \pi]$. In more exact mathematical formalism
$$P \rightarrow I_\eta \triangleq I + \left(e^{j\theta} - 1\right)|\eta\rangle\langle\eta|. \tag{3.12}$$
The matrix of I_η is a modified identity matrix with diagonal element $I_{\beta_{xx}} = e^{j\theta}$ if $x = \eta$.

4. Finally the initial state of the index register at the input of the first Grover gate is considered as
$$|\gamma_1\rangle \triangleq \sum_{x=0}^{N-1} \gamma_{1x}|x\rangle, \tag{3.13}$$
where $\sum_{x=0}^{(N-1)} |\gamma_{1x}|^2 = 1$ as appropriate.

Next the two basis vectors $|\alpha\rangle$ and $|\beta\rangle$ comprising the indexes leading to unmarked items (set $\overline{S}$) and that of ending in a marked entry (set S) should be redefined, which were originally set in (3.5) and (3.6), respectively

$$|\alpha\rangle = \frac{1}{\sqrt{\sum_{x\in\overline{S}} |\gamma_{1x}|^2}} \sum_{x\in\overline{S}} \gamma_{1x}|x\rangle, \tag{3.14}$$

$$|\beta\rangle = \frac{1}{\sqrt{\sum_{x\in S} |\gamma_{1x}|^2}} \sum_{x\in S} \gamma_{1x}|x\rangle. \tag{3.15}$$

Observing the new basis vectors $|\alpha\rangle$ and $|\beta\rangle$ orthogonality is still given between them, $\langle\alpha|\beta\rangle = 0$, since during the pairwise multiplication within the inner product one of the probability aplitudes is always zero.

Remark: In order to avoid the division by zero in (3.14) and (3.15) we require that at least one non-zero probability amplitude exists for the marked and unmarked indices. If all the entries are marked then we have only vector $|\beta\rangle$ and a measurement before the search will result in a marked state with certainty. Contrary if the database does not contain the requested item at all then only vector $|\alpha\rangle$ exists. As we will discuss later at the end of Section 3.2.3 both scenarios can be recognized by means of a phase estimation. Therefore in the forthcoming analysis we assume that both vectors exist that is neither of the two sets are empty.

Now it is time to construct the generalized Grover operator Q from previously defined gates $(G \rightarrow Q)$

$$\begin{aligned} Q &\triangleq -UI_\eta U^\dagger I_\beta = -U\left(I + \left(e^{j\theta} - 1\right)|\eta\rangle\langle\eta|\right)U^\dagger I_\beta \\ &= -\left(UIU^{-1} + \left(e^{j\theta} - 1\right)U|\eta\rangle\langle\eta|U^\dagger\right)I_\beta \\ &= -\left(I + \left(e^{j\theta} - 1\right)|\mu\rangle\langle\mu|\right)I_\beta, \end{aligned} \tag{3.16}$$

where

$$|\mu\rangle \triangleq U|\eta\rangle \tag{3.17}$$

and relation $U^\dagger = U^{-1}$ is exploited in consequence of the unitary property.

In possession of N-dimensional Q first we have to prove that its output vector always remains in the 2-dimensional space of $|\alpha\rangle$ and $|\beta\rangle$, which helps us to preserve our rotation based visualization. This requires the proof of the following theorem:

Theorem 3.1. *If the state vectors $|\alpha\rangle$ and $|\beta\rangle$ are defined according to (3.5) and (3.6) and both of them contain at least one nonzero probability amplitude, as well as the unitary operator U and an arbitrary state $|\eta\rangle$ are taken in such a way that $U|\eta\rangle$ lies within the vector space V spanned by the state vectors $|\alpha\rangle$ and $|\beta\rangle$, then the generalized Grover operator Q preserves this 2-dimensional vector space. In other words for any $|v\rangle \in V$, $Q|v\rangle \in V$ is true.*

Proof. Following the geometrical definition of inner product, the projection of $U|\eta\rangle$ on vector $|\beta\rangle$ can be calculated as $\langle\beta|U|\eta\rangle \cdot |\beta\rangle$. Since $U|\eta\rangle$ is defined in the vector space V and it has unit length, therefore vector $U|\eta\rangle - \langle\beta|U|\eta\rangle|\beta\rangle$ is parallel to $|\alpha\rangle$ and it can be computed in the following way

$$U|\eta\rangle - \langle\beta|U|\eta\rangle|\beta\rangle = \sqrt{1 - |\langle\beta|U|\eta\rangle|^2}|\alpha\rangle,$$

from which $|\alpha\rangle$ can be expressed in the nontrivial case i.e. if $|\langle\beta|U|\eta\rangle| \neq 1$ as

$$|\alpha\rangle = \frac{1}{\sqrt{1-|\langle\beta|U|\eta\rangle|^2}}\left(U|\eta\rangle - \langle\beta|U|\eta\rangle|\beta\rangle\right).$$

Vector $|\mu\rangle$ is considered as an arbitrary unit vector in V

$$|\mu\rangle_2 = \cos(\Omega)\,|\alpha\rangle + \sin(\Omega)\,e^{j\Lambda}|\beta\rangle, \tag{3.18}$$

where $\Omega, \Lambda \in [-\pi, \pi]$ and the superscript 2 refers to the 2-dimensional representation of originally N-dimensional $|\mu\rangle$. The global phase was omitted in (3.18) since it does not influence the operation and the final result.

In order to reach the well-tried rotation based picture of searching the generalized Grover operator should be determined in V where the required 2-dimensional Grover matrix is searched in the form of

$$\mathbf{Q_2} = \begin{bmatrix} Q_{11} & Q_{12} \\ Q_{21} & Q_{22} \end{bmatrix}. \tag{3.19}$$

Now we are able to compute the effect of Q on the basis vectors $|\alpha\rangle$ and $|\beta\rangle$. Provided the resulting vectors remain in V then this property will be valid for their arbitrary linear combination (superposition) $|v\rangle = a|\alpha\rangle + b|\beta\rangle$ because of the superposition principle. Therefore we apply Q for basis vector $|\beta\rangle$ first

$$Q|\beta\rangle = -\left(I + \left(e^{j\theta}-1\right)|\mu\rangle\langle\mu|\right) I_\beta|\beta\rangle. \tag{3.20}$$

As I_β multiplies[3] every index leading to a marked entry by $e^{j\phi}$, i.e. $|\beta\rangle$ is an eigenvector of I_β with eigenvalue $e^{j\phi}$ thus

$$I_\beta|\beta\rangle = e^{j\phi}|\beta\rangle. \tag{3.21}$$

Substituting (3.21) into (3.20) we get

$$Q|\beta\rangle = -e^{j\phi}\left(\left(e^{j\theta}-1\right)\langle\mu|\beta\rangle|\mu\rangle + |\beta\rangle\right). \tag{3.22}$$

Applying (3.18) and relation $\langle\mu|\beta\rangle = \langle\beta|\mu\rangle^* = \sin(\Omega)\,e^{-j\Lambda}$

$$\begin{aligned} Q|\beta\rangle &= -e^{j\phi}\left(e^{j\theta}-1\right)\sin(\Omega)\,e^{-j\Lambda}\left(\cos(\Omega)\,|\alpha\rangle + \sin(\Omega)\,e^{j\Lambda}|\beta\rangle\right) - e^{j\phi}|\beta\rangle \\ &= \underbrace{-e^{j\phi}\left(e^{j\theta}-1\right)\sin(\Omega)\cos(\Omega)\,e^{-j\Lambda}}_{Q_{21}}|\alpha\rangle \\ &\quad + \underbrace{-e^{j\phi}\left[\left(e^{j\theta}-1\right)\sin^2(\Omega)+1\right]}_{Q_{22}}|\beta\rangle. \end{aligned} \tag{3.23}$$

Moreover, the other two entries in $\mathbf{Q}$ can be determined by feeding Q with $|\alpha\rangle$

$$Q|\alpha\rangle = -\left(I + \left(e^{j\theta}-1\right)|\mu\rangle\langle\mu|\right) I_\beta|\alpha\rangle, \tag{3.24}$$

[3]The Oracle O did the same using multiplication factor -1.

where $I_\beta|\alpha\rangle = |\alpha\rangle$, because only those indices belonging to solutions of the searching problem are rotated by I_β others are left unchanged[4]. Exploiting the relation

$$\langle\mu|\alpha\rangle = \langle\alpha|\mu\rangle^* = \cos(\Omega) \tag{3.25}$$

we get the missing two elements

$$Q|\alpha\rangle = \underbrace{-\left[1+\left(e^{j\theta}-1\right)\cos^2(\Omega)\right]}_{Q_{11}}|\alpha\rangle + \underbrace{-\left[\left(e^{j\theta}-1\right)\cos(\Omega)\sin(\Omega)\,e^{j\Lambda}\right]}_{Q_{12}}|\beta\rangle \tag{3.26}$$

Now, the reader may conclude from (3.23) and (3.26) that $Q|\alpha\rangle$ and $Q|\beta\rangle$ did not leave vector space V, therefore all their linear superpositions $|v\rangle = a|\alpha\rangle + b|\beta\rangle$ transformed by Q still remain in V. □

Based on equations (3.23) and (3.26) we have matrix $\mathbf{Q_2}$ in a suitable 2-dimensional form

$$\begin{aligned}\mathbf{Q_2} &= -\begin{bmatrix} 1+\left(e^{j\theta}-1\right)\cos^2(\Omega) & e^{j\phi}\left(e^{j\theta}-1\right)\sin(\Omega)\cos(\Omega)\,e^{j\Lambda} \\ \left(e^{j\theta}-1\right)\cos(\Omega)\sin(\Omega)\,e^{-j\Lambda} & e^{j\phi}\left[1+\left(e^{j\theta}-1\right)\sin^2(\Omega)\right]\end{bmatrix} \\ &= -\begin{bmatrix} e^{j\theta}\cos^2(\Omega)+\sin^2(\Omega) & e^{j\phi}e^{-j\Lambda}\left(e^{j\theta}-1\right)\frac{\sin(2\Omega)}{2} \\ \left(e^{j\theta}-1\right)e^{j\Lambda}\frac{\sin(2\Omega)}{2} & e^{j\phi}\left[e^{j\theta}\sin^2(\Omega)+\cos^2(\Omega)\right]\end{bmatrix}.\end{aligned}$$

From this point forward $\mathbf{Q}$ always refers to the 2-dimensional Grover matrix, if not indicated otherwise.

3.2.2 Required number of iterations in the generalized Grover algorithm

Having obtained the 2-dimensional generalized Grover operator Q, we try to follow the rotation based representation of the search. Therefore the optimal number of iterations (Grover gates) l_s required to find a marked item with sure success should be derived. Starting from initial state $|\gamma_1\rangle$ sure success can be provided if

$$\langle\alpha|Q^{l_s}|\gamma_1\rangle = 0, \tag{3.27}$$

which stands for having an index register orthogonal to the vector including all the indices which do not lead to a solution. Because $|\alpha\rangle$ and $|\beta\rangle$ are orthogonal and $|\gamma_1\rangle \in V$, this assumption can be interpreted as $Q^{l_s}|\gamma_1\rangle$ is parallel to $|\beta\rangle$ i.e. $Q^{l_s}|\gamma_1\rangle = e^{j\delta}|\beta\rangle$. In this case sure success can be reached after a single measurement. Since Q is unitary and therefore it is a normal operator too, hence it has a spectral decomposition

$$Q = q_1|\psi_1\rangle\langle\psi_1| + q_2|\psi_2\rangle\langle\psi_2|, \tag{3.28}$$

[4]Thus $|\alpha\rangle$ and 1 are eigenvector and eigenvalue of I_β respectively.

where $q_{1,2}$ denote the eigenvalues of Q and $|\psi_{1,2}\rangle$ stand for the corresponding eigenvectors, respectively. Thus the following equalities hold

$$Q|\psi_{1,2}\rangle = q_{1,2}|\psi_{1,2}\rangle, \tag{3.29}$$

where $\langle\psi_1|\psi_2\rangle = 0$, because of the orthogonality property of the eigenvectors of any normal operators. The eigenvalues which can be determined from the characteristic equation $\det(\mathbf{Q} - q\mathbf{I}) = 0$ are

$$q_{1,2} = -e^{j\left(\frac{\theta+\phi}{2} \pm \Upsilon\right)}. \tag{3.30}$$

In addition we claim the following restriction on angle Υ

$$\cos(\Upsilon) = \cos\left(\frac{\theta-\phi}{2}\right) + \sin^2(\Omega)\left(\cos\left(\frac{\theta+\phi}{2}\right) - \cos\left(\frac{\theta-\phi}{2}\right)\right). \tag{3.31}$$

In possession of the eigenvalues the next step towards the optimal number of iterations is the determination of the normalized eigenvectors $|\psi_{1,2}\rangle$, which are

$$|\psi_1\rangle = \cos(z)\, e^{j\left(\frac{\phi}{2}-\Lambda\right)}|\alpha\rangle + \sin(z)\,|\beta\rangle, \tag{3.32}$$

$$|\psi_2\rangle = -\sin(z)\, e^{j\left(\frac{\phi}{2}-\Lambda\right)}|\alpha\rangle + \cos(z)\,|\beta\rangle, \tag{3.33}$$

where

$$\sin^2(z) = \frac{\sin^2(2\Omega)\sin^2\left(\frac{\theta}{2}\right)}{2\left(1 - \cos\left(\frac{\theta}{2}\right)\cos\left(\frac{\phi}{2} - \Upsilon\right) - 2\cos(2\Omega)\sin\left(\frac{\theta}{2}\right)\sin\left(\frac{\phi}{2} - \Upsilon\right)\right)}.$$

The detailed derivation of the eigenvectors and eigenvalues can be found in Appendices 16.1 and 16.2.

Having the required elements of the spectral decomposition of Q in our hand we are able to calculate the operator representing the l-times repetition of Q

$$\begin{aligned} Q^l &= q_1^l|\psi_1\rangle\langle\psi_1| + q_2^l|\psi_2\rangle\langle\psi_2| = (-1)^l\, e^{j\cdot l\left(\frac{\theta+\phi}{2}\right)} \cdot \\ &\cdot \begin{bmatrix} e^{j2\left(\frac{\phi}{2}-\Lambda\right)}\left(e^{jl\Upsilon}\cos^2(z) + e^{-jl\Upsilon}\sin^2(z)\right) & j\sin(l\Upsilon)\sin(2z)\, e^{j\left(\frac{\phi}{2}-\Lambda\right)} \\ j\sin(l\Upsilon)\sin(2z)\, e^{-j\left(\frac{\phi}{2}-\Lambda\right)} & e^{jl\Upsilon}\sin^2(z) + e^{-jl\Upsilon}\cos^2(z) \end{bmatrix}, \end{aligned} \tag{3.34}$$

where we exploited the fact that $\langle\psi_1|\psi_2\rangle = \langle\psi_2|\psi_1\rangle = 0$. Based on (3.34) the optimal l_s enabling sure success can be derived using (3.27) which is fulfilled if both – the real and the imaginary – parts of $\langle\alpha|Q^{l_s}|\gamma_1\rangle$ are equal to zero.

Let $|\gamma_1\rangle$ be defined as an arbitrary unit vector in V standing for the initial state of the index qregister

$$|\gamma_1\rangle = \cos\left(\frac{\Omega_\gamma}{2}\right)|\alpha\rangle + \sin\left(\frac{\Omega_\gamma}{2}\right)e^{j\Lambda_\gamma}|\beta\rangle. \tag{3.35}$$

Thus (3.27) becomes

$$\begin{aligned}\langle\alpha|Q^{l_s}|\gamma_1\rangle &= \cos\left(\frac{\Omega_\gamma}{2}\right)Q_{11}^{l_s}+\sin\left(\frac{\Omega_\gamma}{2}\right)e^{j\Lambda_\gamma}Q_{12}^{l_s}= \\ &= \cos\left(\frac{\Omega_\gamma}{2}\right)\left[e^{jl_s\Upsilon}\cos^2(z)+e^{-jl_s\Upsilon}\sin^2(z)\right]+ \\ &+ je^{j\left(\frac{\phi}{2}-\Lambda+\Lambda_\gamma\right)}\sin(l_s\Upsilon)\sin(2z)\sin\left(\frac{\Omega_\gamma}{2}\right)=0. \qquad (3.36)\end{aligned}$$

First we calculate the real part of (3.36)

$$\begin{aligned}\Re\left\{\langle\alpha|Q^{l_s}|\gamma_1\rangle\right\} &= \cos\left(\frac{\Omega_\gamma}{2}\right)\underbrace{\left[\cos(l_s\Upsilon)\cos^2(z)+\cos(l_s\Upsilon)\sin^2(z)\right]}_{\cos(l_s\Upsilon)}- \\ &- \sin\left(\Lambda_\gamma-\Lambda+\frac{\phi}{2}\right)\sin(l_s\Upsilon)\sin(2z)\sin\left(\frac{\Omega_\gamma}{2}\right) \\ &= \cos\left(\frac{\Omega_\gamma}{2}\right)\cos(l_s\Upsilon)-\sin\left(\frac{\Omega_\gamma}{2}\right)\sin(l_s\Upsilon)\sin(2z)\sin\left(\Lambda_\gamma-\Lambda+\frac{\phi}{2}\right)=0, \qquad (3.37)\end{aligned}$$

which is followed by the imaginary part

$$\begin{aligned}\Im\left\{\langle\alpha|Q^{l_s}|\gamma_1\rangle\right\} &= \cos\left(\frac{\Omega_\gamma}{2}\right)\underbrace{\left[\sin(l_s\Upsilon)\cos^2(z)-\sin(l_s\Upsilon)\sin^2(z)\right]}_{\sin(l_s\Upsilon)\cos(2z)}+ \\ &+ \cos\left(\Lambda_\gamma-\Lambda+\frac{\phi}{2}\right)\sin(l_s\Upsilon)\sin(2z)\sin\left(\frac{\Omega_\gamma}{2}\right)=0. \qquad (3.38)\end{aligned}$$

Let us first consider that $\sin(l_s\Upsilon)=0\Rightarrow\cos(l_s\Upsilon)=1$. In this case the real part of (3.37) is simplified to

$$\cos\left(\frac{\Omega_\gamma}{2}\right)\cos(l_s\Upsilon)=\cos\left(\frac{\Omega_\gamma}{2}\right)=0\Rightarrow\Omega_\gamma=0\pm k\pi,$$

while the imaginary part equals constantly 0. Therefore this scenario represents the situation where all the entries are unmarked. Contrary if $\sin(l_s\Upsilon)\neq 0$ then

$$\frac{\Im\left\{\langle\alpha|Q^{l_s}|\gamma_1\rangle\right\}}{\sin(l_s\Upsilon)}=\cos\left(\Lambda_\gamma-\Lambda+\frac{\phi}{2}\right)\sin(2z)\sin\left(\frac{\Omega_\gamma}{2}\right)+\cos\left(\frac{\Omega_\gamma}{2}\right)\cos(2z)=0. \qquad (3.39)$$

Equation (3.39) does not depend on l_s, which makes it suitable to determine the so called „*matching condition*" (MC), the relationship between θ and ϕ

$$\cos\left(\Lambda_\gamma-\Lambda+\frac{\phi}{2}\right)=-\cot(2z)\cot\left(\frac{\Omega_\gamma}{2}\right),$$

and thus

$$\tan\left(\frac{\phi}{2}\right)=\frac{\cos(2\Omega)+\sin(2\Omega)\cdot\tan\left(\frac{\Omega_\gamma}{2}\right)\cos(\Lambda-\Lambda_\gamma)}{\cot\left(\frac{\theta}{2}\right)-\tan\left(\frac{\Omega_\gamma}{2}\right)\sin(2\Omega)\sin(\Lambda-\Lambda_\gamma)}. \qquad (3.40)$$

It is worth emphasizing that according to (3.31) Υ seems to be 4π periodical in function of θ, which implies 4π periodicity for ϕ as well when determining ϕ form θ because Υ also depends on ϕ. This seems to be inconsistent with the fact that eigenvalues $q_{1,2}$ should be 2π periodical in θ and ϕ, see (3.30). This problem can be resolved if $\phi(\theta)$ is calculated for the range $[-2\pi, 2\pi]$ in function of $\theta \in [-2\pi, 2\pi]$. Practically $\pm 2\pi$ should be added to ϕ if it has a cut-off at certain θs. The points where $\phi(\theta)$ has cut-offs within the range of $[-2\pi, 2\pi]$ can be determined easily in the following manner

$$\phi = \pm\pi \Rightarrow \tan\left(\frac{\phi}{2}\right) = \pm\infty.$$

Since the numerator of the matching condition in (3.40) is constant in θ, hence the denominator has to be zero to achieve the condition $\phi = \pm\infty$. The cut-off angles $\theta_{co_{1,2}}$ can be derived from denominator of (3.40) as follows

$$\cot\left(\frac{\theta}{2}\right) = \tan\left(\frac{\Omega_\gamma}{2}\right)\sin(2\Omega)\sin(\Lambda - \Lambda_\gamma)$$

thus the cut-off angles in $[-2\pi, 2\pi]$ are

$$\theta_{co_1} = 2\mathrm{arccot}\left(\tan\left(\frac{\Omega_\gamma}{2}\right)\sin(2\Omega)\sin(\Lambda - \Lambda_\gamma)\right), \tag{3.41}$$

$$\theta_{co_2} = \theta_{co_1} \pm 2\pi. \tag{3.42}$$

We depicted $\phi(\theta)$ with and without the $\pm 2\pi$ correction in Fig. 3.3. The cut off points are in this case $\theta = \pm\pi$. By means of this correction 2π periodicity of Υ is achieved, hence the eigenvalues and eigenvectors of Q, even Q itself can boast a 2π periodicity in θ.

Now, the way is open to determine l_s from (3.37) supporting a final measurement with $P_s = 1$. The matching condition (3.40) should also be considered leading to

$$\cos\left(l_s\Upsilon + \arcsin\left(\sin\left(\frac{\phi}{2} - \Lambda + \Lambda_\gamma\right)\sin\left(\frac{\Omega_\gamma}{2}\right)\right)\right) = 0,$$

which is equivalent to

$$l_s\Upsilon = \pm\frac{\pi}{2} \pm i\pi - \arcsin\left(\sin\left(\frac{\phi}{2} - \Lambda + \Lambda_\gamma\right)\sin\left(\frac{\Omega_\gamma}{2}\right)\right), \tag{3.43}$$

where $\pm i\pi, i > 1$ can be omitted from the right hand side, because it would result in a bigger l_s than absolutely necessary. Unlike the basic algorithm where $i > 0$ could result in a more accurate measurement – in exchange of increased number of rotations – in case of the generalized algorithm $i = 0, 1$ can provide $P_\varepsilon = 0$. Expression (3.43) can be interpreted in the following way. The generalized Grover operator (Q) rotates the new initial state $|\gamma_1\rangle'$ having the initial angle

$$\frac{\Omega'_\gamma}{2} = \arcsin\left(\sin\left(\frac{\phi}{2} - \Lambda + \Lambda_\gamma\right)\sin\left(\frac{\Omega_\gamma}{2}\right)\right) \tag{3.44}$$

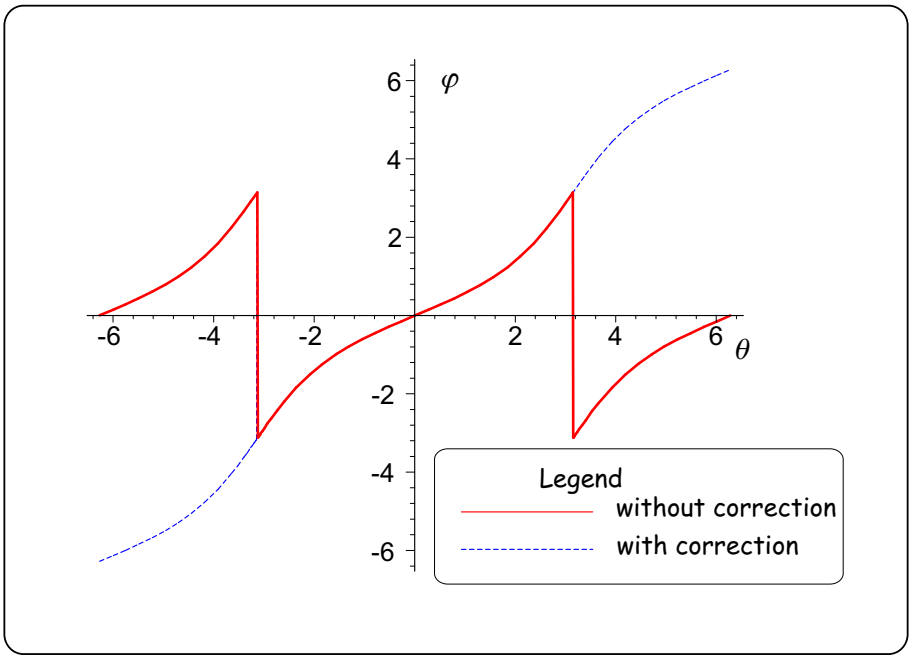

Fig. 3.3 The matching condition between ϕ and θ with and without correction assuming $\Omega = 0.5$, $\frac{\Omega_\gamma}{2} = 0.0001$, $\Lambda_\gamma = 0.004$, $\Lambda = 0.004$

in a plane V' spanned by the basis vectors $|\alpha\rangle'$ and $|\beta\rangle'$ with a rotation angle Υ towards $|\beta\rangle'$ as it is depicted in Fig. 3.4. It has to be remarked that $|\alpha\rangle'$ and $|\beta\rangle'$ are real valued axes while $|\alpha\rangle$ and $|\beta\rangle$ are complex valued. Because of the arbitrary sign of $\sin\left(\frac{\phi}{2} - \Lambda + \Lambda_\gamma\right)$, $\frac{\Omega'_\gamma}{2}$ can take different values depending on

$$\nu = \arcsin\left(\sin\left(\frac{\phi}{2} - \Lambda + \Lambda_\gamma\right)\sin\left(\frac{\Omega_\gamma}{2}\right)\right), \tag{3.45}$$

where $\arcsin(\cdot)$ is defined as

$$|\arcsin(\cdot)| \leq \frac{\pi}{2}.$$

If ν is positive the initial angle $\frac{\Omega'_\gamma}{2}$ could be $(\pi - \nu)$ or (ν), in the other case the possible values are $(-\pi + \nu)$ or $(-\nu)$ (see Fig. 3.5). Substituting matching condition into (3.31) it becomes obvious that

$$\Upsilon \in \begin{cases} [0, \frac{\pi}{2}] & \text{if } \frac{\Omega'_\gamma}{2} \in \text{I. or III. quadrant} \\ [-\frac{\pi}{2}, 0) & \text{if } \frac{\Omega'_\gamma}{2} \in \text{II. or IV. quadrant} \end{cases}$$

and because $+|\beta\rangle'$ is as appropriate for final state as $-|\beta\rangle'$ therefore $\pm|\beta\rangle'$ can be reached from any interpretation of $\frac{\Omega'_\gamma}{2}$ by means of an overall rotation smaller than $\frac{\pi}{2}$ (see Fig. 3.5). Υ can be seen in function of θ in Fig. 3.6. The number of iterations l_s ensuring sure success

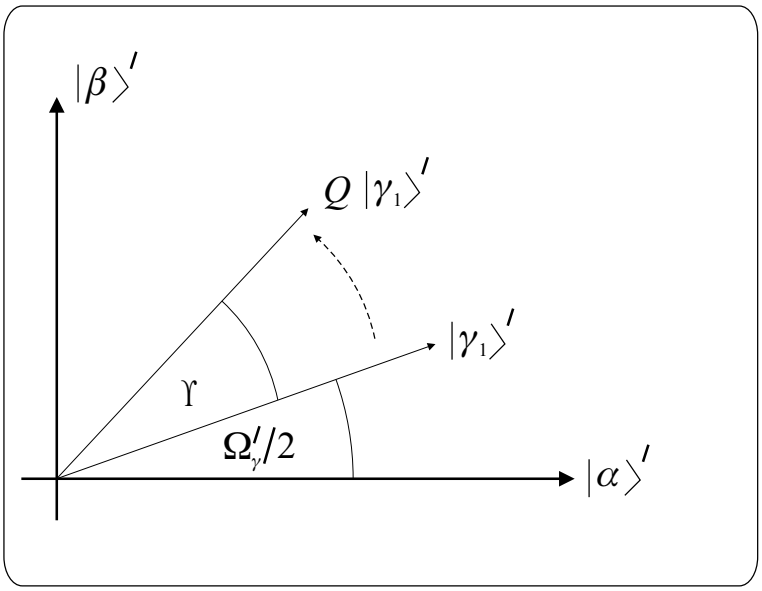

Fig. 3.4 Geometrical interpretation of the generalized Grover iteration

can be expressed from (3.43) as

$$l_s = \frac{\frac{\pi}{2} - \left|\arcsin\left(\sin\left(\frac{\phi(\theta)}{2} - \Lambda + \Lambda_\gamma\right)\sin\left(\frac{\Omega_\gamma}{2}\right)\right)\right|}{\Upsilon}, \tag{3.46}$$

where the absolute value operator omitted in the denominator because

$$0 \leq \arccos(\cdot) \leq \pi$$

has been assumed.

However, we need an integer number of rotations in practice, moreover it is worth investigating the effect of different variables determining l_s especially ϕ which is restricted by the matching condition, therefore the next subsection is dedicated to these questions.

3.2.3 Design considerations of the generalized Grover operator

In order to build the generalized Grover operator one has to define θ, ϕ and $|\mu\rangle$. On one hand the first two parameters have fixed relation via the matching condition, on the other hand Q provides sure success therefore the design process of Q can be traced back to minimizing l_s in function of θ and $|\mu\rangle$. To achieve this goal we investigate several scenarios differing in the amount of available information.

The basic Grover algorithm

As the first scenario we analyze the original Grover algorithm (see Section 3.1) as a special case of the generalized one. Thus we have the following setup: $\theta = \phi = \pi$, $U = H$,

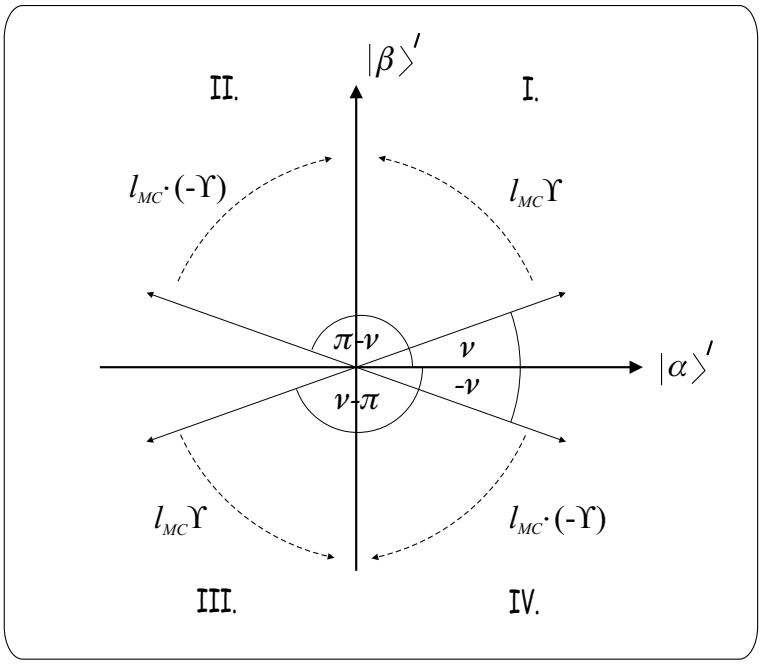

Fig. 3.5 Different possible interpretations of $|\gamma_1\rangle'$

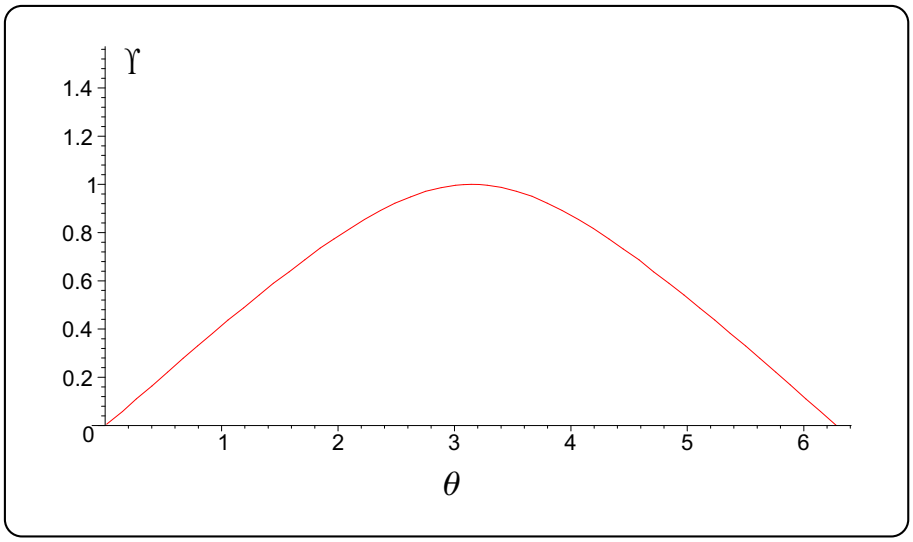

Fig. 3.6 Υ vs. θ assuming $\Omega = 0.5$, $\frac{\Omega_\gamma}{2} = 0.0001$, $\Lambda_\gamma = 0.004$, $\Lambda = 0.004$

$|\eta\rangle = |\mathbf{0}\rangle$. Furthermore we know that input state $|\gamma_1\rangle$ equals the axis of the inversion about average $|\mu\rangle$ that is $\Lambda = \Lambda_\gamma = 0$ as well as $\Omega = \frac{\Omega_\gamma}{2} = \arcsin\left(\sqrt{M/N}\right)$.

In possession of this information let us calculate the corresponding Υ using (3.31)

$$\begin{aligned}\cos(\Upsilon) &= \overbrace{\cos\left(\frac{\theta-\phi}{2}\right)}^{=1} + \sin^2(\Omega)\cdot\left(\overbrace{\cos\left(\frac{\theta+\phi}{2}\right)}^{=-1} - \overbrace{\cos\left(\frac{\theta-\phi}{2}\right)}^{=1}\right)\\ &= \cos^2\left(2\frac{\Omega_\gamma}{2}\right) - \sin^2\left(2\frac{\Omega_\gamma}{2}\right) = \cos(\Omega_\gamma), \end{aligned} \tag{3.47}$$

from which $\Upsilon = \Omega_\gamma$ and thus the optimal number of iterations from (3.46)

$$l_{opt} = \frac{\frac{\pi}{2} - \left|\arcsin\left(\sin\left(\frac{\phi}{2} - \Lambda + \Lambda_\gamma\right)\sin\left(\frac{\Omega_\gamma}{2}\right)\right)\right|}{\Upsilon} = \frac{\frac{\pi}{2} - \frac{\Omega_\gamma}{2}}{\Omega_\gamma},$$

which is nothing else than the required number of rotations l_{opt_0} (3.8) in the basic Grover algorithm. Unfortunately choosing the predefined fixed relation $\theta = \phi = \pi$ it does not guarantee sure success by all means, because the matching condition may be violated.

Providing sure success by modifying the basic Grover algorithm

Now we try to measure one of the marked entries with $P_s = 1$. To achieve this we keep all the previous parameters except θ and ϕ are adjusted according to the matching condition i.e $\phi(\theta)$ becomes a function of θ. Remember that Ω_γ is available from performing a quantum counting (see Section 4.1) with $\theta = \phi = \pi$. The optimal θ_{opt} which minimizes l_s can be computed solving

$$\frac{dl_s(\phi(\theta),\theta)}{d\theta} = \frac{\partial l_s(\phi(\theta),\theta)}{\partial\phi(\theta)}\cdot\frac{d\phi(\theta)}{d\theta} + \frac{\partial l_s(\phi(\theta),\theta)}{\partial\theta} = 0,$$

i.e. we determine the minimum point of l_s in Fig. 3.7. In order to be able to substitute $\phi(\theta)$ into (3.31) and (3.46) one has to evaluate the matching condition (3.40) assuming the given parameter setup

$$\begin{aligned}\tan\left(\frac{\phi}{2}\right) &= \frac{\cos\left(2\frac{\Omega_\gamma}{2}\right) + \sin\left(2\frac{\Omega_\gamma}{2}\right)\cdot\tan\left(\frac{\Omega_\gamma}{2}\right)\overbrace{\cos(\Lambda-\Lambda_\gamma)}^{=1}}{\cot\left(\frac{\theta}{2}\right) - \tan\left(\frac{\Omega_\gamma}{2}\right)\sin\left(2\frac{\Omega_\gamma}{2}\right)\underbrace{\sin(\Lambda-\Lambda_\gamma)}_{=0}}\\ &= \tan\left(\frac{\theta}{2}\right)\cdot\left(\cos(\Omega_\gamma) + \sin(\Omega_\gamma)\tan\left(\frac{\Omega_\gamma}{2}\right)\right)\\ &= \tan\left(\frac{\theta}{2}\right)\cdot(\cos(\Omega_\gamma) + 1 - \cos(\Omega_\gamma)) = \tan\left(\frac{\theta}{2}\right),\end{aligned}$$

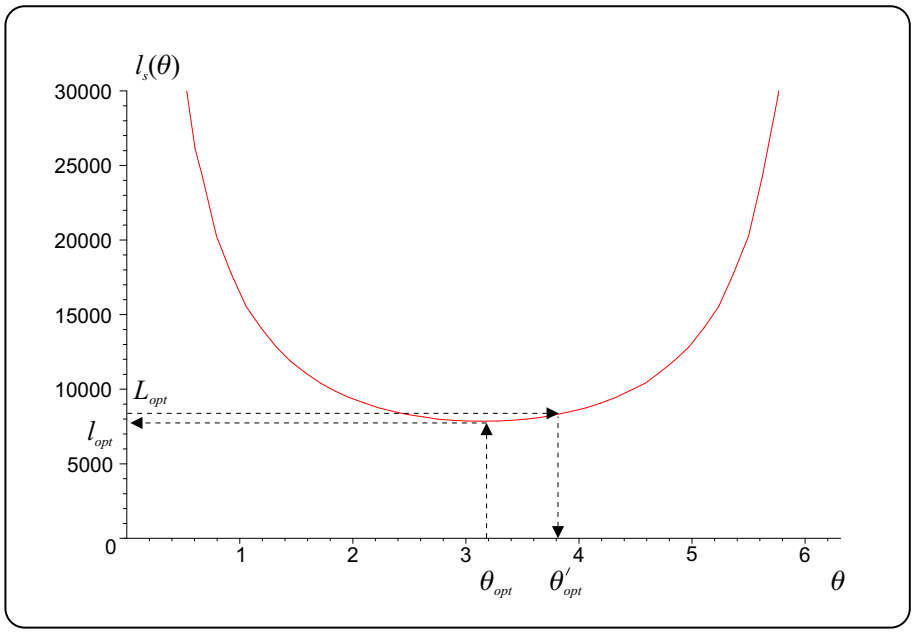

Fig. 3.7 Number of iterations l_s vs. θ assuming the matching condition is fulfilled and $\Omega = 0.0001$, $\frac{\Omega_\gamma}{2} = 0.0001$, $\Lambda_\gamma = \Lambda = 0$

where we exploited basic trigonometric relation $\tan\left(\frac{x}{2}\right) \equiv \frac{1-\cos(x)}{\sin(x)}$. We reached an important result, namely to provide sure success we need $\theta = \phi$. Substituting this special matching condition into (3.31)

$$\begin{aligned}\cos(\Upsilon) &= \cos\left(\frac{\phi-\phi}{2}\right) + \sin^2\left(\frac{\Omega_\gamma}{2}\right)\cdot\left(\cos\left(\frac{\phi+\phi}{2}\right) - \cos\left(\frac{\phi-\phi}{2}\right)\right) \\ &= \cos(\phi)\sin^2\left(\frac{\Omega_\gamma}{2}\right) + \cos^2\left(\frac{\Omega_\gamma}{2}\right).\end{aligned}$$

Now we can turn to minimize l_s in θ

$$l_s(\theta) = \frac{\frac{\pi}{2} - \left|\arcsin\left(\sin\left(\frac{\phi}{2}\right)\sin\left(\frac{\Omega_\gamma}{2}\right)\right)\right|}{\arccos\left(\cos(\phi)\sin^2\left(\frac{\Omega_\gamma}{2}\right) + \cos^2\left(\frac{\Omega_\gamma}{2}\right)\right)}.$$

However, instead of beginning long lasting derivations the reader may realize that the denominator has maximum if $\cos(\phi) = 1 \Rightarrow \phi = \pi$ and the numerator has minimum if $\sin\left(\frac{\phi}{2}\right) = 1 \Rightarrow \phi = \pi$ therefore $\theta_{opt} = \phi_{opt} = \pi$, which is the original setup of the basic Grover algorithm. *Thus the basic Grover algorithm proves to be optimal in terms of the number of database queries if we have no a priori information about the database i.e. it is really unsorted.*

We depicted $l_s(\theta)$ in Fig. 3.7. Since $l_{opt} = l_s(\theta_{opt})$ is not an integer for sure, the nearest superior integer L_{opt} has to be taken into account. In consequence of this deferral, the matching condition is harmed, which requires the calibration of angle θ and ϕ. In

possession of L_{opt} we can calculate ϕ'_{opt} from (3.46) and substituting it into (3.40) we get θ'_{opt}. Obviously there are two such values for θ but we presented only one of them in Fig. 3.7.

Finally we would like to emphasize that to achieve a sure success searching algorithm we did not need to increase the number of database queries compared to the basic algorithm, instead the Oracle and the phase gate were modified!

Starting from an arbitrary initial state

The initial state of the index qreqister was set to $|\gamma_1\rangle = H|\mathbf{0}\rangle$ in case of the basic Grover algorithm since we had no information about the structure of the database i.e. it was considered being unsorted. However, as we mentioned in the introduction of this subsection there are practical problems where we have some pieces of a priori information about the database. Based on this information one can preprocess the index qregister amplifying the probability amplitudes of the marked states – even not uniformly – producing an arbitrary $|\gamma_1\rangle$, see (3.13). Is it possible to exploit this fact by means of the generalized Grover algorithm or shall we loose this advantage when returning to the uniformly distributed initial probability amplitudes of the index qregister of the basic algorithm? To answer this question we have to determine θ, ϕ and $|\mu\rangle$ in possession of $|\gamma_1\rangle$.

Obviously if we were familiar with which states are marked and unmarked then we were able to calculate $|\mu\rangle$ in such a way that a single rotation would provide sure success. As an example let us consider the basic Grover algorithm. Provided the axis of the inversion about the average is chosen to $\Omega = \frac{\frac{\pi}{2}+\frac{\Omega_\gamma}{2}}{2}$ then the reflection about $|\mu\rangle$ after applying the Oracle (reflecting $|\gamma_1\rangle$ onto $|\alpha\rangle$) will result in $|\beta\rangle$ (see Fig. 3.2).

Unfortunately when searching is needed this information is not available. Therefore the best we can do is to set $|\mu\rangle = |\gamma_1\rangle$ that is $\Omega = \frac{\Omega_\gamma}{2}$ and $\Lambda = \Lambda_\gamma$. Since the matching condition and thus l_{opt} depend only on the difference between Λ and Λ_γ therefore their actual values do not influence the design of Q i.e. $\Lambda - \Lambda_\gamma \equiv 0$. Since $|\gamma_1\rangle$ is known hence $|\mu\rangle$ can be easily produced using an appropriate U. In order to minimize l_s in θ the only missing parameter is Ω. We showed in (3.30) that the eigenvalues of Q have the following form $q_{1,2} = -e^{j\left(\frac{\theta+\phi}{2}\pm\Upsilon\right)}$. Hence using a phase estimation with $\theta = \phi = \pi$ it gives back Υ unambiguously from which Ω can be computed exploiting (3.31) and bearing in mind the actual values of θ and ϕ, namely $\Omega = \frac{\Upsilon(\theta=\pi,\phi=\pi)}{2}$ (see (3.47)). Next the same technique can be applied as for the enhanced basic Grover algorithm to determine ϕ'_{opt}, θ'_{opt} and the corresponding L_{opt}.

4

Searching for Extreme Values in an Unsorted Database

"Creativity exists more in the searching than in the finding."

Stephen Nachmanovich

Many computing and engineering problems can be traced back to an optimization process which is aiming to find the extreme value (minimum or maximum point) of a so called cost function or a database. We list here only several well-known cases of these type of problems. For instance global infocom networks require to find the optimum route between two terminals located on different continents in terms of the shortest path or optimal signal detection on the air interfaces of state of the art mobile networks needs to perform maximum likelihood hypothesis testing based on finding the largest conditional probability density function (pdf) among say 10^{30} pdfs. Unfortunately because of their huge computational complexity these problems are typically answered by means of suboptimal solutions. However, quantum computing and related parallel processing capabilities offers a more efficient way to solve the above mentioned problem.

From this point on we use notions *database* and *function* as synonyms from the discussed problem point of view.

This Chapter is organized in the following way. Phase estimation based quantum counting is discussed in Section 4.1 which can be used both as a stand alone algorithm or enables minimizing the error probability when searching for a given entry in the database. A special and often used case of counting is when we are interested whether a database contains a certain entry at all. It is called existence testing and it is explained in Section 4.2. We show how to use quantum existence testing when one is interested in the largest or smallest entry of an unsorted database/cost function in Section 4.3.

4.1 QUANTUM COUNTING

"You see, the chemists have a complicated way of counting: instead of saying 'one, two, three, four, five protons', they say, 'hydrogen, helium, lithium, beryllium, boron.'"

Richard Feynman

Readers having followed carefully the previous analysis of Grover algorithm may hit on an important shortcoming. Namely in order to determine the optimal number of iterations L_{opt_0} in (3.8) we require indirectly exact knowledge about the order of multiplicity M. One may imagine engineering problems where it is available, but this is typically not the case. It looks like as if we have fallen into a very serious trap which may call the conduciveness of all the already achieved results in question. Fortunately quantum computing is dropping a rope to escape from this serious problem because it supports us with an algorithm being able to compute M efficiently.

4.1.1 Quantum counting based on phase estimation

It is widely known that the matrix of the Grover operator can be expressed in the basis of $|\alpha\rangle$ and $|\beta\rangle$ as

$$\mathbf{G} = \begin{bmatrix} \cos(\Omega_\gamma) & -\sin(\Omega_\gamma) \\ \sin(\Omega_\gamma) & \cos(\Omega_\gamma) \end{bmatrix}.$$

Furthermore it is easy to show that G has two eigenvalues namely $e^{\pm j\Omega_\gamma}$. Recalling phase estimation from [87, 82] which aimed to determine the phase belonging to a given eigenvalue of an operator we are out from the trap. A phase estimation applying $U = G$ and using appropriate parameters and initialization will give back a good estimation of Ω_γ with high probability which is in direct connection with M via (4.1).

$$\sin\left(\frac{\Omega_\gamma}{2}\right) = \frac{\sqrt{\frac{M}{N}}}{1} \Rightarrow \Omega_\gamma = 2\arcsin\left(\sqrt{\frac{M}{N}}\right). \tag{4.1}$$

We depicted the quantum counting circuit in Fig. 4.1.

Before celebrating our clever 'discovery', however, we have to set some parameters for the circuit of Fig. 4.1. As one can learn at the phase estimation we need a lower section comprising now n qbits and initialized by the eigenvectors of the expected eigenvalue. Some short calculations provide the corresponding eigenvectors

$$|g_1\rangle = \frac{e^{j\xi}}{\sqrt{2}}\begin{bmatrix} j \\ 1 \end{bmatrix}, |g_2\rangle = \frac{e^{j\xi}}{\sqrt{2}}\begin{bmatrix} -j \\ 1 \end{bmatrix}, \xi \in \mathbb{R},$$

but unfortunately we are not able to feed the circuit neither with $|g_1\rangle$ nor $|g_2\rangle$ because it would require $|\alpha\rangle$ or $|\beta\rangle$ i.e. the complete knowledge about the marked and unmarked sets.

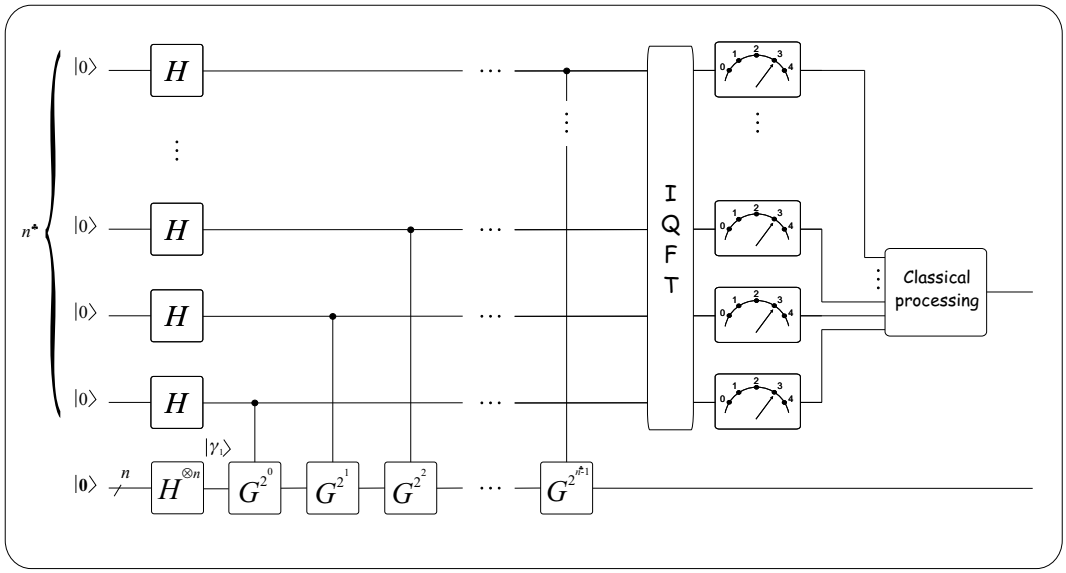

Fig. 4.1 Quantum counting circuit

Thus another trap is seeming to crop up but we have all the required capabilities to avoid it. We know that using a superposition of the eigenvectors as the lower input one gets one of the eigenvalues after the measurement at the upper output. Luckily we have only two and easily distinguishable phases Ω_γ and $-\Omega_\gamma = 2\pi - \Omega_\gamma$ in our very special case since $\Omega_\gamma \leq \frac{\pi}{4}$. Therefore without being familiar in advance with Ω_γ we are able to compute it from the measurement result. For the sake of simplicity we use $|\gamma_1\rangle$ for this purpose which is trivially a superposition of $|\alpha\rangle$ and $|\beta\rangle$. Because $|g_1\rangle$ and $|g_2\rangle$ form an orthonormal basis of the space spanned by $|\alpha\rangle$ and $|\beta\rangle$ hence $|\gamma_1\rangle$ can be expressed as a linear combination of $|g_1\rangle$ and $|g_2\rangle$.

Finally we have to set up the size of the upper quantum register. In order to avoid the confusion using notation n in two different meanings hence the number of qbits in the upper section of the counting circuit will be denoted by $n^{\clubsuit}$. As one can learn form [82] practical setting of $n^{\clubsuit}$ depends on both classical accuracy 2^{-c} of Ω_γ and allowed quantum uncertainty $\breve{P}_{\varepsilon P}$ of the phase estimation in the following manner

$$n^{\clubsuit} = c - 1 + \left\lceil \mathrm{ld}(2\pi) + \mathrm{ld}\left(3 + \frac{1}{\breve{P}_{\varepsilon P}}\right)\right\rceil . \tag{4.2}$$

4.2 QUANTUM EXISTENCE TESTING

A special case of quantum counting if one is interested in whether a given entry exists in the database at all instead of the number M of occurrences. Clearly speaking our goal is to determine whether the initial vector of the index qregister is parallel or angular to basis state $|\alpha\rangle$ in the 2-dimensional rotation based picture of the Grover operator that is

we would like to distinguish the case $\frac{\Omega_\gamma}{2} = 0 \Rightarrow \Omega_\gamma = 0$ from $\frac{\Omega_\gamma}{2} \neq 0$. Trivially we can use quantum counting to solve this problem, namely if we yield $M \neq 0$ then the database contains the requested entry else it does not. However, quantum counting involves some amount of overhead information because from existence point of view the accurate value of M is indifferent. Hence it is worth discussing a bit the required number of qbits for the upper section (based on (4.2)) and suitable error analysis.

Concerning this question let us deal first with classical accuracy. If $M = 0$ then the output of the IQFT should be unambiguously $|\mathbf{0}\rangle$ while provided $M \neq 0$ we can accept any other computational basis states except $|\mathbf{0}\rangle$. So we do not need the precise value of M in the latter case instead classically less accurate results are as appropriate as the exact one. Thus the worst case scenario occurs when $\frac{\Omega_\gamma}{2}$ is the smallest that is we have the smallest angle between $|\gamma_1\rangle$ and $|\alpha\rangle$. Hence the classical accuracy c should be chosen such that in case $M = 1$ the measured output of the IQFT contains at least one nonzero bit which allows distinguishing it from $|\mathbf{0}\rangle$. Let us assume again without loss of generality that we have a database $N = 2^n$ entry of size, therefore using (4.1) we need

$$\min(\Omega_\gamma) = 2\arcsin\left(\sqrt{\frac{1}{N}}\right) \cong 2\sqrt{\frac{1}{N}} = 2^{(-n/2+1)} \geq 2^{-c} \tag{4.3}$$

where we applied the well-known relation $\arcsin(y) = y$ if $y \ll 1$, from which we get

$$c = \left\lceil \frac{n}{2} \right\rceil - 1.$$

Of course we have to take care of quantum uncertainty of phase estimation as well, hence we need all together

$$n^{\clubsuit} = \left\lceil \frac{n}{2} + \mathrm{ld}(2\pi) + \mathrm{ld}\left(3 + \frac{1}{\breve{P}_{\varepsilon P}}\right) \right\rceil - 2$$

qbits, where $\breve{P}_{\varepsilon P}$ stands for the allowed maximum quantum uncertainty and correction $\mathrm{ld}(2\pi)$ is required because c refers to the accuracy of the estimated phase instead of the phase ratio itself. Since the -2 term has marginal influence on the complexity therefore we omit it during the further discussion that is

$$n^{\clubsuit} = \left\lceil \frac{n}{2} + \mathrm{ld}(2\pi) + \mathrm{ld}\left(3 + \frac{1}{\breve{P}_{\varepsilon P}}\right) \right\rceil. \tag{4.4}$$

Moreover if one gets $n^{\clubsuit} < 1$ then $n^{\clubsuit}$ has to be set to 1.

4.2.1 Error analysis

Formula (4.4) gives a rule of thumb when roughly estimating the required qbits in the upper section of the phase estimator. However, as we have seen in the previous subsection the interpretation of classical accuracy was a bit different in case of counting and existence

testing (in the latter case we have a softer constraint). Thus we expect that a similar effect will emerge when investigating quantum inaccuracy precisely. Therefore let us derive the required number p of additional qbits in the upper section of the device if we have a constraint $\breve{P}_\varepsilon$ of quantum uncertainty.

It is easy to see that if $M = 0$ then $\Omega_\gamma = 0$ is measured *always* with certainty since the phase ratio $\kappa = \Omega_\gamma/2\pi$ is also equal to zero, which corresponds to the idealistic phase estimation. Hence only the case $\Omega_\gamma \neq 0$ should be taken into consideration from quantum error point of view when seeking the relationship between the required number of additional qbits and $P_{\varepsilon E}$, where subscript E refers to *Existence testing*. For the sake of controlling precisely this $P_{\varepsilon E}$ one needs p additional qbits to $\frac{n}{2} + \mathrm{ld}(2\pi)$ qbits in the upper qregister to guarantee classical accuracy 2^{-c}. An error occurs if $\tilde{\Omega}_\gamma = 0$ is measured although $\Omega_\gamma \neq 0$ which is equivalent to the case when we get a computational basis state having mere zero bits on the $(n^{\clubsuit} - p)$ MSB positions that is

$$P_{\varepsilon E} = \underbrace{P(\tilde{\Omega}_\gamma \neq 0 | \Omega_\gamma = 0)}_{\equiv 0} P(\Omega_\gamma = 0) + \sum_{\Omega_\gamma \neq 0} P(\tilde{\Omega}_\gamma = 0 | \Omega_\gamma) P(\Omega_\gamma) \tag{4.5}$$

On one hand the conditional error probability can be calculated in the following way

$$P(\tilde{\Omega}_\gamma = 0 | \Omega_\gamma) = \sum_{i=0}^{2^p - 1} \left| \varphi_i(n^{\clubsuit}, \Omega_\gamma) \right|^2 \tag{4.6}$$

where $\varphi_i(n^{\clubsuit}, \Omega_\gamma)$ is the probability amplitude of state $|i\rangle$ and $i \in [0, 2^n)$

$$\varphi_i(n^{\clubsuit}, \Omega_\gamma) = \frac{1}{2^{n^{\clubsuit}}} \frac{1 - e^{j2\pi(2^{n^{\clubsuit}} \frac{\Omega_\gamma}{2\pi} - i)}}{1 - e^{j2\pi(\frac{\Omega_\gamma}{2\pi} - \frac{i}{2^{n^{\clubsuit}}})}}. \tag{4.7}$$

On the other hand we assume that $P(M)$ is uniformly distributed as a worst case approach. Furthermore since $M \in [0, N-1]$ and M is connected to Ω_γ via a reversible function (4.1) therefore $P(\Omega_\gamma) = \frac{1}{N}$.

Unlike (4.5) in order to build a useful connection between $P_{\varepsilon E}$ and overhead p it is worth searching for an appropriate upperbound P_{upper} for $P(\tilde{\Omega}_\gamma = 0 | \Omega_\gamma)$, which is independent from Ω_γ

$$P_{\varepsilon E} = \sum_{\Omega_\gamma \neq 0} P(\tilde{\Omega}_\gamma = 0 | \Omega_\gamma) P(\Omega_\gamma) \leq P_{upper} \frac{N-1}{N}. \tag{4.8}$$

In order to majorize $|\varphi_i(n^{\clubsuit}, \Omega_\gamma)|^2$ we upperbound its numerator and lowerbound its denominator applying the same inequalities $|1 - e^\alpha| \leq 2$ and $|1 - e^\alpha| \geq \frac{2|\alpha|}{\pi}$ as we used for the phase estimation, respectively. Thus we get

$$\left| \varphi_i(n^{\clubsuit}, \Omega_\gamma) \right|^2 \leq \frac{1}{4} \frac{1}{2^{n^{\clubsuit}} \left(\frac{\Omega_\gamma}{2\pi} - \frac{i}{2^{n^{\clubsuit}}} \right)^2},$$

which can be further majorized exploiting $\min(\Omega_\gamma)$ from (4.3)

$$\left|\varphi_i(n^{\clubsuit},\Omega_\gamma)\right|^2 \leq \frac{1}{4}\frac{1}{\left(\frac{2^{n^{\clubsuit}}}{\pi\sqrt{N}}-i\right)^2} \tag{4.9}$$

Considering that $\sqrt{N}=2^{\frac{n}{2}}$ and $n^{\clubsuit}=\frac{n}{2}+\mathrm{ld}(2\pi)+p$ the right hand side of (4.9) simplifies to

$$\left|\varphi_i(n^{\clubsuit},\Omega_\gamma)\right|^2 \leq \frac{1}{4}\frac{1}{(2^{p+1}-i)^2}.$$

Now we are able to derive a suitable P_{upper}

$$P(\tilde{\Omega}_\gamma=0|\Omega_\gamma) \leq \sum_{k=0}^{2^p-1}\frac{1}{4}\frac{1}{(2^{p+1}-k)^2} \tag{4.10}$$

If $(2^{p+1}-k)^2$ were strictly monotonously increasing in $[0,2^p]$ then the sum in (4.10) could be upperbounded by the corresponding integral i.e.

$$\sum_{k=0}^{2^p-1}\frac{1}{4}\frac{1}{(2^{p+1}-k)^2} \leq \int_0^{2^p}\frac{1}{4}\frac{1}{(2^{p+1}-k)^2}dk.$$

This requires that $2^{p+1}-k\geq 0 \Rightarrow 2^{p+1}\geq 2^p$ which is trivially satisfied. Evaluating the above integral one obtains

$$\begin{aligned} P(\tilde{\Omega}_\gamma=0|\Omega_\gamma) &\leq \int_0^{2^p}\frac{1}{4}\frac{1}{(2^{p+1}-k)^2}dk = \frac{1}{4}\left(\frac{1}{2^{p+1}-2^p}-\frac{1}{2^{p+1}}\right) \\ &= \frac{1}{8}\frac{1}{2^p} = P_{upper}, \end{aligned} \tag{4.11}$$

which allows upperbounding $P_{\varepsilon E}$ itself based on (4.8)

$$P_{\varepsilon E} \leq \frac{1}{8}\frac{1}{2^p}\frac{2^n-1}{2^n}. \tag{4.12}$$

Provided we have an engineering constraint $\breve{P}_\varepsilon \geq P_{\varepsilon E}$ one needs

$$p=\mathrm{ld}\left(\frac{2^n-1}{8\cdot 2^n\breve{P}_\varepsilon}\right) \leq \mathrm{ld}\left(\frac{1}{8\breve{P}_\varepsilon}\right), \tag{4.13}$$

qbits to fulfil it and the total number of required qbits in the upper section is

$$n^{\clubsuit}=\left\lceil \frac{n}{2}+\mathrm{ld}(2\pi)+\mathrm{ld}\left(\frac{1}{8\breve{P}_\varepsilon}\right)\right\rceil. \tag{4.14}$$

Using the above derived existence tester, in order to separate the two outcome categories it is enough to check whether the output of the device contains at least one nonzero bit or not. If yes then the database comprises the requested item else it is not in. Furthermore we emphasize that this method does not suffer any classical errors!

Concerning the computational complexity we can state that the quantum existence tester saves $n/2$ qbits and 3 qbits in classical accuracy and quantum uncertainty compared to the quantum counting circuit, which can be significant if $N\gg 1$.

4.3 FINDING EXTREME VALUES IN AN UNSORTED DATABASE

From quantum computing point of view we should consider the Grover algorithm as the most promising candidate. Unfortunately as we shortly summarized in the corresponding *Further Reading* the proposed Grover based solutions are efficient only in terms of expected number of database queries. In order to overcome this major shortcoming we decided to exploit the quantum existence testing algorithm as a core function. This is because our special problem does not require quantum counting on the whole that is we do not need to determine the number of occurrences of a certain entry in the database but we are rather interested in whether the database contains it at all.

Having introduced the quantum existence testing algorithm in Section 4.2 we are ready to turn to extreme value searching. We will embed our special core function into a classical logarithmic search (see e.g. [88, 60]). Let us assume that we have a function $y = g[x]$ which has integer input $x \in [0, N-1]$ and integer output $y \in [G_{\min 0}, G_{\max 0}]$ that is we have a rough estimation about the range of y (e.g. we know that y is non-negative thus $G_{\min 0} = 0$ proves to be a suitable lower bound). Using these notations the problem can be formulated as follows. We are interested in y_{opt} such that $\min_x(g[x]) = g[x_{opt}] = y_{opt}$. We emphasize that although minimum value search is considered here, the suggested technique can be trivially transformed to find the maximal entry of a database. The best classical solutions require N queries to the database to find x_{opt} hence our aim is to design a more efficient algorithm based on quantum computing.

To solve the above mentioned problem we combine the well-known logarithmic (often referred as binary) search algorithm – which is intended originally for searching a given item in a *sorted* database – with quantum existence testing. Hereby we produce an algorithm which keeps the efficiency of binary search while processing an *unsorted* database. It operates in a recursive way where in the s^{th} step we halve the actual searching region splitting it into two subregions. Let $G_{\text{med}s}$ denote that y value which separates the subregions. Next we launch the quantum existence testing algorithm – represented here by function $QET(z)$ – to check whether there is a $y < z$ marked state in the lower subregion or not. If the answer is YES then we use the lower subregion as the input of the next searching step else the upper one has to be chosen. In order to being more precise the proposed algorithm is given now in detail

1. We start with $s = 0$: $G_{\min 1} = G_{\min 0}$, $G_{\max 1} = G_{\max 0}$ and $\Delta G = G_{\max 0} - G_{\min 0}$
2. $s = s + 1$
3. $G_{\text{med}s} = G_{\min s} + \left\lceil \frac{G_{\max s} - G_{\min s}}{2} \right\rceil$
4. $flag = QET(G_{\text{med}s})$
   - if $flag = YES$ then $G_{\max s+1} = G_{\text{med}s}$, $G_{\min s+1} = G_{\min s}$

- else $G_{\max\, s+1} = G_{\max\, s}$, $G_{\min\, s+1} = G_{\mathrm{med} s}$.

5. if $s < \mathrm{ld}(\Delta G)$ then go to (2) else stop and $y_{opt} = G_{\mathrm{med} s}$.

We have two additional remarks to this algorithm. First it can be used obviously in case of multiple minimum values, too. Next if one is interested in the corresponding $x_{opt} = g^{-1}[y_{opt}]$ then a single quantum counting followed by a single Grover search has to be performed resulting the number of different x values belonging to y_{opt} and to obtain one of them according to a uniform distribution.

Finally computational complexity should be considered. Obviously the best classical strategy the exhaustive search needs $O(N)$ steps to find y_{opt} with sure success. Already available quantum computing based solutions require $O(\sqrt{N} + \mathrm{ld}^2(N))$ [13, 2] iterations (i.e. Grover operators) in *expected value*. Contrary the proposed new approach obtains y_{opt} using $O(\sqrt{N} \cdot \mathrm{ld}(\Delta G))$ database access.

If one considers elementary quantum gates and exploits the benefits of modular exponentiation then only $O(\mathrm{ld}(\Delta G)\mathrm{ld}^3(\sqrt{N}))$ elementary steps needed. The initial searching range has influence on the complexity as well, but in many practical applications one has some pieces of information about $G_{\min\, 0}$ and $G_{\max\, 0}$, which can be quite rough without causing difficulties thanks to the $\mathrm{ld}(\cdot)$ function.

5

Quantum Based Multiuser Detection

"Although this may seem a paradox, all exact science is dominated by the idea of approximation."

Bertrand Russell

Every telecommunication system designed to provide services for more than one subscriber has to cope with the problem of medium access control (MAC) which regulates how to share the common medium (channel) among the users. Unlike traditional solutions where subscribers are separated in time, frequency or space state of the art 3rd/4th generation mobile systems differentiate the users based on special individual codes assigned to each customer. Unfortunately performing optimal detection proves to be hard task classically, therefore suitable suboptimal solutions are in the focus of international research. However, quantum computing offers a direct way to the optimal solution because of its parallel processing capabilities.

Hence we introduce a mobile telecommunication oriented application based on Grover search and quantum counting in this chapter following the next steps: Section 5.1 explains the theoretical background of code division multiple access systems, highlights the related detection problem and gives the most trivial answer to it. Optimal detection criteria and their complexity are summarized and classical optimum detectors are discussed in Section 5.2. Finally we trace back the optimal detection to quantum-based solution in Section 5.3.

5.1 DS-CDMA IN PRACTICE

DS-CDMA works very-well, in theory, where signals from different users remain still orthogonal at the receiver. In practice, however, the radio channel proves to be much more hostile. It has deterministic modifications and e.g. random variations in signal strength and delay. Deterministic channel attenuation originates form the fact that mobile terminals are typically in different distances from the base station. We can fight against this effect using power control that is the base station instructs the mobiles to adjust their transmission powers so that all the signals are received with almost the same signal strength at the base station. Since the speed of light and thus that of electromagnetic radiation is constant hence terminal positions with different distances around the base station cause differences in delays as well. This effect is further complicated if one considers that a transmitted signal may travel in different tracks with different lengths at the same time. This latter effect is referred as *multi-path propagation*. Assuming that Alice is transmitting to Bob, who is tying to detect the signal, Bob does not know exactly when he has to start the inner product operation (detection). If he is late or in a hurry then orthogonality may be upset. While orthogonal code families can be produced easily by the reader as well, such code families whose members' are orthogonal to any shifted versions of other members proves to be a really hard task even for experts. The suggested remedy to this problem is the so called Rake receiver which applies the inner product operation with different shifted versions of the corresponding chip sequence at the same time and combines the results.

Remark: We can conclude that orthogonality means the common basis of different medium access schemes. They achieve this property in different ways using frequency bands, time slots, spatial regions or codes. The difference lies in the important fact that the first three approaches have *hard limits* regarding the admitted users in the network that is if we run out e.g. form time slots then no subscriber can be accepted until somebody leaves the system. On the other hand a new user entering in a CDMA system only decreases the orthogonality in the receivers, which produces more errors as a consequence but the number of acceptable users is only asymptotically limited i.e. the more users we have the less transmission rates can be offered. Thus CDMA networks are much more flexible from this point of view, therefore we call them *soft limited* systems.

Random effects, however, are more dangerous. Random attenuation and delay may cause different weighting and shift of the individual signals in the received signal, which is advantageous for certain signal and disadvantageous for others in the detector when inner product operation is performed. In order to describe these phenomena we derive the received signal $r(t)$ at the base station using appropriate mathematical formalism. Clearly speaking we are interested in the baseband signals. Complex baseband-equivalent description allows omitting carriers in price of using complex valued functions instead of real ones e.g. $r_{ekv}(t)$

instead of $r(t)$. From this point we consider complex baseband-equivalent signals and symbols therefore we leave the subscript *eqv*! We suggest to follow the steps of producing $r(t)$ in Fig. 5.1 which depicts the block diagram of the transmitter and the channel.

In this case an uplink DS-DCDMA system is investigated. The i^{th} symbol of the k^{th} $(k = 1, 2, \ldots, K)$ user is denoted by $b_k[i] \in \{+1, -1\}$. This assumption corresponds to the simplest scenario where symbols remain real-valued although we use the complex equivalent description (Binary Phase Shift Keying, BPSK). From our problem point of the level of modulation would not influence the theoretical background of the detection therefore we decided to use BPSK for the sake of simplicity.

In DS-CDMA systems an information bearing bit is encoded by means of a user specific chip code having the length of the processing gain (PG). Let $c_k[q]$ refer to the q^{th} chip of the code word of subscriber k, and we chose again the simplest alphabet $c_k[q] \in \{+1, -1\}$. Since only continuous electromagnetic waveforms can be transmitted in the radio channel in practice hence each chip has to be multiplied with the so called chip elementary waveform denoted by $g_k(t)$. Thus the analogue version of the chip sequence is referred as the user continuous *signature waveform*

$$s_k(t) = \sum_{q=0}^{PG-1} c_k[q] g_k(t - qT_c), \tag{5.1}$$

where T_c stands for the time duration of one chip. Obviously members of $\{s_k(t)\}$ are orthogonal concerning the symbol length T_s i.e.

$$\int_0^{T_s} s_k(t) s_l(t) dt \equiv 0, \forall k \neq l, \tag{5.2}$$

and normalized

$$\int_0^{T_s} \Re^2(s_k(t)) dt + \int_0^{T_s} \Im^2(s_k(t)) dt = 1$$

Thus the output signal of the k^{th} user related to the i^{th} symbol, denoted by $v_k(t)$ is given as

$$v_k(i, t) = b_k[i] s_k(t). \tag{5.3}$$

Practically Alice sends strings of consecutive symbols called bursts. Let us assume that each burst consist of $R+1$ symbols. Therefore we introduce vector $\mathbf{b}_k = [b_k[0], ..., b_k[R]]^T$ denoting the data symbols of the k^{th} user in a certain burst. Thus the k^{th} users's signal during this burst can be expressed as

$$v_k(t) = \sum_{i=0}^{R} b_k[i] s_k(t - iT_s). \tag{5.4}$$

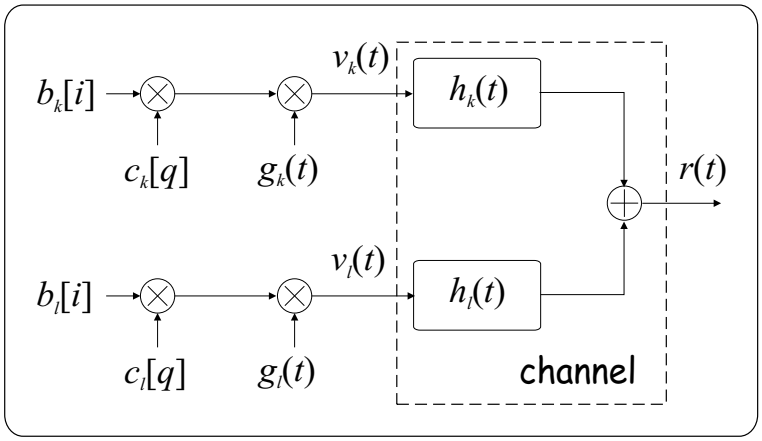

Fig. 5.1 DS-CDMA transmitter and channel

Now, Alice's signal is sent out to the air. We apply here a widely used channel model and remark that of course other, more sophisticated models are also available in the literature (see Chapter 2). However, the selected model contains the most important impacts while does not require us to be lost in details. The channel distortion from the k^{th} user point of view is modelled via an impulse response function as if the channel were a filter

$$h_k(i,t) = a_k[i]\delta(t-\tau_k),$$

where $a_k[i] = A_k[i]e^{j\alpha_k[i]}$ with real $A_k[i]$ and $\alpha_k[i]$. $a_k[i]$ comprises phenomena causing the random nature of the channel and it is called *fading*. $A_k[i]$, $\alpha_k[i]$ and τ_k are typically independent random variables while let us suppose as the worst case that they are uniformly distributed on the following regions:

$$A_k[i] \in [-A, A]; \alpha_k[i] \in [0, 2\pi]; \tau_k \in [0, T_s].$$

Deterministic attenuation is omitted since it can be handled using power control. Similarly we do not consider Gaussian noise because CDMA systems are strongly interference limited one thus Gaussian noise has marginal influence on detection. Finally we assume that τ_k remains constant during each burst while $a_k[i]$ varies from symbol to symbol. The channel not only delays and distorts Alice's transmitted signal but also adds together all the signals originating form other users, hence we are able to describe the received signal at the base station via convolving the channel input with its impulse response in the following manner

$$r(t) = \sum_{k=1}^{K}\sum_{i=0}^{R} h_k(i,t) * v_k(i,t) = \sum_{k=1}^{K}\sum_{i=0}^{R} a_k[i]b_k[i]s_k(t - iT_S - \tau_k). \qquad (5.5)$$

5.2 OPTIMAL MULTI-USER DETECTION

Now, having received $r(t)$ at the base station Bob would like to extract (demodulate) Alice's signal. Let us assume for a short roundabout that $\tau_k = 0$ and $a_k = 1$ deterministically (equivalently the channel is regarded as a shortcut or an identity transformation). In this case the received signal becomes

$$r(i,t) = \sum_{k=1}^{K} b_k[i] s_k(t), \tag{5.6}$$

considering the interval belonging to the i^{th} symbol.

Bob tries to obtain a fairly good estimation $\tilde{b}_k[i]$ exploiting the orthogonality of signature waveforms according to (5.2). This requires multiplication with Alice's waveform $s_k(t)$ and integration on $[0, T_s]$ (see Fig. 5.2). This operation is nothing else than calculation of the inner product for continuous variables. Bearing in mind the often used notion for this operation in the literature we call it *matched filter*. Let us denote the output of the matched filter in case of the i^{th} symbol with $y_k[i]$

$$y_k[i] = \int_0^{T_s} r(i,t) s_k(t) dt = \int_0^{T_s} b_k[i] s_k(t) s_k(t) dt + \int_0^{T_s} \sum_{l=1, l\neq k}^{K} b_l[i] s_l(t) s_k(t) dt = b_k[i]. \tag{5.7}$$

Thus theoretically the output of the matched filter contains information only about $b_k[i]$ and its sign can be used to decide which symbol has been sent by applying a comparator. Therefore Bob can use $y_k[i]$ directly to determine $\tilde{b}_k[i] = \mathrm{sgn}(y_k[i])$.

As we discussed earlier orthogonality may be violated because of the random delays in the channel. In a realistic scenario the above introduced detector may fail with certain probability. Optimal solutions minimizes this probability having in sight available side information. If we insist of using only Alice's signature waveform to detect symbols originating from Alice then this technique is referred as *single-user detection*. This approach can be appropriate when the detector is located in a mobile terminal whose computational power is moderated. However, sitting in a bases station's receiver module we are allowed to be more pragmatic. Since all the signals arriving from different users must be detected all the signature waveforms are available! Why not to exploit this possibility? Thus those schemes which perform combined detection are called *multi-user detectors* (MUD) .

Before explaining how the optimal MUD operates it is worth classifying our scenario. Since different τ_k delays are considered therefore the channel is *asynchronous*. Furthermore $a_k[i]$ is assumed being completely unknown in the receiver hence we have to solve a *non-coherent* detection problem.

In possession of the concept standing behind the single-user DS-CDMA detectors and being familiar with the effects of the radio channel waiting for naive subscribers we are ready to design an optimal detector architecture.

First of all we have to realize that in case of random delays to detect the i^{th} symbol it is not enough to take into account the incoming signal during the corresponding symbol period. Instead we need to consider the whole burst. Therefore we concentrate on vector $\mathbf{b}_k$ representing the data symbols of the k^{th} user's burst under detection.

Next we require to give a suitable definition for optimality. Two extreme answer and many intermediate criteria can be found in the literature. The most popular definition is based on the *maximum likelihood sequence* (MLS) decision principle – often referred as *jointly optimum decision* – while the other end ensures *minimum bit error rate* (MBER) and cited as *individually optimum* decision.

In order to formulate more precisely these two decision techniques and explain the origin of their names let us introduce matrix

$$\mathbf{B} = [\mathbf{b}_1, \mathbf{b}_2, ..., \mathbf{b}_K] \Rightarrow B_{ik} = b_k[i], k = 1, ..., K; i = 0, ..., R. \tag{5.8}$$

Furthermore Bob collects the outputs of the matched filters

$$y_k[i] = \int_{iT_s}^{(i+1)T_s} r(t)s_k(t - iT_s)dt \tag{5.9}$$

into $\mathbf{Y}$ such that

$$\mathbf{Y} = [\mathbf{y}_1, \mathbf{y}_2, ..., \mathbf{y}_K] \Rightarrow Y_{ik} = y_k[i], k = 1, ..., K; i = 0, ..., R. \tag{5.10}$$

In case of an MLS decision we have $2^{K(R+1)}$ different hypotheses according to the different $\mathbf{B}_m$ vectors

$$\begin{aligned} &H_1 : \mathbf{Y} = w(\mathbf{B}_1) \\ &H_2 : \mathbf{Y} = w(\mathbf{B}_2) \\ &\vdots \\ &H_{2^{K(R+1)}} : \mathbf{Y} = w(\mathbf{B}_{2^{K(R+1)}}). \end{aligned} \tag{5.11}$$

where $w(\mathbf{B}_m)$ denotes a matrix-matrix function producing the matrix of the matched filters' outputs provided $\mathbf{B}_m$ contains the symbols sent by all the users during the burst in question related to the m^{th} hypothesis ($m = 1, ..., 2^{K(R+1)}$). The corresponding architecture is depicted in Fig. 5.3. It is independent whether we use MLS or MBER detectors. The difference lies in the decision boxes. Obviously $w(\cdot)$ depends not only on the transmitted symbols but on random channel parameters too. Moreover $w(\cdot)$ is not reversible. Therefore Bob is not able to compute unambiguously that $\mathbf{B}$ which is leading to $\mathbf{Y}$. Instead he invokes decision theory. The optimal decision in MLS sense 'simply' requires to find that hypothesis with maximal conditional probability density function i.e.

$$\tilde{\mathbf{B}}_{MLS} : \max_m f(\mathbf{Y}|\mathbf{B}_m). \tag{5.12}$$

Let us suppose that we quantize the random variables characterizing the radio channel into sufficiently small pieces from the detector point of view. Say N_A, N_α and N_τ represents the number of different values of $A_k[i], \alpha_k[i]$ and τ_k respectively. Furthermore we collect the supposed values of these parameters during the detected burst into the following matrices and vector

$$\mathbf{A} : A_{ik} = A_k[i]; \mathbf{C} : C_{ik} = \alpha_k[i]; \mathbf{d} : d_k = \tau_k.$$

Next we form a single matrix in the following manner

$$\mathbf{Z} = [\mathbf{A}, \mathbf{C}, \mathbf{d}].$$

Bearing in mind that all the random variables are uniformly distributed in order to calculate the conditional density functions in (5.12) one has to count those $\mathbf{Z}$ matrices which lead to $\mathbf{Y}$ i.e.

$$f(\mathbf{Y}|\mathbf{B}_m) = \frac{\#(\mathbf{Z} : \mathbf{Y} = u(\mathbf{B}_m, \mathbf{Z}))}{\#(\mathbf{Z})}, \tag{5.13}$$

where $u(\mathbf{B}_m, \mathbf{Z})$ represents a matrix-matrix function computing the matrix of the matched filters' outputs if $\mathbf{B}_m$ and $\mathbf{Z}$ is assumed.

While an MLS detector tries to estimate all the symbols jointly during a given burst in case of MBER detectors we decide for $\tilde{b}_k[i]$ from symbol to symbol. Thus we have to perform $K(R+1)$ decisions each of which selects one of the following two hypotheses

$$H_1 : y_k[i] = w'(b_k[i] = 1)$$

$$H_2 : y_k[i] = w'(b_k[i] = -1)$$

where function $w'(b_k[i])$ calculates the output of the k^{th} user's matched filter matched filter after the i^{th} symbol interval. This hypothesis testing requires to maximize the following conditional pdfs

$$\tilde{b}_k[i] : \max_{b_k[i]=\pm 1} f(y_k[i]|b_k[i]) \tag{5.14}$$

and $\tilde{\mathbf{B}}_{MBER} = [\tilde{b}_k[i]]$. In order to express conditional pdfs in (5.14) we introduce

$$\mathbf{Z}_{\pm 1} = [\mathbf{B}_{\pm 1}, \mathbf{A}, \mathbf{C}, \mathbf{d}],$$

where matrices $\mathbf{B}_{\pm 1}$ consist of possible values for $b_l[c]$ ($l \neq k$ and $c \neq i$ at the same time) while $b_k[i]$ is set either $+1$ or -1. Since each $b_l[c]$ can be assumed as an independent equiprobable random variable

$$f(y_k[i]|b_k[i] = \pm 1) = \frac{\#(\mathbf{Z}_{\pm 1} : y_k[i] = u'(\mathbf{Z}_{\pm 1}))}{\#(\mathbf{Z}_{\pm 1})}, \tag{5.15}$$

where $u'(\mathbf{Z}_{\pm 1})$ calculates the outcome of the corresponding matched filter.

Unfortunately both MUD techniques are rather time-consuming. In case of MLS approach one needs to test $2^{K(R+1)}$ different hypotheses which grows exponentially with

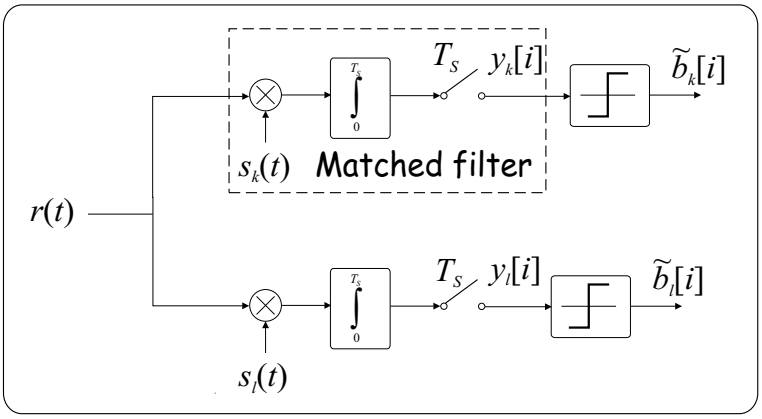

Fig. 5.2 Single-user DS-CDMA detector with matched filter, idealistic case

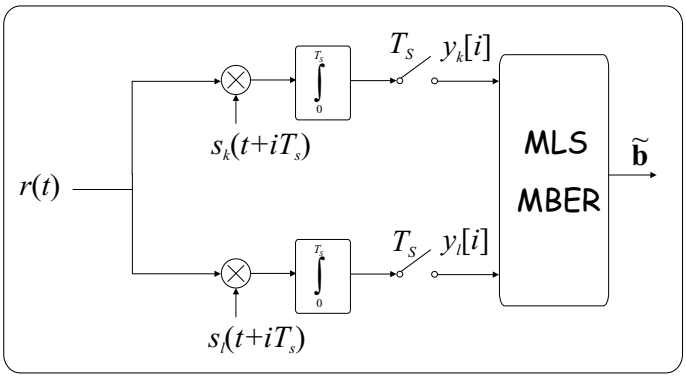

Fig. 5.3 Multi-user DS-CDMA detector

the number of active users. On the other hand MBER detection requires $2K(R+1)$ evaluation of the conditional pdfs. Furthermore the evaluation of the conditional pdfs are rather hard tasks especially in the latter case. Therefore they can not be used in practice and suboptimal approximations are in the focus of research and used in practical applications such as single-user, interference cancelling, decorrelating detectors (see *Further Reading*).

5.3 QUANTUM BASED MULTI-USER DETECTION

Although MLS based optimal multi-user detectors are a bit popular than the MBER based ones because of their less computational complexity as we mentioned before both approaches are far away from practical implementations. However, quantum assisted computing exploiting quantum parallelism may help us to attack the optimum MUD problem directly.

Let us discuss the MBER problem and concentrate on the detection of the $b_k[i]$ symbol. As we deduced in (5.14) Bob needs to evaluate two conditional pdfs. We derived some hints how to perform this in (5.15). Since we are interested only in the larger pdf thus the denominators can be omitted. Both numerators require to solve a special counting problem. Because all the channel parameters and other symbols are independent and uniformly distributed Bob has to decide whether the number of $\mathbf{Z}_{+1}$ or $\mathbf{Z}_{-1}$ leading to $y_k[i]$ is bigger, which is equivalent to the question whether $b_k[i] = +1$ or $b_k[i] = -1$ have the larger probability of being the originator of $y_k[i]$?

We have already discussed the counting problem related to the search in an unstructured database in Section 4.1, where a fairly efficient quantum based solution was proposed exploiting phase estimation on the Grover operator. Concerning our special multi-user detection scenario we have a virtual database encoded into function $u'(\cdot)$ instead of a real one.

In possession of a promising idea and knowledge about quantum counting next we determine the architecture and initialization parameters of the quantum based MUD (QMUD) detector. We apply the top-down design principle thus we depicted the system concept in Fig. 5.5. We define two counting circuits according to the two hypotheses one that assumes $b_k[i] = +1$ and another for $b_k[i] = -1$. Their outputs representing the numerators in (5.15) are denoted by

$$e_{\pm 1} = \#(\mathbf{Z}_{\pm 1} : y_k[i] = u'(\mathbf{Z}_{\pm 1})). \tag{5.16}$$

Each quantum counter is feeded with the outcome $y_k[i]$ of the matched filter, the corresponding hypothesis $b_k[i] = \pm 1$ and the set $S = \{s_k(t)\}$ of individual signature waveforms of all the active users. Next the outputs $e_{\pm 1}$ are compared and the result determines Bob's estimation $\tilde{b}_k[i] = \arg\max_{\pm 1}\{e_{\pm 1}\}$.

Following the top-down concept we have to face the design of the Grover operator. Without harming generality we use the basic Grover box introduced in Section 3.1. First of all it requires an index register input denoted by $|\gamma\rangle$. As Fig. 5.6 presents we form each computational basis state $|x\rangle$ of $|\gamma\rangle$ from consecutive blocks. Each block is responsible for the storage of different parameters. First we use all together $K(R+1)-1$ qbits to represent different $b_l[c]$ symbols $l = 1, ..., K; c = 0, ..., R$, only $b_k[i]$ is omitted because there is an individual input defined for it directly to the Oracle. This is followed by three other blocks consisting of $K(R+1)n_A, K(R+1)n_\alpha$ and Kn_τ qbits and comprising values for $A_k[i], \alpha_k[i]$ and τ_k respectively, where

$$n_A = \lceil \mathrm{ld}(N_A) \rceil; n_\alpha = \lceil \mathrm{ld}(N_\alpha) \rceil N_\alpha; n_\tau = \lceil \mathrm{ld}(N_\tau) \rceil.$$

Therefore Bob requires

$$n = K(R+1)(n_A + n_\alpha + 1) + Kn_\tau - 1$$

qbits to describe a given configuration. Having defined the size of the index register we turn to the Oracle. Originally it calls the database and compares DB[x] with the requested item. Now, we use $u"(b_k[i], x)$ as 'database' which computes the matched filter output as if $b_k[i] = \pm 1$ and x were given to it and the Oracle compares the result with $y_k[i]$ in the following way

$$f(x) = \begin{cases} 1 & \text{if } y_k[i] = u"(b_k[i], x)\,, \\ 0 & \text{otherwise.} \end{cases} \tag{5.17}$$

As the last design step we remember that phase estimation and thus quantum counting includes quantum uncertainty, which can be controlled by means of additional qbits in the upper section of the phase estimator according to (4.2). Considering the worst case scenario i.e. (4.2), this means in our case

$$n^{\clubsuit} = n + \underbrace{\left\lceil \mathrm{ld}(2\pi) + \mathrm{ld}\left(3 + \frac{1}{\breve{P}_\varepsilon}\right) \right\rceil}_{p},$$

where $\breve{P}_\varepsilon$ stands for the maximum allowed quantum uncertainty. Taking a look at Fig. 5.4 the reader can conclude that a fairly good quantum uncertainty from air interface point of view say less than 10^{-8} can be achieved by using about 25 extra qbits which is negligible to n.

Finally the computational complexity of the QMUD algorithm inherited from quantum counting, namely we need $O(n^3)$ elementary gates, where 2^n represents the size of the database [82].

Remark: The above explained method can be trivially extended to that case when we use multi-level symbols instead of binary ones. If M-level symbols are applied than Bob need to run M quantum counter parallel or sequentially.

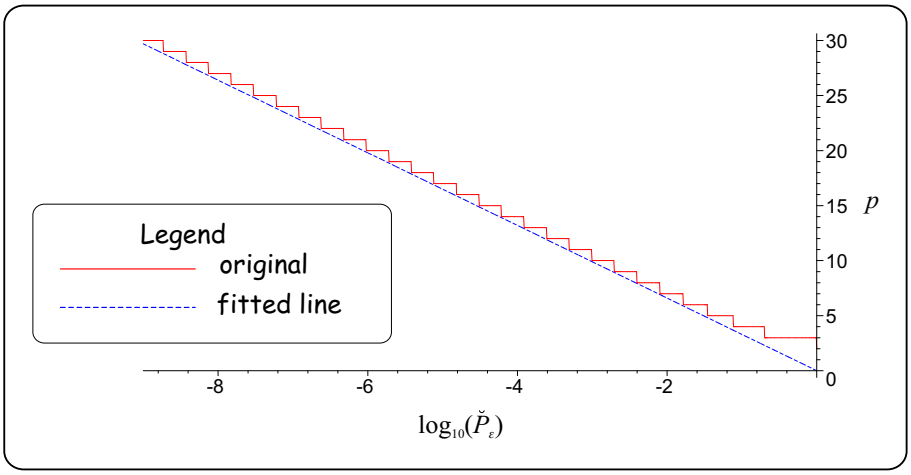

Fig. 5.4 Quantum error probability $\log_{10}(\breve{P}_{\varepsilon})$ vs. number of required additional qbits p

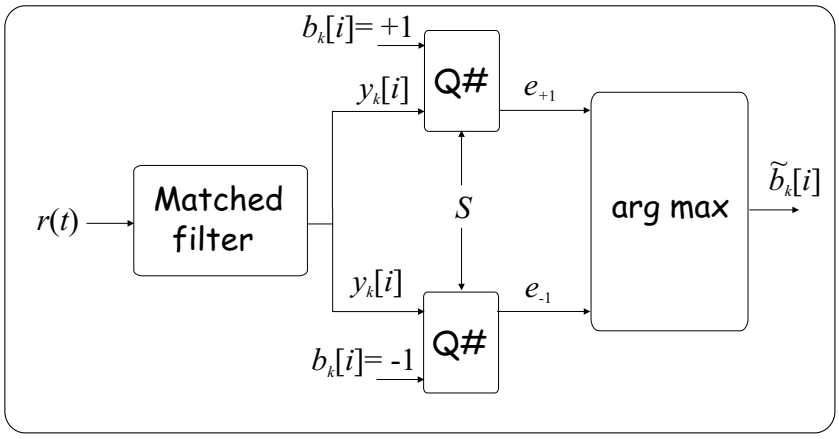

Fig. 5.5 System concept of quantum counting based multi-user DS-CDMA detector

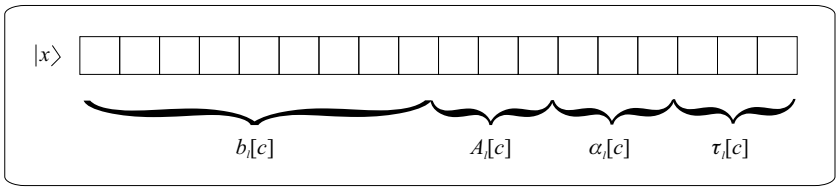

Fig. 5.6 The structure of the index register

Part II

CAC in Spread Spectrum Systems

6

Introduction to Call Admission Control in CDMA Systems

Before starting to design new efficient CAC algorithms for wireless systems first we should take a sort walk around the problem. The first iteration of rephrasing CAC to become mobile leads to the following definition: A new call can be accepted from air interface point of view only if the system is able to put enough radio resources at the users' disposal. Such resources can be e.g. time slots, frequency sub channels, signal to noise ratio (SNR) or signal to interference ratio (SIR), etc. However, if we would like to catch the essence of CAC we have to concentrate on SNR/SIR because successful detection of a radio signal symbol depends basically on receiving enough signal energy during a given period of time while the received interference/noise energy remains under a well defined limit. Therefore all the resources can be traced back to SNR/SIR. Furthermore definition of CAC in wireless environment can be recomposed as follows: A new call can be accepted only if the SNR/SIR values influenced by the new call enables signal detection at all the receivers with declared QoS levels (e.g. BER, Bit Error Ratio). Here should be emphasized that unlike wired networks where the reliable transmission medium (e.g. optical fiber) has almost negligible impact on delay and routers/switches are responsible for introducing delay variations, in case of air interfaces fading often causes retransmission of packets. Hence radio link delay properties mainly depend on SNR/SIR, too. Mobile telecommunication systems can be categorized according to the operational environment, more precisely whether they are working in a licensed or unlicensed (e.g. ISM) band. Cellular Public Land Mobile Networks (PLMNs) such as GSM, IS95, UMTS belong to the former group while Wireless LANs (WLANs) or Bluetooth form the latter set [31]. Operation of systems in unlicensed band is mainly influenced by noise, where we refer to noise as signals from other systems and equipment (e.g. WLAN cards share the common ISM band with microwave ovens' "signals") and of course Gaussian noise of the Nature counted here as well. Licensed band PLMNs, however, suffer mainly from

interference caused by other subscribers of the same system. Several efficient interference suppression techniques were applied from the beginning of radio telecommunications such as controlling the access of users to the channel in FDMA or TDMA manner. In this way only reduced amount of so called neighboring channel interference remains to overcome. Some common channel interference may appear in cellular networks but applying cell clustering (constructing frequency plans) it can be easily eliminated. Frequency and time domain multiplexing not only offer a simple way to reduce interference but furthermore they provide very trivial CAC. For example in case of GSM [66] available band is divided into carriers with 200 KHz spacing and each carrier consists of eight timeslots (i.e. traffic or control channel). Hence the decision about the acceptance of an arriving call means to check whether an unused timeslot is available or not. The advent of CDMA (Code Division Multiple Access) [92] combined spread spectrum technology in public networks (WLANs, IS95, 3G systems) turned upside down the situation. CDMA subscribers use the same frequency band and the same time frame for transmission but apply different codes, therefore CDMA based air interfaces are mainly influenced by interference caused by other users from the same network instead of Gaussian noise. Theoretically code orthogonality supports the separation of different users' signals, which can not be maintained perfectly in multipath environment. This fact causes relevant differences between first/second and the third/fourth generation mobile system's CAC policies. FDMA and TDMA based networks have hard limit (e.g. number of time slots and carriers) for the number of users operating on the air interface at the same time. In 3G/4G WCDMA systems [18], however, there is no hard limit for the number of simultaneously admitted subscribers because their number is determined by the signal to interference ratio. Therefore, a soft margin can be applied by the CAC which is limited only by the Quality of Service contracts, i.e. more users cause more interference that causes degraded QoS (BER) for each user. This type of CAC decision proves to be a computationally rather complex problem in 3G/4G systems because checking of available unused slots (channels) is replaced by estimation of SIR values. This is the price we shall pay for the increased spectral efficiency and flexible limit for the number of admitted users. Unfortunately CAC is inconsistent with computationally complex algorithms since incoming users have to be handled as soon as possible. On the other hand decreasing complexity results in inaccurate CAC decisions i.e. in unutilized system resources. Therefore, the main goal is to create sophisticated and efficient call admission control methods that are able to adapt dynamically to an ever-changing (mobility and fading) environment while providing suitable trade-off between decision efficiency and complexity. The variation between the CAC algorithms lies in the criteria with which a new call should be admitted:

The number-based CAC randomly chooses the new calls based on the current and maximum number of users that the system can tolerate per service, i.e fixed cost per service

is assumed [93, 98, 51]. Number-based CAC results in simple decisions but its efficiency is strongly limited, therefore another successful approach emerged.

The MAI-based/SIR-based CAC predicts the co-channel interference that would be caused by the new connection to the same and other cells. Various approaches can be found in the literature. Two simple SIR-based solutions were proposed first by Liu and El Zarki [101]. Later out-of-cell interference was approximated by means of Gaussian distribution [17]. SIR-based CAC algorithms also appear in [50] predicting the additional inter-cell interference the new call will produce. Ying et. al. used different threshold values in two-layer hierarchical cell structure in [94]. Geijer-Lundin and his colleagues proposed the so-called noise rise estimate methods [34, 30]. Real-time SIR measurement offers another way to ensure QoS [23]. A two-round dynamic CAC and optimization algorithm was discussed in [33]. Mobility-based CAC algorithm for arbitrary call-arrival rates was proposed in [72]. SIR-based CAC in compliance with radio network planning was investigated in [58]. In [98], interference-level-based CAC and number-of-users-based CAC are compared.

The dropping of a handover call is generally considered more serious than blocking of a new call. Therefore, various handoff priority-based CAC schemes have been proposed; they can be classified into two broad categories.

1. Guard Channel (GC) Schemes: Some channels are reserved for handoff calls. There are four different schemes.

    - The cutoff priority scheme is to reserve a portion of channel for handoff calls; whenever a channel is released, it is returned to the common poll of channels [22, 95].
    - The fractional guard channel schemes is to admit a new call with certain probability (which depends on the number of busy channels). This scheme was first proposed by Ramjee et al. [73] and shown to be more general than the cutoff priority scheme.
    - The rigid division-based CAC scheme divides all channels allocated to a cell into two groups: one for the common use for all calls and the other for handoff calls only [64].
    - Finally we can limit the number of new calls admitted to the network as Fang proposed in [96].

2. Queueing Priority (QP) Schemes: In this scheme, calls are accepted whenever there are free channels. When all channels are busy, new calls are queued while handoff calls are blocked [47], new calls are blocked while handoff calls are queued [29, 16], or all arriving calls are queued with certain rearrangements in the queue [12, 90].

Soft handover in CDMA systems enables parallel communications to several base stations in order to improve the efficiency (delay, packet loss) of cell change. Therefore, soft handover and CAC have to be combined [7]. Ma and co-authors considered a stochastic model for an admission controller in CDMA cellular networks that prioritizes soft handover calls using soft guard channels [99].

7

CAC Model for CDMA Networks

A sophisticated model of CDMA-based cellular networks from CAC point of view is introduced in this section. We consider here uplink scenario i.e. CAC provides QoS for reception at base stations, however, later in Section 11 the model is extended for the downlink as well.

According to [54, 97], individual mobile terminals (we assume here one service for one terminal, but the model can be trivially extended for multi-service terminals) are grouped into traffic classes. Each user i belonging to the jth class is characterized by its transmission rate $X_{ij} \geq 0$ measured in [bps] and described with pdf $f_{X_{ij}}(x)$. Because each subscriber from a given class has the same traffic characteristics therefore index i is omitted if we do not want (if it is not required) to distinguish individual users of a certain class. In these cases X_j and $f_{X_j}(x)$are used respectively.

Remark: Generally in case of any variable having indices *ij* is written only with index j means that it represents one variable from class j and this variable is the same for all terminals in the given class.

7.1 BASIC MODEL FOR CAC DECISION

QoS provisioning requires CAC decision at each call/service arrival whether the outage probability that for each call/service i from class j the actual BER exceeds a certain limit (*maxBER*$_{ij}$), remains smaller than the contracted QoS parameter i.e.

$$P\left(BER_{ij} > maxBER_{ij}\right) < e^{-\gamma} for \forall i, j. \tag{7.1}$$

In order to connect physical system resources to BER requirements CAC is often traced back to SIR/SNR [25, 17, 24, 50]. Since BER can be expressed as $BER = g(SIR)$ where g(.) is typically strictly non-decreasing function of its argument and differs according to

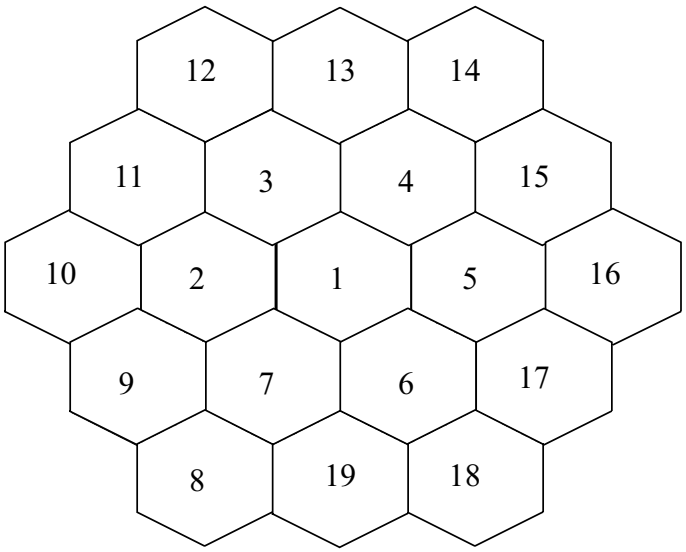

Fig. 7.1 System model with reference and neighboring cells

the applied modulation/spreading scheme e.g. DS-CDMA, OFDM, MC-CDMA, etc. [74]. Therefore CAC rule can be reformulated in the following way

$$P\left(g(SIR_{ij}) > maxBER_{ij}\right) = P\left(SIR_{ij} < minSIR_{ij}\right) < e^{-\gamma} for\, \forall i,j \qquad (7.2)$$

where

$$minSIR_{ij} = g^{-1}(maxBER_{ij}).$$

7.2 INVOLVING CELLULAR STRUCTURE INTO CAC

SIR values at a certain base station strongly depend on positions of interfering terminals, hence from CAC point of view an appropriate cell structure is presented in Fig.7.1. We assume that the new call arrives in the cell positioned in the middle (Cell 1). The newly entering terminal will cause interference in all the cells located in its interference region. Those cells are forming the *interference region* of a terminal which the terminal interference effect can not be ignored in. For the sake of simplicity we use the traditional two-ring model, where the first and second neighboring cell rings are taken into account, see Fig. 7.1. However, for the proposed CAC method, an arbitrary set of cells in the interference region can be defined as an input. Base stations (cells) in the interference region are identified by sequence number $k^{\#}$ ($k^{\#}$=1...K). In case of two-ring model K=1+6+12=19. Cell 2-7 belong to the first neighboring ring while the second ring consists of cell 8-19. Therefore, cell 2-19 form the interference region for a mobile located in Cell 1.

Let us moreover define the set of those base stations, located around a given base station $k^{\#}$, whose terminals' interference regions contain cell $k^{\#}$ i.e. transmitted signals from these cells cause interference at the base station in question. This set is called *CAC region* of base station $k^{\#}$ and its cells are referred by means of cell IDs k=1..$K_{k^{\#}}$. Moreover it contains cell $k^{\#}$ too.

So *interference region* and *CAC region* typically cover the same area but the former one represents the same notion from interference source point of view while the latter one constitute the drain of interference.

Now we can give the first SIR-based coarse definition of CAC: In case of a new call request CAC shall be performed for each $k^{\#}$ and during each CAC decision $K_{k^{\#}}$ cells shall be taken into account for SIR calculation. (In case of basic two-ring model $K = K_{k^{\#}} = 19$). A given CAC decision is called *positive* if at base station $k^{\#}$in question for each terminal i from class j located in cell $k^{\#}$ (i.e. i=1.. $N_{jk^{\#}}$, where $N_{jk^{\#}}$ refers to the number of users from class j in cell $k^{\#}$) communicating with base station $k^{\#}$ the following inequality holds

$$P\left(SIR_{ijk^{\#}} \geq minSIR_{ijk^{\#}})\right) < e^{-\gamma} for \forall i, j, k^{\#}, \tag{7.3}$$

where $SIR_{ijk^{\#}}$ denotes the received SIR at base station $k^{\#}$ from terminal i of class j located in cell $k^{\#}$.

The new call can only be admitted if all the CAC decisions ($k^{\#}$=1...K) are positive.

7.3 GENERALIZATION OF EVANS&EVERITT'S CAC MODEL

In order to derive a practical definition of CAC problem an accurate mathematical description of CAC has to be derived based on the previous definition's model.

We start from the basic idea of Evans and Everitt [54], which proposes to express SIR by means of target power levels. However, in order to overcome the shortcomings and inaccuracy of that model, we introduce

- generalized traffic model instead simple ON/OFF model,
- generalized channel model instead of simple deterministic two-way propagation model,
- thermal noise and interference from other systems instead of omitting them,

These enhancements require calculating SIR at base stations using mobile terminals' transmission power P_{ijk}, where i identifies the call (terminal), j denotes the traffic class the call belongs to and k is the cell ID where the mobile is located respectively.

The radio channel effect on transmitted signal power P_{ijk} from a terminal i of class j in cell k is represented at the receiver of base station $k^{\#}$ by means of path gain $V_{ijkk^{\#}}$ which

is typically modelled by means of a random variable whose pdf originates from different propagation models (Rayleigh, Rice, lognormal, Nakagami, etc.) [19]

$$V_{ijkk^{\#}} = \frac{p_{ijkk^{\#}}}{P_{ijk}}, \tag{7.4}$$

where $p_{ijkk^{\#}}$ represents the received (target) power level at base station $k^{\#}$form terminal i of class j located in cell k.

Transmit power levels and gain values allow us to introduce a more detailed calculation of $SIR_{ijk^{\#}}$

$$SIR_{ijk^{\#}} = \frac{P_{ijk^{\#}} V_{ijk^{\#}k^{\#}}}{\underbrace{\sum_{h=1}^{J}\sum_{l=1}^{N_{hk^{\#}}} P_{lhk^{\#}} V_{lhk^{\#}k^{\#}}}_{\text{own cell interference}} + \underbrace{\sum_{\substack{k=1 \\ k\neq k^{\#}}}^{K_{k^{\#}}}\sum_{h=1}^{J}\sum_{l=1}^{N_{hk}} P_{lhk} V_{lhkk^{\#}}}_{\text{other cell interference}} + \underbrace{(N_0 + I_{OS})\, B}_{\substack{\text{thermal noise and} \\ \text{other system interference}}}}, \tag{7.5}$$

where the numerator denotes the received power of the wanted signal at the base station's receiver, the first term of the denominator represents the interference originating from the cell we perform CAC for (*own cell interference*), furthermore second term refers to interference coming from other cells of CAC region and finally N_0 and I_{OS} stand for the one-sided spectral density of the thermal noise and interference from other systems respectively. B [Hz] defines the bandwidth of the system.

One may put the question why not to combine the first and second interference terms as it was done in [54]. We can give two answers to this question a practical and a theoretical one. From practice point of view unlike own cell interferer other cell interference typically modelled with a single random variable representing all the interference sources [26], which could simplify the evaluation of CAC inequality.

In this paper we do not exploit this idea because of its introduced inaccuracy. Instead we distinguish each interference source. The reason why we decided to separate the two interference terms comes from theoretical considerations, which will be explained later in this subsection.

Having defined more precisely one of the two important parameters of inequality (7.3) now we concentrate on minimum SIR requirement.

Required minimum signal to interference density ratio for proper detection of $X_{ijk^{\#}}$ [bps] bits during each second at the base station receiver ($k^{\#}$) for a j type user i is defined as

$$SIDR_{ijk^{\#}} = \left(\frac{E_b}{I_0}\right)_j X_{ijk^{\#}}, \left[\frac{\text{J / bit}}{\frac{\text{J / s}}{\text{Hz}}}\frac{\text{bit}}{\text{s}}\right] = [\text{Hz}]\,. \tag{7.6}$$

where E_b [J/bit] refers to the bit energy and I_0 [W/Hz] is the power-density of all the interference effects i.e. I_0 equals to the denominator of (7.5) divided by the system bandwidth B. Therefore $minSIR_{ijk^{\#}}$ can be expressed as

$$minSIR_{ijk^{\#}} = \frac{SIDR_{ijk^{\#}}}{B} = \left(\frac{E_b}{I_0}\right)_j \frac{X_{ijk^{\#}}}{B}. \tag{7.7}$$

Now in possession of both CAC decision parameters we can substitute them into (7.3) to get a much deeper insight into the heart of CAC in CDMA systems: if the following set of inequalities holds for the outage probability

$$P\left(\frac{P_{ijk^{\#}}V_{ijk^{\#}k^{\#}}}{\underbrace{\sum_{h=1}^{J}\sum_{l=1}^{N_{hk^{\#}}} P_{lhk^{\#}}V_{lhk^{\#}k^{\#}}}_{\text{own cell interference}} + \underbrace{\sum_{\substack{k=1\\k\neq k^{\#}}}^{K_{k^{\#}}}\sum_{h=1}^{J}\sum_{l=1}^{N_{hk}} P_{lhk}V_{lhkk^{\#}}}_{\text{other cell interference}} + \underbrace{(N_0 + I_{OS})\,B}_{\substack{\text{thermal noise and}\\ \text{other system interference}}}} < \frac{SIDR_{ijk^{\#}}}{B}\right) < e^{-\gamma}$$
$$for\ \forall i, j, k^{\#} \tag{7.8}$$

then QoS contracts can be provided for all the terminals in the network.

Assuming perfect power control transmission power values in (7.8) loose their independence, furthermore they become random variables depending on user's traffic behavior and channel gain, therefore evaluation of inequality (7.8) seems to be rather complex. However, by means of practical considerations it can be rewritten in a more useful manner.

If we assume that received power level at the base station for a given user is directly proportional to the required minimum signal to interference density ratio

$$p_{ijk^{\#}k^{\#}} = P_{ijk^{\#}}V_{ijk^{\#}k^{\#}} = \lambda \cdot SIDR_{ijk^{\#}}, \tag{7.9}$$

where λ has dimension of [W/Hz] then the left hand side of (7.8) is upper bounded. This statement can be proven easily generalizing results in [54, 55]. Of course constraint (7.9) is valid only for terminals communicating with the own base station ($k^{\#}$), because other terminals adjust their power according to their target base stations. Exploiting this fact P_{lhk} values of other cell interference term in (7.8) can be expressed by means of target power levels and gain factors as

$$P_{lhk} = \frac{p_{lhkk}}{V_{lhkk}} = \frac{\lambda \cdot SIDR_{lhk}}{V_{lhkk}}. \tag{7.10}$$

Applying these considerations in (7.8)

$$P\left(\frac{\lambda \cdot SIDR_{ijk^{\#}}}{\underbrace{\sum_{h=1}^{J}\sum_{l=1}^{N_{hk^{\#}}} \lambda \cdot SIDR_{lhk^{\#}}}_{\text{own cell interference}} + \underbrace{\sum_{\substack{k=1 \\ k \neq k^{\#}}}^{K_{k^{\#}}} \sum_{h=1}^{J}\sum_{l=1}^{N_{hk}} \lambda \cdot SIDR_{lhk} \frac{V_{lhkk^{\#}}}{V_{lhkk}}}_{\text{other cell interference}} + \underbrace{(N_0 + I_{OS})\, B}_{\substack{\text{thermal noise and} \\ \text{other system interference}}}} < \frac{SIDR_{ijk^{\#}}}{B}) \right) < e^{-\gamma} \tag{7.11}$$

$$for\ \forall i, j, k^{\#}$$

Now we can explain why the own cell and other cell interference terms are not allowed to join theoretically. If we did so, factor $\frac{V_{lhkk^{\#}}}{V_{lhkk^{\#}}}$ would appear in own cell interference term. In [54] this fact did not cause any problem since gain factors were assumed to be deterministic, therefore $\frac{V_{lhkk^{\#}}}{V_{lhkk^{\#}}} = 1$ eliminates the differences. In our generalized case, however, gain factors in the numerator and denominator of the other cell interference term are considered independent random variables; hence their quotient typically differs from 1.

Having made several simple algebraic steps in (7.11) CAC inequality reaches its almost final form (only statistical behavior of radio channel will be involved later into the model)

$$P\left(B\left(1 - \underbrace{\frac{N_0 + I_{OS}}{\lambda}}_{\substack{\text{thermal noise and} \\ \text{other system interference}}} \right) < \underbrace{\sum_{h=1}^{J}\sum_{l=1}^{N_{hk^{\#}}} SIDR_{lhk^{\#}}}_{\text{own cell interference}} + \underbrace{\sum_{\substack{k=1 \\ k \neq k^{\#}}}^{K_{k^{\#}}} \sum_{h=1}^{J}\sum_{l=1}^{N_{hk}} SIDR_{lhk} \frac{V_{lhkk^{\#}}}{V_{lhkk}}}_{\text{other cell interference}} \right) < e^{-\gamma} \tag{7.12}$$

$$for\ \forall i, j, k^{\#}$$

Inequality (7.12) in its form gives clear representation of CAC problem. B stands for the capacity of the system in Hz that is decreased because of the thermal noise and other system interference, which renders the proper detection more difficult. On the right hand side, randomly changing capacity requirements of individual users are summarized. If the total amount of required resources exceeds the capacity of the system then outage occurs. CAC is responsible for providing guarantee that this outage probability remains smaller than the agreed QoS parameter.

One may wonder why index j disappeared from inequality (7.12)? To answer this question we have to emphasize that i is counted from 1 up to $N_{jk^{\#}}$, hence j remains present in the future too.

7.4 INVOLVING RADIO CHANNEL MODEL INTO CAC

As we mentioned earlier in this section the effect of radio channel on transmitted signal power from terminal i from class j of cell k is represented at the receiver of base station $k^{\#}$ by means of power gain $V_{ijkk^{\#}}$ which in our case consists of the well-known two-way propagation model extended with multiplicative fading Y. Gain of deterministic two-way model can be defined [31] as

$$A(d_{kk^{\#}}) = \left(\frac{h_T \cdot h_R}{d_{kk^{\#}}^2}\right)^2, \tag{7.13}$$

where h_T is the height of the transmitter antenna, h_R stands for the height of the receiving base station's antenna (i.e. uplink scenario) and $d_{kk^{\#}}$ denotes the averaged distance between them. Because of the always changing position of mobile terminals practically only averaged distances can be taken into account with the same $d_{kk^{\#}}$ value for all the terminals located in the same cell k, i.e. $V_{ijkk^{\#}}$ does not depend on i and j. Hence notation $V_{ijkk^{\#}}$ is replaced by $V_{kk^{\#}}$.

This simple model becomes more realistic if we introduce multiplication factor Y^2 representing the channel's stochastic behavior (so called fading) and characterized by pdf $f_Y(y)$ of its amplitude gain

$$f_Y(y) \begin{cases} \geq 0 & if\ y > 0 \\ 0 & if\ y \leq 0 \end{cases}.$$

Therefore, overall channel gain is given by

$$V_{kk^{\#}} = A(d_{kk^{\#}})Y^2, Y > 0. \tag{7.14}$$

Without loss of generality we show how to handle the two-ring cell architecture from gain point of view.

Let us assume that the interference is investigated (CAC is performed) at the base station of the cell $k^{\#}$ (which is located in the middle in Fig.7.1 and called reference cell). The interference originates from mobile terminals located in the reference and neighboring cells (own and other cell interferences). Because of the regular structure three different types of cells have to be taken into account depending on the distances from the reference base station.

A *first type cell* is the reference cell ($k = 1$ in Fig.7.1). *Second type cells* are the directly neighboring cells of the reference cell ($k = 2..7$ in Fig.7.1) and *third type cells* are located in the second cell ring around the reference cell ($k = 8..19$ in Fig.7.1). Interference from any other cells is not considered because the distance dependency of the path gain makes the interference effect of those cells negligible.

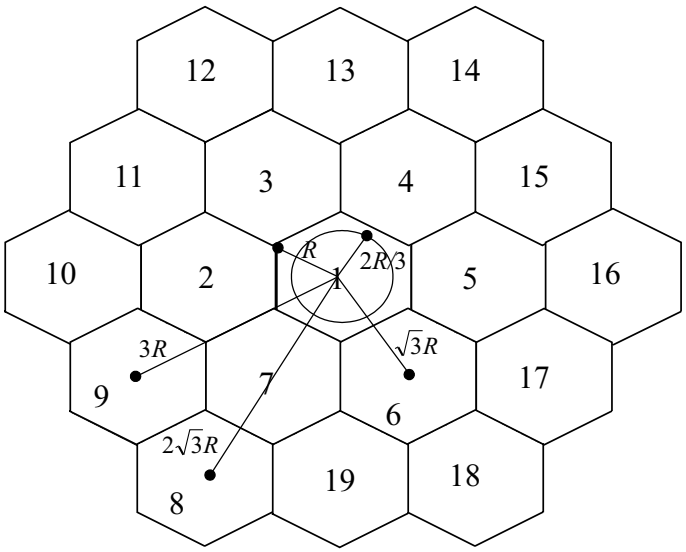

Fig. 7.2 Average distances for different cell types

Exact $d_{kk\#}$ values can be derived in the following manner (see Fig. 7.2). Assuming uniformly distributed terminals in the cell and approximating hexagon with circle having cell radius R, the probability that a mobile is in the range $[r, r + dr)$ is

$$P\left(r \leq x < r + dr\right) = \frac{1}{R^2\pi}(2r\pi\, dr) = \frac{2r}{R^2}dr, \tag{7.15}$$

from which one obtains

$$d_{k\#k\#} = \int_0^R r \cdot \frac{2r}{R^2}dr = \frac{2}{R^2}\int_0^R r^2 dr = \frac{2}{R^2}\left[\frac{r^3}{3}\right]_0^R = \frac{2}{3}R. \tag{7.16}$$

For the second and third type cells distances are calculated, as if the mobiles were concentrated at the middle of the cells. Hence, for second type cells $d_{kk\#} = \sqrt{3}R$ and for the third type cells we have two distances according to Fig. 7.2 $d_{kk\#} = 3R$ and $d_{kk\#} = 2\sqrt{3}R$.

Of course being in possession of user distribution (the system can provide such information based on measurement) accuracy of this simple approach can be increased very easily.

8

Call Admission Control in General

A sophisticated model of WCDMA system from call admission point of view has been introduced in the previous chapter. Before introducing the new solution of the CAC problem general background of CAC is discussed in Section 8.1 and an appropriate reference method is explained in Section 8.2.

8.1 ABSTRACT FORMULATION OF CAC PROBLEM

In order to give an abstract description of call admission procedures we introduce the following scenario. Virtual sources are grouped into classes. Every source i in a certain class j is characterized by a random variable Q_{ij} according to its resource demand (e.g. bandwidth). The random variable is given with its pdf $f_{Q_{ij}}(q) = f_{Q_j}(q)$ i.e. sources from the same class have the same statistical behavior. The number of active sources in the jth class is denoted by N_j. Therefore the state of the system can be described in every moment by means of a state vector

$$\mathbf{N} = (N_1, N_2, \ldots, N_J) \tag{8.1}$$

in a J dimensional state space, where J refers to the number of virtual classes.

Now, the call admission procedure means that it should be decided whether a new call can be accepted without violating the QoS parameter guaranteed for other users or not. This CAC problem can be approached in a geometric way. All the state vectors can be divided into two subspaces. Vectors which can be accepted without violating the QoS contracts belong to the first (or acceptable) set and states that must be rejected to the second (or rejected) one

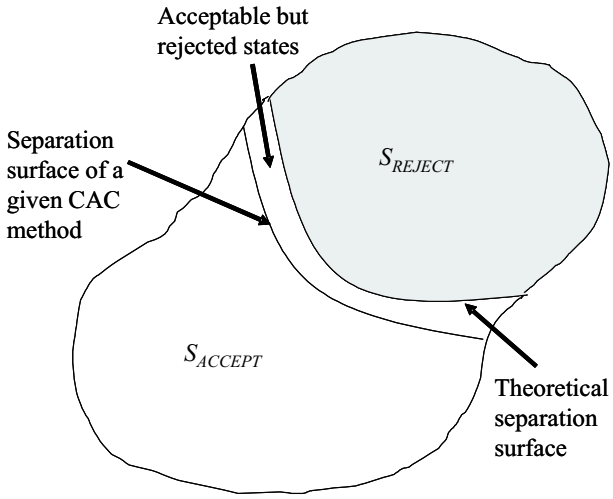

Fig. 8.1 Geometric interpretation of CAC

$$S_{ACCEPT} \triangleq \{\mathbf{N} : P\left(Q > B^*\right) < e^{-\gamma}\},$$
$$S_{REJECT} \triangleq \{\mathbf{N} : P\left(Q > B^*\right) \geq e^{-\gamma}\}, \tag{8.2}$$

where $Q \geq 0$ refers to the random variable representing the overall capacity demand of the sources

$$Q = \sum_{j=1}^{J} \sum_{i=1}^{N_j} Q_{ij}, \tag{8.3}$$

and B^* denotes the capacity of the system and γ stands for the QoS parameter.

Therefore, the task of CAC can be regarded as a space separation problem (see Fig. 8.1.) i.e. how to determine the surface separating the two regions and how to decide whether the new state vector is located on the acceptable or rejected side of the separation surface.

Unfortunately the CAC decision cannot be carried out directly on the basis of the theoretical surface. On one hand because of the high computational complexity of convolution required to determine the overall resource requirement of the sources, calculation of exact separation surface seems to be quiet hard task. On the other hand the typically large number of the states in the theoretical surface needs enormous large storage capacity. Therefore suboptimal solutions are required in form of CAC algorithms.

Different CAC methods can compete in the property of being as close to the theoretical separation surface as they can. The tighter the CAC surface the smaller is the region in Fig. 8.1. representing the theoretically acceptable but by the given CAC algorithm rejected states.

Moreover there exists a strict condition that has to be fulfilled: in order to provide QoS guarantee any approximation separation surface of any CAC methods should remain within the acceptable subspace. This is the reason why e.g. Gaussian approximation of the sum of random variables representing individual capacity demands can not be used.

8.2 EFFECTIVE BANDWIDTH BASED CAC

In order to find less complex but near to optimal solutions for

$$P\left(Q > B^*\right) = P\left(\sum_{j=1}^{J}\sum_{i=1}^{N_j} Q_{ij} > B^*\right) \leq e^{-\gamma} \tag{8.4}$$

several methods were introduced. One of the most promising classes of algorithms among them is based on Effective Bandwidth concept which was originally introduced for wired networking CAC [59, 6, 11, 41, 100, 85].

Inequality (8.4) represents the well-known tail distribution estimation problem that requires the convolution of large number of random variables. Because the calculation of convolution is rather time consuming task so the theoretical amount of required capacity is approximated by deterministic values.

In case of effective bandwidth methods sources are grouped into classes and a deterministic so called effective bandwidth value is assigned to each type of source which is somewhere between the mean and the peak demand. Then the actual value of the overall resource requirement is estimated by means of multiplying the number of the sources in different classes with the corresponding effective bandwidth values and summing up these terms for all the classes. Of course effective bandwidth values depend on the QoS parameters and on the stochastic behavior of the sources as well.

This effective bandwidth technique was adapted to wireless environment by Evans and Everitt [54, 55, 83, 84, 76, 86].

Using effective bandwidth concept (8.3) is replaced by the following simple inequality

$$P\left(\sum_{j=1}^{J} \kappa_j N_j > B^*\right) \leq e^{-\gamma}, \tag{8.5}$$

where κ_j refers to the effective bandwidth value of the jth class. Different ideas were introduced in the literature to find appropriate effective bandwidth values [6, 11, 41]. In order to determine κ_j in WCDMA environment two solutions were proposed in [54].

The first one is to use Gaussian approximation to estimate the density function of the overall traffic. However, this approximation is not able to guarantee the validity of inequality (8.4), therefore this solution should be rejected.

The other much promising way to calculate the effective bandwidth values is application of the Chernoff bound, which always upper bounds the tail distribution.

Remark: If random variables representing individual capacity requirements are bounded by say H_j then until $\sum_{j=1}^{J} N_j \cdot H_j \geq B^*$ evaluation of inequality (8.4) can be traced back to a simple summation of individual H_j values instead of calculating convolution. This constrain for bounded sources is typically fulfilled in wired systems where randomness of individual capacity requirement depends only on traffic characteristics (number of emitted packets within a given time interval) which is obviously limited. In case of wireless systems, however, this is not so evident because many effects beside traffic parameters influence the stochastic behavior of individual capacity requirement (e.g. channel gain).

8.2.1 Problems with Effective bandwidth based CAC

The main indisputable advantage of effective bandwidth based CAC methods lies in the fact that once effective bandwidth values are known they are very fast during CAC decisions because the applied fairly simple mathematical operations (floating point multiplications and additions).

Unfortunately one has to pay high prices for this benefit:

1. Calculation of effective bandwidth values is computationally very complex task. Therefore it must be performed in advance.

2. Effective bandwidth based CAC is in certain cases rather inaccurate. In order to highlight the reason of this property let us turn back to geometrical interpretation of CAC. Any effective bandwidth based solution approximates the theoretical separation hypersurface with a (linear) hyperplane (e.g. in two dimensions it estimates a curve with a line), which is far from the optimal solution (see Fig. 8.2.). Of course this is why it enables fast CAC decisions. Therefore CAC accuracy can be increased using CAC algorithms implementing nonlinear separation surfaces. From another viewpoint inaccuracy of effective bandwidth methods lies in the fact that they do not exploit statistical behavior of the sources. Although they avoid convolution of source distributions and reduce decision time in this way, but on the other hand they enable loose approximation of required resources.

3. The most important drawback of effective bandwidth methods in wireless environment follows from first reason. Namely the large computational complexity makes impossible the dynamic adaptation to the changes of system parameters. These are system capacity and individual resource requirements. The former one is more or less fixed in mobile networks but the latter ones are definitely NOT. Unlike e.g. wired ATM where individual demand can be characterized by means of a random variable

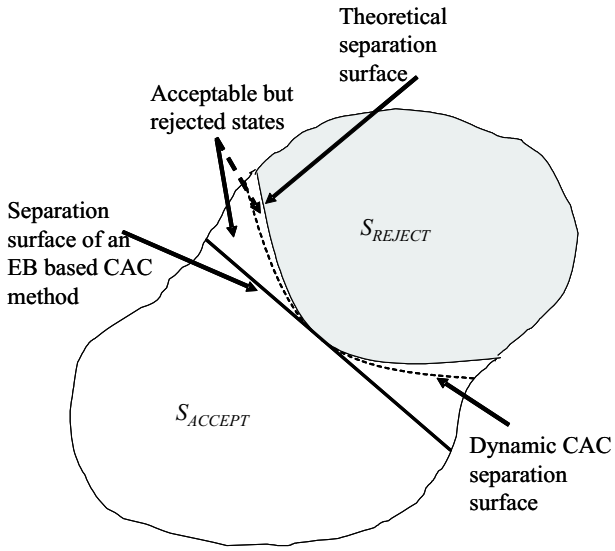

Fig. 8.2 Effective bandwidth based and dynamic separation surfaces

representing user' traffic, in case of wireless this random variable contains target minimum signal to interference density ratio requirement, channel model, averaged distances and the user traffic. So each time when we introduce a new service or the averaged distances change (e.g. during a soccer match we have different average distance then before or after) or the applied channel parameters change (e.g. because of weather conditions) the static CAC has to perform a quiet complex optimization task in order to determine the new effective bandwidth values. So in a continuously changing wireless environment static effective bandwidth based CAC would fail because its philosophy. The name of the game is the same as it was in case of 802.11 WLAN security. They borrowed a popular cryptographic solution from wired world under the name WEP (Wired Equivalent Privacy) which performs quiet well in the original static systems but dramatically fails in wireless scenarios. The reason is trivial and clear: because of the continuously and dynamically changing wireless environment ciphering keys are very often changed, which results in repeated keys within short intervals. Monitoring encrypted messages with the same key plain texts can be eavesdropped.

9

Dynamic Call Admission Control

One straightforward solution of tail estimation problem depicted in (8.4) is based on the so called Chernoff bound which originates from Markov inequality utilizing the strictly increasing nature of ln(·). We know from Galleger [42] that:

Let $Q \geq 0$ be a random variable which has expected value m_Q. For all $B^* > 0$ and $s > 0$ real numbers the following Chernoff inequality holds:

$$P\left(Q > B^*\right) < e^{\ln\left(\mathbb{E}(e^{s\cdot Q})\right) - s\cdot B^*} \tag{9.1}$$

If we *can* guarantee that

$$e^{\ln\left(\mathbb{E}(e^{s\cdot Q})\right) - s\cdot B^*} < e^{-\gamma}, \tag{9.2}$$

then CAC inequality (8.4) is also fulfilled. The main advantage of the Chernoff bound lies in the optimization parameter s that allows comparing the minimum of the left hand side of (9.2) to the QoS parameter, i.e. finding the tightest upper bound for the tail.

Taking the natural logarithm of both sides of (9.2) we get

$$\ln\left(\mathbb{E}(e^{s\cdot Q})\right) - s\cdot B^* < -\gamma. \tag{9.3}$$

Restructuring inequality (9.3)

$$\ln\left(\mathbb{E}(e^{s\cdot Q})\right) - s\cdot B^* + \gamma < 0, \tag{9.4}$$

where on the left-hand side we have the so called logarithmic moment generator function (LMGF) of $e^{s\cdot Q}$ random variable

$$M_Q(s) \triangleq \ln\left(\mathbb{E}(e^{s\cdot Q})\right). \tag{9.5}$$

Hence we derived an alternative of CAC inequality (18)

$$\Psi(s) = M_Q(s) - s \cdot B^* + \gamma < 0. \tag{9.6}$$

In order to apply (9.6) in practice one has to solve the following vital problems:

1. Problem 1: The logarithmic moment generating function of the overall demand should be traced back to LMGFs of individual sources because we have information only about individual sources (Q_{ij}).

2. Problem 2: Unfortunately (9.2) does not provide any hint how to determine the optimum value for s denoted by s^* from now on. Hence suitable method should be found to seek s^*: $\min_s \Psi(s) = \Psi(s = s^*)$.

9.1 CALCULATION OF LOGARITHMIC MOMENT GENERATING FUNCTION OF THE AGGREGATED TRAFFIC

We utilize the practical assumption that individual sources Q_{ij} are independent. So definition (9.5) can be transformed into the following form

$$\begin{aligned} M_Q(s) &= \ln\left(\mathbb{E}(e^{s\cdot Q})\right) = \ln\left(\prod_{j=1}^{J}\mathbb{E}\left(e^{s\cdot\sum_{j=1}^{J}\sum_{i=1}^{N_j}Q_{ij}}\right)\right) \\ &= \sum_{j=1}^{J}\sum_{i=1}^{N_j}\ln\left(\mathbb{E}(e^{s\cdot Q_{ij}})\right) = \sum_{j=1}^{J}\sum_{i=1}^{N_j}M_{Q_{ij}}(s). \end{aligned} \tag{9.7}$$

Since resource demands in a given class is modelled with the same pdf, hence LMGFs within the same class do not differ that is $M_{Q_j}(s) = M_{Q_{ij}}(s)$, therefore

$$M_Q(s) = \sum_{j=1}^{J} N_j M_{Q_j}(s), \tag{9.8}$$

which results in the simple addition of individual LMGFs! Now let us draw the consequences:

- Convolution has been converted to addition, therefore individual LMGFs can be used as effective bandwidth values.

- In order to solve Problem 1. one has to derive the individual LMGFs from descriptors (e.g. pdfs) of individual sources. We are going to accomplish this task for WCDMA environment later in Chapter 10.

9.2 EFFICIENT METHOD TO DETERMINE THE OPTIMAL VALUE OF THE CHERNOFF PARAMETER

One proposed brute force method to find s^* in WCDMA scenarios has been introduced in [54], but this solution mainly based on wired equivalents [59, 6, 11]. The common idea behind all this type of algorithms can be summarized in the following way: recalling the geometrical interpretation of CAC they try to find out the hyperplane with the largest subspace of accepted states. In possession of that hyperplane's normal vector corresponding s^* can be calculated.

The most serious shortcomings of this approach are on one hand the required large computational power and therefore its static nature and on the other hand an optimal linear separation surface belongs to each system state and the selected one represents only a trade off for them instead of being optimal for all the states.

In order to improve accuracy and introducing resilience in CAC we present how to calculate s^* in real time at each CAC decision. This allows fast adaptation to changing system parameters and determines always the optimal separation surface for all the systems states instead of making compromise among them!

9.2.1 On the Properties of s^*

The next theorem emphasizes an important property of s^* (see proof in Section 17.1).

Theorem 9.1. *Let Q≥0 be a random variable with expected value m_Q . If $B^* > m_Q$ and s>0 then there exist one and only one s^* for which $\min_s \Psi(s) = \Psi(s = s^*)$ and $s^* \in (0, \infty]$.*

Unfortunately s^* can not be expressed directly from $\frac{d\Psi(s=0)}{ds} = 0$ since the integration and (8.3).

In order to find a suitable algorithm that is able to find s^* we exploit the shape of the first derivative. Since it is strictly monotonous, therefore intersection of first derivative and axis s can be found using a logarithmic search algorithm on a properly chosen interval $[s_{min}, s_{max}]$.

9.2.2 Upper and Lover Bounds of the Logarithmic Search region

The efficiency of logarithmic search algorithm (how many iteration steps are required to find s^* with a predefined error) mainly depends on the appropriate selection of the boundaries of the search interval. One obvious setup comes from Theorem 9.1

$$[s_{\min} = 0, s_{\max} = +\infty].$$

Of course this approach would fail in practice. Therefore the next theorem provides a much narrower region for potential s^*.

Theorem 9.2. *Let $Q_{ij} \geq 0$ be random variables with expected values $m_{Q_{ij}}$ and $Q = \sum_{j=1}^{J} \sum_{i=1}^{N_j} Q_{ij}$. Let t denote the system time measured in number of call events (call arrival or call termination). If event t is a new call arrival then $s^*(t) < s^*(t-1)$ and in case of event t refers to a finished call then $s^*(t) > s^*(t-1)$.*

Exploiting the results in Theorem 9.2 we can define the following rule to choose appropriate bounds of the logarithmic search region. When a new call is entering it is reasonable to set $s_{min}(t) = s_{min}(t-1)$ and $s_{max}(t) = s^*(t-1)$, or in case of a finished call $s_{min}(t) = s^*(t-1)$ and $s_{max}(t) = s_{\max}(t-1)$.

9.2.3 Main Steps of the Logarithmic Search Algorithm

Let us assume that the CAC is currently processing the tth call event.

1. Using the final results of the previous subsection we set up the bounds of the search region [$s_{min}(t,u$=0), $s_{max}(t,u$=0)] where index $u$refers to the actual logarithmic search iteration step.
2. Interval $[s_{min}(t,u), s_{max}(t,u)]$ has to be mediated: $s_{med}(t,u) = s_{min}(t,u) + \frac{s_{max}(t,u) - s_{min}(t,u)}{2}$.
3. One has to calculate $\frac{d\Psi(s=s_{med}(t,u))}{ds}$ and $\Omega(s = s_{med}(t,u))$ where $\Omega(s) = e^{\Psi(s)}$.
4. If $|\Omega(s = s_{med}(t,u)) - \Omega(s = s_{med}(t,u-1))| \leq \frac{d}{e^{\gamma}}$ then $s_{med}(t,u)$ approximates s^* satisfactorily and the algorithm stops. d refers to the halting criterion.
5. If $\frac{d\Psi(s=s_{med}(t,u))}{ds} > 0$, then s^* is smaller than $s_{med}(t,u)$ because $\frac{d\Psi(s)}{ds}$ is strictly monotonously increasing function of s, hence we set $s_{min}(t,u+1) = s_{min}(t,u)$ and $s_{max}(t,u) = s_{med}(t,u)$. Go to 2!
6. If $\frac{d\Psi(s=s_{med}(t,u))}{ds} < 0$, then s^* is greater than $s_{med}(t,i)$, therefore we set $s_{min}(t,u+1) = s_{med}(t,u)$ and $s_{max}(t,u+1) = s_{max}(t,u)$. Go to 2!

Remark1: Halting criterion d at Step 4 determines both the accuracy of estimation of s^* and thus the accuracy of our outage probability estimation, since $\Omega(s)e^{\gamma}$ represents the Chernoff upper bound of outage probability, see (9.1) and (17.1). The criterion applied at Step 4 is appropriate since the second derivative of $\Omega(s)$ is always positive, hence it has no inflexion points i.e. the right hand side of the inequality proves to be monotonously decreasing in u. The more precise estimation of resource demand is requested the more

accurate estimation of s^* is needed and the large will be the number of required iteration steps.

Remark2: Because $\Omega(s)$ and therefore $\Psi(s)$ has minimum place at s^* hence any error in $s^*(d \neq 0)$ will not cause underestimation of required resource to provide contracted QoS.

Remark3: Conditions in Step 5 and 6 do not contain investigation on equality. The reason comes from Step 4 where the algorithm stops if equality happens.

Only one but very important question remained open with a serious contradiction. In possession of $s_{min}(t)$ and $s_{max}(t)$ we are able to calculate $s^*(t)$ or having $s^*(t)$ one can determine the searching region of the next search but these parameters are not independent. In order to break out from this vicious circle one should propose suitable initial values for $s_{min}(t=1)$ and $s_{max}(t=1)$ i.e. the searching range for s at the first call arrival.

Obviously $s_{min}(t=1)=0$ is a trivial solution for $\inf\{s_{min}(t)\}$. To find an appropriate upper bound for $s^*(t=1)$ we propose the following simple method

1. $n=0$; $s^*(t=1,n=-1)=0$; $s_{min}(1,n)=0$,
2. $s_{max}(1,n)=2^n$,
3. search for $s^*(1,n)$ using logarithmic search in $[s_{min}(1,0), s_{max}(1,n)]$,
4. if $s^*(1,n) \neq s^*(1,n)$ then $n=n+1$ and go to 2!
   else $s_{min}(1)=2^{n-1}$ and $s_{max}(1)=2^n$.

Another alternative solution to find a suitable s_{max}(1) originates from the Gaussian approximation. Based on the central limit theorem random variable Q in (17.1) can be approximated by means of a Gaussian random variable i.e.

$$f_Q(q)=\frac{1}{\sqrt{2\pi\sigma_Q^2}}e^{-\frac{(q-m_Q)^2}{2\sigma_Q^2}}, \tag{9.9}$$

where mean value m_Q and squared variation σ_Q^2 are the sum of individual mean values and squared variations (i.e. they are known values). Our goal is to find an s such that

$$\frac{d\Omega(s)}{ds}=\int_{-\infty}^{+\infty}(q-B^*)e^{s\cdot(q-B^*)+\gamma}f_Q(q)dq=0. \tag{9.10}$$

Substituting (9.9) into (9.10) one gets

$$\int_{-\infty}^{+\infty}(q-B^*)e^{s\cdot(q-B*)+\gamma}\frac{1}{\sqrt{2\pi\sigma_Q^2}}e^{-\frac{(q-m_Q)^2}{2\sigma_Q^2}}dq=0,$$

which can be simplified to

$$\int_{-\infty}^{+\infty}(q-B^*)e^{s\cdot q}\frac{1}{\sqrt{2\pi\sigma_Q^2}}e^{-\frac{(q-m_Q)^2}{2\sigma_Q^2}}dq=0,$$

simplifying with parameters which are independent from q. Now we combine the *exp* functions in the following way

$$\int_{-\infty}^{+\infty}(q-B^*)\frac{1}{\sqrt{2\pi\sigma_Q^2}}e^{-\frac{q^2-2qm_Q+m_Q^2-sq2\sigma_Q^2}{2\sigma_Q^2}}dq=\int_{-\infty}^{+\infty}(q-B^*)\frac{1}{\sqrt{2\pi\sigma_Q^2}}e^{-\frac{q-2q(m_Q+s\sigma_Q^2)+m_Q^2}{2\sigma_Q^2}}dq=$$
$$\int_{-\infty}^{+\infty}(q-B^*)\frac{1}{\sqrt{2\pi\sigma_Q^2}}e^{-\frac{(q-(m_Q+s\sigma_Q^2))^2}{2\sigma_Q^2}}e^{-\frac{s^2\sigma_Q^4+2m_Qs\sigma_Q^2}{2\sigma_Q^2}}dq=0.$$

Finally omitting the second exp. factor (it does not depend on q) we reach

$$\int_{-\infty}^{+\infty}(q-B^*)\frac{1}{\sqrt{2\pi\sigma_Q^2}}e^{-\frac{(q-(m_Q+s\sigma_Q^2))^2}{2\sigma_Q^2}}dq=0, \tag{9.11}$$

which contains a modified Gauss pdf with shifted mean value. Now, it is known that a Gaussian pdf is symmetric onto its mean value, furthermore $g(q)=q-B^*$ has intersection with the horizontal axis $q=B^*$ and it is point-symmetric onto this intersection point, therefore the integral in (9.11) equals 0 if the sifted mean value is located exactly in $q=B^*$ i.e. $(m_Q+s\sigma_Q^2)=B^*$. This leads to

$$s=\frac{B^*-m_Q}{\sigma_Q^2},$$

which is a suitable guess for $s_{max}(1)$. Of course we used Gaussian approximation, hence this potential $s_{max}(1)$ has to be checked whether $\frac{d\Psi(s=s_{max}(1))}{ds}>0$ if not we have to turn to the previous method but applying the current $s_{max}(1)$.

One may wonder whether the rough estimation of bounds introduces to much delay into CAC. We emphasize in this context that CAC is applied in multi user systems where system capacity is planned to serve large number of subscribers, therefore when the first terminals enter into the system they can be accepted without performing CAC so CAC has enough time to calculate the bounds in the background.

10

Applying Dynamic CAC in WCDMA Environment

In this section the bridge between the general CAC approach and its specific application in WCDMA-based spread spectrum systems is built.

10.1 MAPPING GENERAL CAC PARAMETERS AND WCDMA MODEL

If one compares WCDMA CAC inequality (7.12) and that one (8.4) of general CAC first we can map trivially general system capacity B^* with WCDMA system capacity

$$B^* = B \cdot \left(1 - \frac{N_0 + I_{OS}}{\lambda}\right). \tag{10.1}$$

From individual resource demand point of view we define in WCDMA scenario virtual sources described by random variables $SIDR_{ijk^\#}$ and $Q_{ijkk^\#} = SIDR_{ijk}\frac{V_{ijkk^\#}}{V_{ijkk}}$ [Hz]. So CAC inequality (7.12) can be rewritten in WCDMA environment in the following way

$$P\left(\overbrace{\underbrace{\sum_{h=1}^{J}\sum_{l=1}^{N_{hk^\#}} SIDR_{lhk^\#}}_{\text{own cell interference}} + \underbrace{\sum_{\substack{k=1\\k\neq k^\#}}^{K_{k^\#}}\sum_{h=1}^{J}\sum_{l=1}^{N_{hk}} Q_{lhkk^\#}}_{\text{other cell interference}}}^{Q_{ijk^\#}} > B^*\right) < e^{-\gamma} \quad for\ \forall i,j,k^\# \tag{10.2}$$

It should be highlighted that unlike wired networks where each user traffic type represents one traffic class, in case of wireless systems several virtual classes belong to each traffic type depending on the cell structure and gain factors, which dramatically increases the CAC state space. For example if we have two user classes and we define three types of

cells (in terms of distances, see Fig. 7.1) then all together we will have eight virtual types of sources (according to the four different distances). Therefore efficient suboptimal CAC are essencial.

Taking into consideration that SIDR requirements and gain factors in (7.12) are non-negative and positive random variables respectively, hence Chernoff bound based dynamic CAC explained in Section 9 can be applied for WCDMA based wireless systems, which requires the evaluation of the following inequalities instead of (10.2)

$$\Psi(s) = M_{Q_{jk^{\#}}}(s) - s \cdot B^{*} + \gamma < 0 \quad for\, \forall j, k^{\#}, \tag{10.3}$$

where $M_{Q_{jk^{\#}}}(s)$ denotes LMGF of the aggregate resource demand in case terminals from traffic class j in cell $k^{\#}$ are investigated (note that calls in a given class are not distinguished) during CAC decision. This function can be traced back in compliance with (9.8) and (10.2) to

$$M_{Q_{jk^{\#}}}(s) = N_{jk^{\#}} M_{SIDR_j}(s) + \sum_{\substack{h=1 \\ h \neq j}}^{J} N_{hk^{\#}} M_{SIDR_h}(s) + \sum_{\substack{k=1 \\ k \neq k^{\#}}}^{K_{k^{\#}}} \sum_{h=1}^{J} N_{hk} M_{Q_{hkk^{\#}}}(s), \tag{10.4}$$

where

$$Q_{hkk^{\#}} = \underbrace{SIDR_h}_{\substack{\text{depends only} \\ \text{on user's traffic}}} \cdot \underbrace{\frac{V_{kk^{\#}}}{V_{kk}}}_{\substack{\text{depends only on channel's} \\ \text{behavior}}} = \left(\frac{E_b}{I_0}\right)_h X_h \frac{A(d_{kk^{\#}})Y^2}{A(d_{kk})W^2}. \tag{10.5}$$

The advantages of our proposed dynamic CAC scheme can only be exploited if corresponding individual LMGFs and their first derivatives are known.

10.2 LMGFS OF VIRTUAL SOURCES

As a next step forward we calculate first the LMGFs for generalized case i.e. we assume arbitrary continuous memoryless traffic distributions and generalized multiplicative fading in the radio channel. Next the general result is applied for special practical and in the literature often referred cases such as ON/OFF traffic and faded channel.

Remember that $f_{X_j}(x)$denotes the pdf of a jth class user's traffic and the impact of radio channel on transmitted signal is given by $V_{kk^{\#}} = A(d_{kk^{\#}})Y^2$, where $A(d_{kk^{\#}})$ refers to the distant dependent two-way deterministic path gain and random variable Y stands for the channel's stochastic behavior (so called fading) and characterized by pdf $f_Y(y)$ of its amplitude gain. First, we determine the LMGFs for own cell term of (10.4)

$$M_{SIDR_j}(s) = \ln\left(\int_0^{+\infty} e^{s\cdot q} f_{SIDR_j}(q)dq\right), \tag{10.6}$$

where $f_{SIDR_j}(q)$ is the pdf of $SIDR_j = \left(\frac{E_b}{I_0}\right)_j X_j$.

(10.6) can be calculated easily from pdfs of user traffic using random variable transformation

$$f_{SIDR_j}(q) = f_{X_j}\left(q \cdot \left(\frac{I_0}{E_b}\right)_j\right) \cdot \left(\frac{I_0}{E_b}\right)_j, \tag{10.7}$$

from which one gets

$$M_{SIDR_j}(s) = \ln\left(\left(\frac{I_0}{E_b}\right)_j \cdot \int_0^{+\infty} e^{s\cdot q} \cdot f_{X_j}\left(q \cdot \left(\frac{I_0}{E_b}\right)_j\right)dq\right). \tag{10.8}$$

Now, we turn to solve the much complex problem to derive $M_{Q_{hkk\#}}(s)$. There exist several conditions which guarantee that $M_{Q_{hkk\#}}(s)$ exists. We use the following one: for random variable Q LMGF $M_Q(s)$ always exists if Q is lower and upper bounded. This constrain is trivially fulfilled in case of $SIDR_j$ since user traffic is always in the range of $[0, X_j^{\max}]$.

In case of $Q_{hkk\#}$, however, channel gain $V_{kk\#}$ is typically modelled by a random variable which is continuous on $(0, \infty]$ (i.e. Y and W are e.g. Rayleigh, Rice, etc. distributed), therefore our proposed condition seems to be unusable. This unwanted property of channel models can be avoided if one considers realistic effects which result in a much more precise system model represented by bounded Y' and W', and discussed later in this section in detail.

Firstly let us combine deterministic factors into one single term

$$D_{hkk\#} \triangleq \left(\frac{E_b}{I_0}\right)_h \cdot \frac{A(d_{kk\#})}{A(d_{kk})}, \tag{10.9}$$

which leads to $Q_{hkk\#} = D_{hkk\#} X_h Y^2 \frac{1}{W^2}$, where Y and W have the same pdf representing the channel's stochastic behavior.

Since

$$M_{Q_{hkk\#}}(s) = \ln\left(\int_0^{+\infty} e^{s\cdot q} f_{Q_{hkk\#}}(q)dq\right), \tag{10.10}$$

where $f_{Q_{hkk\#}}(q)$ is the pdf of $Q_{hkk\#}$ we have to define the pdf in question. We deliver it step by step because partial results will be used later in this paper.

Assuming $f_Y(y)$ and $f_W(w)$ are classical channel models i.e. they are continuous on $(0,\infty]$, hence pdfs of variable $T=Y^2$ and $R=1/W^2$ can be derived by simple random variable transformation

$$f_T(t)=\tfrac{1}{2\sqrt{t}}f_Y(\sqrt{t}),$$
$$f_R(r)=\tfrac{r^{-\frac{3}{2}}}{2}f_W\left(\tfrac{1}{\sqrt{r}}\right),$$

respectively.

Taking into account that Y and W are independent random variables hence $f_{T,R}(t,r)=f_T(t)f_R(r)$ so for $L=Y^2/W^2=T\cdot R$ thus

$$\begin{aligned} f_L(l) &= \int_0^{+\infty}\frac{1}{r}\cdot f_R(r)\cdot f_T\left(\frac{l}{r}\right)dr=\int_0^{+\infty}\frac{1}{4r^2\sqrt{l}}\cdot f_W\left(\frac{1}{\sqrt{r}}\right)\cdot f_Y\left(\sqrt{\frac{l}{r}}\right)dr \\ &= \int_0^{+\infty}\frac{1}{4\sqrt{l}}f_W(\sqrt{r})f_Y\left(\sqrt{lr}\right)dr, \end{aligned}$$

where we applied replacement $r=\frac{1}{r}$ in the last step.

Now we turn back to consider realistic effects. First we enhance the modelling of Y. Since the received power can not exceed the transmitted one, therefore in accordance with (7.14)

$$1\geq\frac{p_{lhkk\#}}{P_{lhk}}=V_{lhkk\#}=A(d_{kk\#})Y^2,$$

from which one gets

$$T_{kk\#}^{\max}=\max\{Y^2\}=\frac{1}{A(d_{kk\#})}$$

and pdf of $T'=(Y')^2$ is

$$f_{T'}(t)=\delta(0)\cdot\int_{T_{kk\#}^{\max}}^{+\infty}f_T(u)du+\vartheta(T_{kk\#}^{\max})\cdot f_T(t),$$

where $\delta(.)$ and $\vartheta(.)$ refer to the Dirac and modified Heaviside (step) functions as well (see Definitions in Section 15).

Next, idealistic (in terms of infinite transmission power) power control is replaced by a much realistic one. The illustrative explanation of this problem leads us to (7.10), where we simply applied the reciprocal $\frac{1}{V_{lhkk}}$ of the channel gain to calculate transmission power P_{lhk}. In typical cases the gain V_{lhkk} may have very small or zero value, which implies infinite emitted power. Of course this can not be fulfilled in practice. Therefore we

introduce the maximum output power $P_h^{\max}$ for terminals in class h. (Traffic classes and power capabilities can be independent for a given terminal. In that case maximum output power has to be indexed both by l and h.)

So emitted power of a given terminal can be bounded by

$$P_h^{\max} \geq \frac{p_{lhkk}}{V_{lhkk}} = \frac{\lambda \cdot SIDR_h}{A(d_{kk})} \frac{1}{W^2} = \frac{\lambda}{A(d_{kk})} \cdot \left(\frac{E_b}{I_0}\right)_h X_h R,$$

from which

$$R \leq \frac{P_h^{\max} A(d_{kk})}{\lambda \cdot (X_h = x)} \left(\frac{I_0}{E_b}\right)_h = R_{hk}^{\max}(x)$$

and pdf of $R' = \frac{1}{(W')^2}$

$$f_{R'}(r\,|x) = \delta(0) \cdot \int_{R_{hk}^{\max}(x)}^{+\infty} f_R(u)du + \vartheta(R_{hk}^{\max}(x)) \cdot f_R(r),$$

where the first term corresponds the fact that in case of the terminal should transmit – because bad channel conditions – with higher power than $P_h^{\max}$ then it reduces its power to zero in order to decrease uselessly emitted interference. Further steps to deliver $f_{Q_{hkk\#}}(q)$ can be found in Section 17.2, the final result is the following

$$f_{Q_{hkk\#}}(q) = \delta(q) \left(1 - \int_0^{Q_{hkk\#}^{\max}} G_{hkk\#}(q)dq\right) + G_{hkk\#}(q). \tag{10.11}$$

Substituting (10.11) into (10.10) one reached the final formula of LMGF of other cell interference

$$M_{Q_{hkk\#}}(s) = \ln\left(\int_0^{Q_{hkk\#}^{\max}} e^{s\cdot q}\left(\delta(q)\left(1 - \int_0^{Q_{hkk\#}^{\max}} G_{hkk\#}(q)dq\right) + G_{hkk\#}(q)\right)dq\right) =$$
$$\ln\left(\int_0^{Q_{hkk\#}^{\max}} e^{s\cdot q}\delta(q)dq - \int_0^{Q_{hkk\#}^{\max}} e^{s\cdot q}\delta(q)\int_0^{Q_{hkk\#}^{\max}} G_{hkk\#}(a)dadq + \int_0^{Q_{hkk\#}^{\max}} e^{s\cdot q}G_{hkk\#}(q)dq\right) =$$
$$\ln\left(1 - \int_0^{Q_{hkk\#}^{\max}} G_{hkk\#}(a)da + \int_0^{Q_{hkk\#}^{\max}} e^{s\cdot q}G_{hkk\#}(q)dq\right). \tag{10.12}$$

Moreover, in order to perform dynamic CAC decisions first derivatives $\frac{d\Psi(s)}{ds}$ are needed when logarithmic search is running. Fortunately $\frac{d\Psi(s)}{ds}$ can be traced back to the first derivatives of the individual LMGFs. From (10.10) and (17.14) we have

$$\frac{dM_{SIDR_j}(s)}{ds} = \frac{\mathbb{E}(SIDR_j e^{s\cdot SIDR_j})}{\mathbb{E}(e^{s\cdot SIDR_j})} = \frac{\int_0^{+\infty} qe^{sq} f_{SIDR_j}(q)dq}{\int_0^{+\infty} e^{sq} f_{SIDR_j}(q)dq}$$
$$= \frac{\int_0^{+\infty} q\cdot e^{s\cdot q}\cdot f_{X_j}\left(q\cdot\left(\frac{I_0}{E_b}\right)_j\right)dq}{\int_0^{+\infty} e^{s\cdot q}\cdot f_{X_j}\left(q\cdot\left(\frac{I_0}{E_b}\right)_j\right)dq}. \quad (10.13)$$

Furthermore from (10.11) and (10.10) we get

$$\frac{dM_{Q_{hkk^\#}}(s)}{ds} = \frac{\mathbb{E}(Q_{hkk^\#} e^{s\cdot Q_{jkk^\#}})}{\mathbb{E}(e^{s\cdot Q_{hkk^\#}})} = \frac{\int_0^{+\infty} qe^{sq} f_{Q_{hkk^\#}}(q)dq}{\int_0^{+\infty} e^{sq} f_{Q_{hkk^\#}}(q)dq}$$
$$= \frac{\int_0^{Q^{\max}_{hkk^\#}} qe^{s\cdot q} G_{hkk^\#}(q)dq}{1-\int_0^{Q^{\max}_{hkk^\#}} G_{hkk^\#}(a)da+\int_0^{Q^{\max}_{hkk^\#}} e^{s\cdot q} G_{hkk^\#}(q)dq}. \quad (10.14)$$

Now we have all the required functions in our hand to perform CAC decisions in a code division based spread spectrum network.

10.3 MAIN STEPS OF CAC IN WIRELESS NETWORKS

In this section we summarize the main steps of a CAC decision combining the previous results. Let us assume, that a new call is arriving in cell k*. CAC has to be performed in all the cells with ID $k^\#$ ($k^\#$=1...K, including k*) within its interference region i.e. a CAC decision at a new call entering consists of K partial decision for cells where the new call causes interference or from which the target base station of the new call receives interference. The call can only be accepted if all the partial decisions are positive (call is acceptable).

A partial decision for cell $k^\#$ contains J individual CAC decisions one for each traffic class. Each of them requires the following procedure. First the subnetwork state matrix is updated for CAC region (comprising cells from where interference arrives, k=1..$K_{k^\#}$) of $k^\#$

$$\mathbf{N}^{k\#}_{J\times K_{k\#}} = \begin{bmatrix} N_{11} & N_{12} & \dots & N_{1K_{k\#}} \\ N_{21} & N_{22} & \dots & N_{2K_{k\#}} \\ \vdots & \vdots & N_{jk} & \vdots \\ N_{J1} & N_{J2} & \dots & N_{JK_{k\#}} \end{bmatrix}, \tag{10.15}$$

where J refers to the ID of traffic classes and N_{jk} stands for the number of users from class j in cell k.

Now in order to decide whether $\mathbf{N}^{k\#}_{J\times K_{k\#}}$ is feasible or not we launch a logarithmic search in compliance with Subsection 9.2.3. Having found s^* we substitute it into (10.4) then if inequality (10.3) holds $\mathbf{N}^{k\#}_{J\times K_{k\#}}$ is acceptable.

Remark1: All together $J\cdot K$ CAC decisions shall be performed before a new call enters or after a call has leaved the network (clearly speaking the latter case does not require a complete CAC decision but only updating the optimization bounds for s^*). However, decisions are independent from one another, therefore parallel computations are possible.

Remark2: The reader may be surprised that only a small part of the whole cellular network is involved into the CAC decision. One would expect that a new call rearranges the whole network as the terminals adjust their transmission power to the new scenario starting from the cell of the entering terminal and spreading around in a similar way the waves do when a pebble has fallen into the water. This effect would complicate CAC decisions. Fortunately CAC inequality (7.12) clearly highlights the fact that only terminals from those cells influence CAC decision in a given cell that lie in its CAC region. Moreover, those CAC regions require CAC decision in which one of the N_{jk} values has been changed either because of entering a new call or leaving one.

10.4 LMGFS IN PRACTICAL CASES

In possession of the theoretical background of Chernoff bound based CAC for WCDMA environment we calculate required LMGFs and their first derivatives for practical wireless scenarios.

10.4.1 Lognormal Fading with General Traffic

Let us consider lognormally distributed fading i.e. the path loss is defined as [31]

$$Lp(d_{kk\#})^{dB} = Ls(d_0)^{dB} + 10n\lg\left(\frac{d_{kk\#}}{d_0}\right) + C^{dB}, \tag{10.16}$$

where d_0 stands for the reference distance, $Ls(d_0)^{dB}$ refers to the free space path loss in dB, n denotes the path loss exponent and finally C is a Gaussian random variable with zero mean $m_C = 0$ and deviation σ_C i.e.

$$f_C(c) = \frac{1}{\sqrt{2\pi}\sigma_C} e^{-\frac{y^2}{2\sigma_C^2}}. \tag{10.17}$$

$M_{SIDR_j}(s)$ is not affected by channel characteristics, hence we concentrate on $M_{Q_{hkk\#}}(s)$ and its derivative. In order to perform this calculation, however, one has to derive the pdf of path gain according to (7.14) and (10.16).

First we transform the path loss to gain and replace dB by ratio

$$\sqrt{V_{kk\#}} = 10^{\frac{-Lp(d_{kk\#})^{dB}}{10}} = \frac{1}{Ls(d_0)} \cdot \left(\frac{d_0}{d_{kk\#}}\right) \cdot 10^{\frac{-C}{10}},$$

where the first two terms are estimated by $\sqrt{A(d_{kk\#})}$ (since $A(d_{kk\#})$ is also a constant, this approximation does not influence the introduced CAC technique). Therefore pdf of $Y = 10^{\frac{-C}{10}}$ can be expressed as

$$f_Y(y) = \begin{cases} \frac{10}{\sqrt{2\pi}\sigma_C \ln(10)} \frac{1}{y} e^{-\ln^2(y)\frac{100}{2\sigma_C^2 \ln^2(10)}} & if\ y > 0 \\ 0 & if\ y \leq 0 \end{cases}. \tag{10.18}$$

In order to calculate the corresponding LMGF and its first derivative $G_{hkk\#}(q)$ has to be determined

$$G_{hkk\#}(q) = \vartheta(q - Q^{\max}_{hkk\#}) \int_0^{+\infty} \frac{D_C}{\sqrt{\pi}} \frac{1}{q} e^{-\ln^2\left(\frac{q}{xD_{hkk\#}}\right) D_C^2} f_{X_h}(x)dx, \tag{10.19}$$

where $D_C$refers to the constant

$$D_C = \frac{5}{2\sigma_C \ln(10)}. \tag{10.20}$$

10.4.2 ON/OFF Traffic with Generalized Channel Model

When the user traffic is modelled with worst case ON/OFF sources the corresponding pdf is

$$f_{X_j}(x) = a_j\delta(0) + b_j\delta(H_j), \tag{10.21}$$

where H_j denotes the maximum transmission rate for the jth class user and a_j and b_j refers to the probability of remaining silent or transmitting with H_j respectively. For example assuming speech traffic characterized by Voice Activity Factor (VAF_j)

$$m_{X_j} = H_j \cdot VAF_j, \tag{10.22}$$

$$a_j = 1 - \frac{m_{X_j}}{H_j} = 1 - VAF_j;\;\; b_j = \frac{m_{X_j}}{H_j} = VAF_j. \tag{10.23}$$

Pdf of $SIDR_j$ is expressed considering that $\delta\left(\frac{q}{A} - 0\right) = A \cdot \delta(q)$

$$f_{SIDR_j}(q) = \frac{f_{X_j}\left(q \Big/ \left(\frac{E_b}{I_0}\right)_j\right)}{\left(\frac{E_b}{I_0}\right)_j} = a_j\delta(0) + b_j\delta\left(q - H_j \cdot \left(\frac{E_b}{I_0}\right)_j\right). \tag{10.24}$$

Now we derive $M_{SIDR_j}(s)$ using (10.24)

$$\begin{aligned} M_{SIDR_j}(s) &= \ln\left(\int_0^{+\infty} e^{s\cdot q} a_j\delta(0)dq + \int_0^{+\infty} e^{s\cdot q} b_j\delta\left(q - H_j \cdot \left(\frac{E_b}{I_0}\right)_j\right)dq\right) \\ &= ln\left(a_j + b_j \exp\left(s \cdot H_j \cdot \left(\frac{E_b}{I_0}\right)_j\right)\right). \end{aligned} \tag{10.25}$$

Applying (10.24) $\frac{dM_{SIDR_j}(s)}{ds}$ is calculated considering (10.13)

$$\frac{dM_{SIDR_j}(s)}{ds} = \frac{b_j H_j \cdot \left(\frac{E_b}{I_0}\right)_j \cdot \exp\left(sH_j \cdot \left(\frac{E_b}{I_0}\right)_j\right)}{a_j + b_j \exp\left(sH_j \cdot \left(\frac{E_b}{I_0}\right)_j\right)} = \frac{m_{X_j} \cdot \left(\frac{E_b}{I_0}\right)_j \cdot \exp\left(s \cdot H_j \cdot \left(\frac{E_b}{I_0}\right)_j\right)}{a_j + b_j \exp\left(s \cdot H_j \cdot \left(\frac{E_b}{I_0}\right)_j\right)}. \tag{10.26}$$

Calculation of LMGF of other cell interference is based on (10.12) and (10.14) which requires

$$G_{hkk\#}(q) = \vartheta(q - Q^{\max}_{hkk\#}) \frac{b_h}{4\sqrt{qD_{hkk\#}H_h}} \int_0^{+\infty} f_Y\left(\sqrt{r}\right) \cdot f_Y\left(\sqrt{\frac{qr}{D_{hkk\#}H_h}}\right) dr. \tag{10.27}$$

10.4.3 ON/OFF Traffic with Lognormal Fading Channel

In this subsection we combine the results of the previous subsections in order to achieve LMGFs in a given practical case.

Assuming ON/OFF traffic classes in accordance with (10.21) and wireless channel suffering lognormal fading defined by (10.18) the considered LMGFs and their first derivatives are the following.

$M_{SIDR_j}(s)$and $\frac{dM_{SIDR_j}(s)}{ds}$ have already been calculated, see (10.25) and (10.26). However, $M_{Q_{hkk\#}}(s)$ and $\frac{dM_{Q_{hkk\#}}(s)}{ds}$ require more effort to determine. We start from (10.19)

$$
\begin{aligned}
G_{hkk\#}(q) &= \vartheta(q-Q^{\max}_{hkk\#})\int\limits_0^{+\infty}\frac{D_C}{\sqrt{\pi}}\frac{1}{q}e^{-\ln^2\left(\frac{q}{xD_{hkk\#}}\right)D_C^2}a_h\delta(x-0)dx \\
&+ \vartheta(q-Q^{\max}_{hkk\#})\int\limits_0^{+\infty}\frac{D_C}{\sqrt{\pi}}\frac{1}{q}e^{-\ln^2\left(\frac{q}{xD_{hkk\#}}\right)D_C^2}b_h\delta(x-H_h)dx \\
&= \vartheta(q-Q^{\max}_{hkk\#})\frac{b_hD_C}{\sqrt{\pi}}\frac{1}{q}e^{-\ln^2\left(\frac{q}{H_hD_{hkk\#}}\right)D_C^2}. \qquad (10.28)
\end{aligned}
$$

(10.28) allows us to calculate

$$
1-\int\limits_0^{Q^{\max}_{hkk\#}}G_{hkk\#}(q)dq = 1-\int\limits_0^{Q^{\max}_{hkk\#}}\frac{b_hD_C}{\sqrt{\pi}}\frac{1}{q}e^{-\ln^2\left(\frac{q}{H_hD_{hkk\#}}\right)D_C^2}dq =
$$

$$
= 1-\frac{b_h}{2}\left(1+\text{erf}\left(\ln\left(\frac{P_h^{\max}}{\lambda H_hD_{hkk\#}}\right)\right)\right) = \frac{1}{2}+\frac{a_h}{2}-\frac{b_h}{2}\text{erf}\left(\ln\left(\frac{P_h^{\max}}{\lambda H_hD_{hkk\#}}\right)\right). \qquad (10.29)
$$

It is worth emphasizing the following approximation

$$
\int\limits_0^{Q^{\max}_{hkk\#}}qe^{s\cdot q}G_{hkk\#}(q)dq \approx \sum_{g=0}^{\Gamma}\frac{s^gb_he^{\frac{(g+1)(g+1+4D_C^2\ln(H_hD_{hkk\#}))}{D_C^2}}}{2g!}\text{erfc}\left(\frac{2D_C^2\ln\left(\frac{H_hD_{hkk\#}\lambda}{P_h^{\max}}\right)+g+1}{2D_C}\right), \qquad (10.30)
$$

where for typical system parameters $\Gamma \approx 10$ enables quiet accurate estimation of the above integral. Using results of (10.30) it is easy to derive

$$
\int\limits_0^{Q^{\max}_{hkk\#}}e^{s\cdot q}G_{hkk\#}(q)dq \approx \sum_{g=0}^{\Gamma}\frac{s^gb_he^{\frac{g(g+4D_C^2\ln(H_hD_{hkk\#}))}{D_C^2}}}{2g!}\text{erfc}\left(\frac{2D_C^2\ln\left(\frac{H_hD_{hkk\#}\lambda}{P_h^{\max}}\right)+g}{2D_C}\right). \qquad (10.31)
$$

Substituting (10.29), (10.30) and (10.31) into (10.12) and (10.14) one can compute $M_{Q_{hkk\#}}(s)$ and $\frac{dM_{Q_{hkk\#}}(s)}{ds}$ respectively.

10.4.4 Rayleigh Fading with General Traffic

Rayleigh faded wireless channel can be characterized by means of the following pdf

$$
f_Y(y) = \begin{cases} \frac{y}{\sigma^2}e^{-\frac{y^2}{2\sigma^2}} & if\ y>0 \\ 0 & if\ y\le 0 \end{cases}. \qquad (10.32)
$$

Since $M_{SIDR_j}(s)$ is not affected by channel characteristics, hence we concentrate on $M_{Q_{hkk^{\#}}}(s)$ and its derivative. In order to calculate the corresponding LMGF and its first derivative $G_{hkk^{\#}}(q)$ has to be determined

$$G_{hkk^{\#}}(q) = \vartheta\left(q - \frac{P_h^{\max}}{\lambda}\right) \cdot \int_0^{+\infty} \frac{D_{hkk^{\#}} x}{(q + D_{hkk^{\#}} x)^2} f_{X_h}(x) dx. \tag{10.33}$$

10.4.5 ON/OFF Traffic with Rayleigh Fading Fhannel

In this subsection we combine the results of the previous subsections in order to achieve LMGFs in a given practical case.

Assuming ON/OFF traffic classes in accordance with (10.21) and wireless channel suffering Rayleigh fading defined by (10.32) the considered LMGFs and their first derivatives are the following.

$M_{SIDR_j}(s)$and $\frac{dM_{SIDR_j}(s)}{ds}$ have already been calculated, see (10.25) and (10.26). However, $M_{Q_{hkk^{\#}}}(s)$ and $\frac{dM_{Q_{hkk^{\#}}}(s)}{ds}$ require more effort to determine. We start from (10.33)

$$\begin{aligned}
&G_{hkk^{\#}}(q) = \vartheta(q - Q_{hkk^{\#}}^{\max}) \int_0^{+\infty} \frac{D_{hkk^{\#}} x}{(q + D_{hkk^{\#}} x)^2} f_{X_h}(x) dx \\
&= \vartheta(q - Q_{hkk^{\#}}^{\max}) \int_0^{+\infty} \frac{D_{hkk^{\#}} x}{(q + D_{hkk^{\#}} x)^2} a_h \delta(x - 0) dx + \\
&\vartheta(q - Q_{hkk^{\#}}^{\max}) \int_0^{+\infty} \frac{D_{hkk^{\#}} x}{(q + D_{hkk^{\#}} x)^2} b_h \delta(x - H_h) dx \\
&= \vartheta\left(q - \tfrac{P_h^{\max}}{\lambda}\right) \cdot \tfrac{m_{X_h} D_{hkk^{\#}}}{(q + D_{hkk^{\#}} H_h)^2},
\end{aligned}$$

which allows us to calculate

$$\begin{aligned}
1 - \int_0^{Q_{hkk^{\#}}^{\max}} G_{hkk^{\#}}(q) dq &= 1 - \int_0^{Q_{hkk^{\#}}^{\max}} \frac{b_h D_{hkk^{\#}} H_h}{(q + D_{hkk^{\#}} H_h)^2} dq \\
&= 1 - \frac{b_h Q_{hkk^{\#}}^{\max}}{Q_{hkk^{\#}}^{\max} + D_{hkk^{\#}} H_h} = 1 - \frac{b_h P_h^{\max}}{P_h^{\max} + \lambda D_{hkk^{\#}} H_h},
\end{aligned} \tag{10.34}$$

$$\begin{aligned}
&\int_0^{Q_{hkk^{\#}}^{\max}} q e^{s \cdot q} G_{hkk^{\#}}(q) dq = \\
&m_{X_h} D_{hkk^{\#}} \left(1 - \frac{\lambda D_{hkk^{\#}} H_h e^{\frac{P_h^{\max}}{\lambda} s}}{P_h^{\max} + \lambda D_{hkk^{\#}} H_h} - (1 - D_{hkk^{\#}} H_h s)\, e^{-D_{hkk^{\#}} H_h s} \cdot \right. \\
&\left. \left(\mathrm{Ei}(1, -D_{hkk^{\#}} H_h s) - \mathrm{Ei}\left(1, -s\left(\tfrac{P_h^{\max}}{\lambda} + D_{hkk^{\#}} H_h\right)\right)\right)\right),
\end{aligned} \tag{10.35}$$

$$\int_0^{Q_{hkk\#}^{\max}} e^{s\cdot q} G_{hkk\#}(q)dq = \frac{m_{X_h}}{H_h}\left(1 - \frac{\lambda D_{hkk\#} H_h e^{\frac{P_h^{\max}}{\lambda} s}}{P_h^{\max} + \lambda D_{hkk\#} H_h} + D_{hkk\#} H_h s e^{-D_{hkk\#} H_h s}.\right. \left.\left(\text{Ei}(1, -D_{hkk\#} H_h s) - \text{Ei}\left(1, -s\cdot\left(\frac{P_h^{\max}}{\lambda} + D_{hkk\#} H_h\right)\right)\right)\right), \tag{10.36}$$

where Ei(n,x) refers to the exponential integrals (see Definitions in Section 15).

Substituting (10.34), (10.35) and (10.36) into (10.12) and (10.14) one can compute $M_{Q_{hkk\#}}(s)$ and $\frac{dM_{Q_{hkk\#}}(s)}{ds}$.

11 Extensions

In this section two extensions of the CAC in WCDMA systems are discussed.

11.1 SOFT HANDOVER

Soft handover is one of the very important properties of CDMA-based networks. Compared to GSM – where *hard handover* was applied and therefore a certain terminal was able to communicate only with one base station – CDMA terminals are allowed send and receive packets to/from several surrounding base stations (these links are called *handover legs*). Hence packet loss can be avoided during the handover and thus QoS level is increased. On one hand the technological background of soft handover is fairly simple. Since CDMA transmitters operate on the same carrier frequency and users are distinguished by means of codes thus no frequency adjustment is needed for parallel transmissions with several base stations. This allows building cheap transmitters. On the other hand theoretical background of efficient soft handover proves to be more challenging.

The simple model of the system is depicted in Fig. 11.1 from the reference cell point of view. Theoretically each terminal in the system is able to transmit to the reference base station, however, due to the strong distant-dependent attenuation only soft handover between neighboring cells are considered in practice. Here we assume that mobiles are handovering softly when they are located in the ring bounded by concentric circles with radius R_{s1} and R_{s2} i.e. ring $[R_{s1}, R_{s2}]$. Terminals outside of this ring have only single communication link (handover leg) either to the reference base station or to one of the neighboring base stations.

Now, we describe the soft handover process step by step. Let us assume a mobile moving from the middle of the reference Cell 1 towards the center of Cell 2. When a certain terminal enters into ring $[R_{s1}, R_{s2}]$ a new leg is opened to bases station of Cell 2 (BS2).

(Of course it may happen that more new legs are opened to several base stations, but this fact does not influences the principles of the handover protocol). The new leg, however, causes interference at BS1 and needs to be detected at BS2, therefore before establishing the new leg CAC has to be performed as if a new call arrived. Thus appearance of a new soft handover leg in the system can be regarded form CAC point of view as a new call arrival. So when the mobile crosses circle R_{s1} a CAC decision is required with a new state matrix (see (10.15)). As we mentioned earlier a certain user belonging to a given traffic class means 4 virtual CAC classes because of four different distances. Now, due to soft handover extra classes are needed. We have to calculate a new averaged distance for terminals of interference region $[R_{s1}, R]$ since terminals in this ring communicating with BS2 are causing interference at BS1. Similarly to (7.16) one obtains

$$d_{k\#k\#} = \frac{2}{R^2} \int_{R}^{R_{s1}} r^2 dr = \frac{2}{3} \frac{R_{s1}^3 - R^3}{R^2}, \tag{11.1}$$

and in compliance of this new distance the number of virtual classes has to be increased by 1 for each traffic classes i.e. from 4 to 5.

Cell 2 is not critical from CAC point of view because the mobile is power controlled from Cell 1 (this leg is the so called *main leg*), therefore it does not cause any problem if QoS can not be guaranteed for the terminal at BS2. This extra link only helps to maintain QoS for that terminal. (More sophisticated soft handover schemes can be defined where power control is adjusted taking into account all the soft handover legs, but these approaches are out of the scope of this Thesis and regarded as future topic of research.)

When the user crosses the cell border (circle with radius R) the role of BS1 and BS2 is exchanged. CAC has to decide whether BS2 is able to serve the terminal and BS1 remains only an auxiliary link towards the network.

Finally the handset leaves the soft handover region towards BS2 and the leg to BS1 can be released.

11.2 CAC ON THE DOWNLINK

In case of downlink CAC is less crucial compared to uplink. This is because downlink traffic to different users can be synchronized at the base station, which ensures easier detection. Therefore, one may say that an accepted call on the uplink means the admission on the downlink as well. Asymmetric traffic in infocom networks – where terminals send short request and get long answers (e.g. movie files) – is in compliance with this assumption. However, the more and more popular peer-to-peer systems regularly exchange the role of the two directions. Hence, we consider here the downlink from CAC point of view.

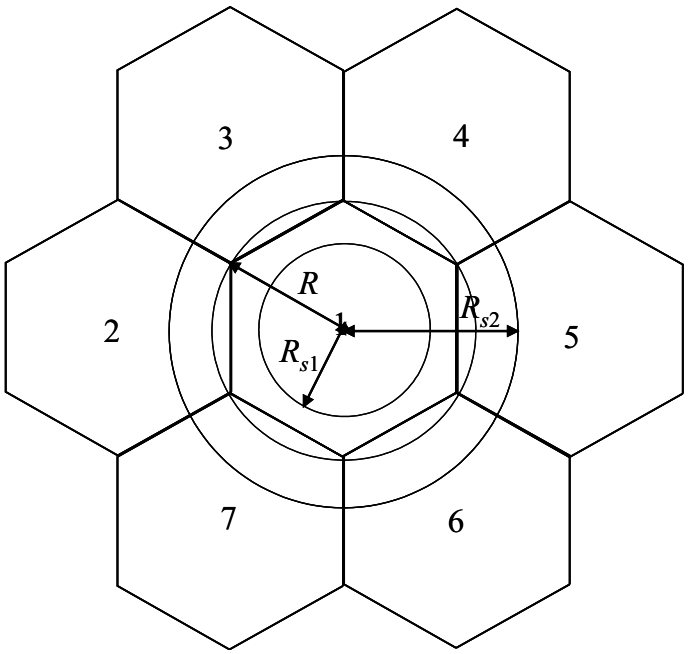

Fig. 11.1 System model with reference and neighboring cells in case of soft handover

The presented solution explains how uplink CAC can be transformed to downlink CAC taking into account the most important effects. The differences compared to the uplink are the following. On one hand terminals are the senders and base stations perform reception. On the other hand this fact results in fixed senders and moving receivers (opposite to the uplink case). Our downlink model is depicted in Fig. 11.2. For the sake of simplicity we consider a worst case scenario for CAC decisions. The terminal is located as far as possible from its base station (BS1) and as close to the interfering base stations as possible i.e. it is assumed standing on the cell border at point T. The figure shows the different distances between the terminal in T and the neighboring bases stations. Obviously one virtual class belong to each distance similar to the uplink case.

Of course the above described downlink CAC can be refined in the frames of future research.

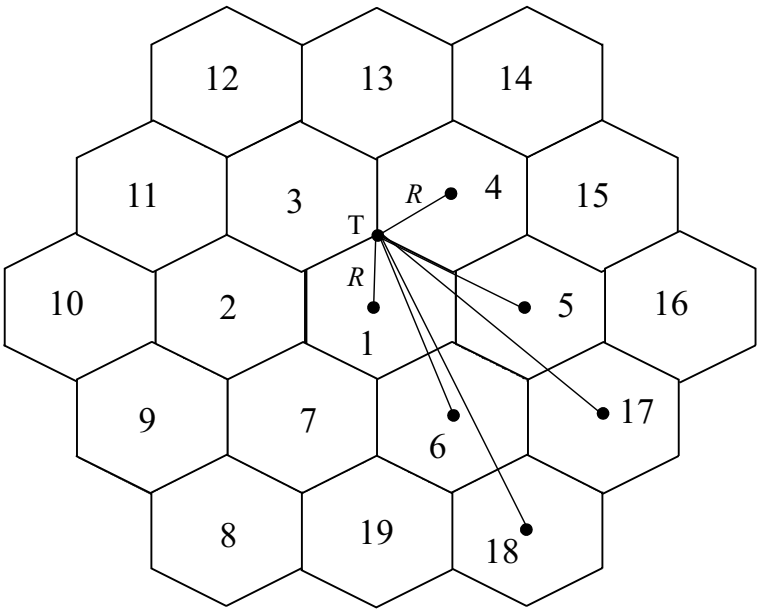

Fig. 11.2 System model with reference and neighboring cells for downlink

12

Simulation Results

The aim of this section is on one hand to compare the performance of the 'Static CAC' from Evans and Everitt as a reference and the proposed new 'Dynamic CAC' algorithms, on the other hand to answer computational complexity related questions.

In order to fulfill these goals appropriate simulation environment was built using open source OMNeT++ discrete event simulator suit [1].

12.1 STATIC PERFORMANCE

Firstly we performed static comparison of the two methods that is we measure the size of the acceptable state space (the number of accepted states of each method is counted performing CAC decision for all the possible network vectors). Another possible interpretation of term "static" can be regarded as no differentiation has been made among traffic states i.e. all the accepted states have the same weighting factor.

The chosen 3G like simulation set up was following:

Two rings of hexagonal cells around the reference cell (where the new call enters into the network) were taken into account. Moreover cell radius r=500 m, transmitter antenna's height: h_T=30 m, receiver antenna's height: h_R=1,5 m, and lognormal fading was assumed acting in the channel.

We considered two ON/OFF traffic classes with parameters:

Peak transmission rates:$H_1 = 144\,\text{kbps}$ and $H_2 = 384\,\text{kbps}$, voice activity factors $VAF_1 = VAF_2 = 0,4$, receiver sensitivity $(E_b/I_0)_{1,2} = 5\text{dB}$ was set up. Required QoS parameter was chosen to $e^{-\gamma} = 10^{-3}$ and the system capacity B^* reduced by other system interference was varied during the simulations from 1 MHz up to 2MHz. Finally halting criterion $d = e^{-\gamma} \cdot 10^{-3} = 10^{-6}$ was used for logarithmic search.

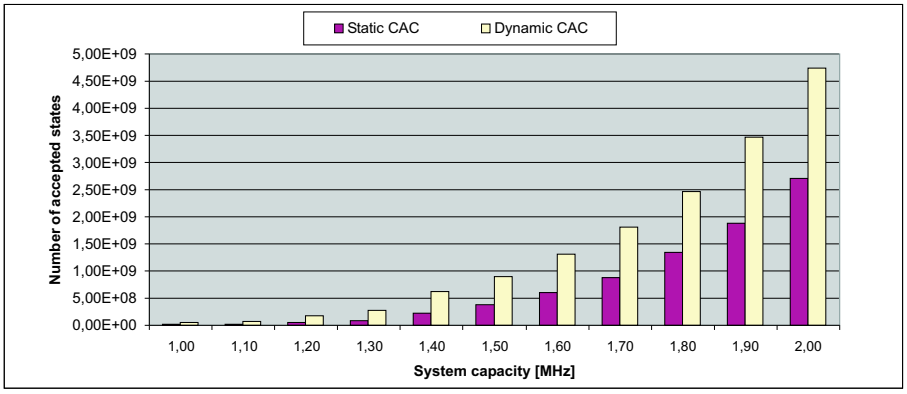

Fig. 12.1 Accepted network states vs. air interface capacity in case of static comparison

The number of accepted network states for the above defined simulation set up can be seen in Fig. 12.1 as the function of system capacity.

Simulation results fulfills our expectations i.e. Dynamic CAC admits about twice as much states as the Static CAC because it finds always the optimum point for a given network state instead of using a pre-calculated optimum for all the states. This is equivalent to the fact that Static CAC applies linear separation surface while Dynamic CAC a much sophisticated curve.

12.2 DYNAMIC PERFORMANCE

In case of dynamic investigations not only traffic, but call generation descriptors were given for each user type.

We assumed Poisson call arrival processes (with parameter λ_j) and exponential call holding times (with parameter μ_j) for each user class in each cell.

In compliance with these parameters call sequences were generated consisting of call arrivals and call terminations. In this case we counted the number of accepted calls in the reference cell for 10000 call arrival events, so only those states ware taken into account that happen during the call sequences. Therefore the state vectors were weighted i.e. some states occurred more than once others had not been passed at all. This type of comparison handles with higher importance the typical network scenarios than the rare ones.

Number of accepted states in function of call arrival intensity λ_2 is depicted in Fig. 12.2 while the call acceptance ratio i.e. the ratio of accepted calls vs. overall number of arrived calls in function of call arrival intensity λ_2 is depicted in Fig. 12.3, where $\mu_2 = 0,01$, $\mu_1 = 0,1$ and $\lambda_1 = 0,01$, $B^* = 2$ MHz.

Evaluation of Fig. 12.2 and Fig. 12.3 leads to relevant consequences. If λ_2 is small i.e. the system is underloaded. ≈ 9800 accepted calls among 10000 attempts means

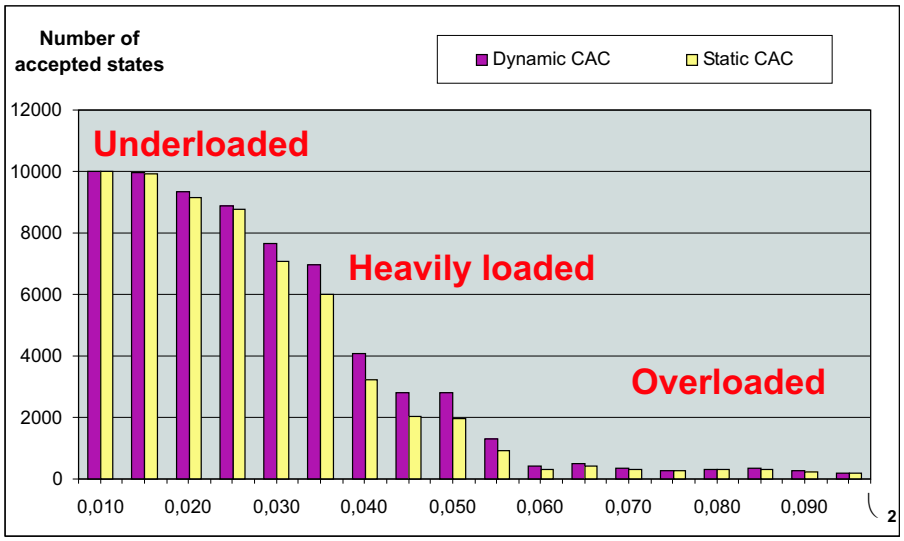

Fig. 12.2 Number of accepted calls as a function of λ_2

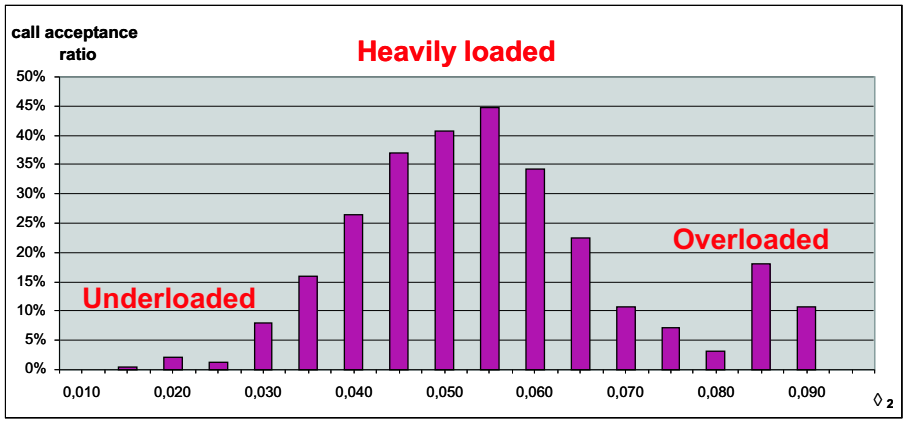

Fig. 12.3 Ratio of accepted calls vs. call attempts as a function of λ_2

2% blocking probability which is typical for UMTS network planning. One can observe no significant differences between the two methods (unlike computational complexity see below). This fact can be explained that Static CAC optimizes for underloaded network scenario, hence its precalculated optimum point is near to that one of Dynamic CAC.

While we increase λ_2 the system becomes more and more heavily loaded and Dynamic CAC performs better and better up to 45%. So we can state that Dynamic CAC is very efficient in call acceptance rate (or blocking probability) in heavily loaded scenarios.

Finally when λ_2 is exceeds a given limit the system becomes overloaded. The differences in performance decrease between the CAC methods but Dynamic CAC remains better. Of course from practical point of view this scenario has marginal importance.

12.3 COMPUTATIONAL COMPLEXITY

While performance has to be evaluated according to quantitative analysis, computational complexity is mainly a question of qualitative comparison. It has to be decided whether the given CAC method can be run real time or not.

In case of Static CAC computational complexity consists of two well separated terms: a precalculated and an online one.

First effective bandwidth values have to be computed in advance considering known values of system parameters such as system bandwidth, traffic and call descriptors, etc. Unfortunately effective bandwidth values are results of quiet complex optimization process, which does not allows their real time calculation.

Next during system operation only simple additions and multiplications (in magnitude of several hundreds/thousand) have to be performed when a new call arrives, which provides very fast CAC decisions.

The real bottleneck of Static CAC can be traced back to the first term, because any changes in system parameters result in long recalculation (update) of effective bandwidth values. Since system parameters in typical wired networks are constant simple effective bandwidth techniques are popular for these systems. However, wireless air interfaces suffer continuously changing radio channel effects, which counteracts the efficient real time application of Static CAC in wireless networks (this is the reason why deterministic radio channels were assumed in [54]!).

In case of Dynamic CAC no precalculation process is required, computation is only performed during call events. Computational complexity of a CAC decision differs in a constant factor from that one of Static CAC. Namely during one iteration of logarithmic search the same number of addition have to performed as in case of Static CAC decision. Hence the real question can be concentrated into the number of required iterations to find optimum value s^*. Therefore, the averaged number of iteration steps in function of d is

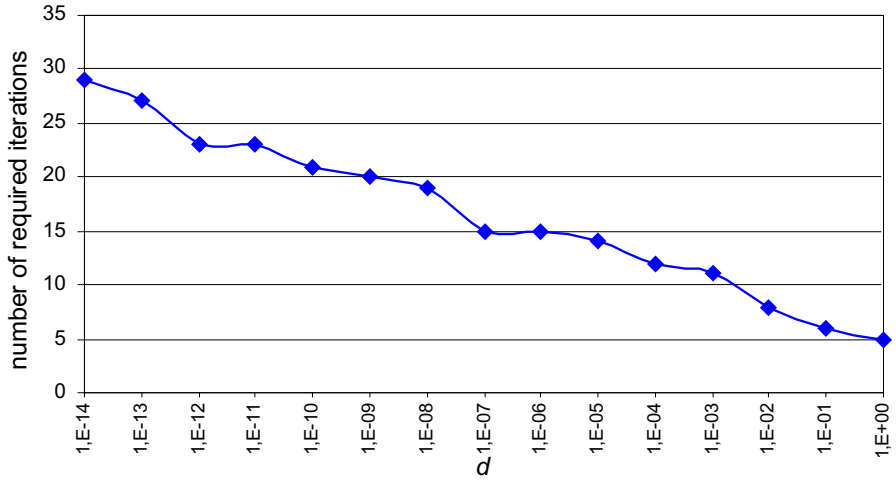

Fig. 12.4 Number of required iterations as a function of d

presented in Fig. 12.4 Two substantial conclusions have to be emphasized. On one hand the number of required iterations at $d = 10^{-6}$ is about only 15, which does not introduce valuable difference in computational complexity and therefore it does not influence real-time operation of Dynamic CAC. On the other hand the curve is almost linear despite the fact that d had been decreased logarithmically, which enables large freedom when d is set up.

12.4 BENEFITS AND EVALUATION OF DYNAMIC CAC

In this section we summarize the main characteristics and benefits of the proposed Dynamic CAC method.

Unlike static, effective bandwidth based solutions Dynamic CAC does not require computationally complex calculations to update the user descriptors used by CAC, therefore its application is quiet suitable in wireless environment.

The proposed new method does not require the classification of users at all. Since the user descriptors (LMGFs) are evaluated in a real-time way and the number of iteration steps depends only indirectly on the number of classes via the number of users in the classes. Therefore only the overall number of users has influence on the number of iteration steps. So any individual user parameter set can be handled and more sophisticated services can be provided.

The proposed CAC method does not depends on the applied modulation and/or spectrum spreading schemes. So it can be applied not only in DS-CDMA based UMTS networks, but frequency hopping, OFDM, MC-CDMA, etc. systems can also be considered.

In case multi-service terminals are assumed Dynamic CAC requires only the convolution of random variables representing the traffic characteristics of services under operation and this aggregated traffic has to be substituted into the equations. Static CAC, however, can handle multi-services of a terminal as individual services, with reasonable performance degradation.

Since calculation of the LMGF of the overall resource requirement can be traced back to the individual LMGFs, different channel models can be applied for each terminal according to the radio environment without increasing computational complexity.

13

Conclusions and Open Problems

The main objective of this Thesis was to show that computationally complex problems originating from the infocom systems can be solved either by sophisticated classical algorithms or quantum computing can be invoked. Furthermore it was demonstrated – e.g. in case of extreme value searching – that combining the two paradigms may open a new dimension in problem-solving.

A sophisticated model and new efficient dynamic CAC method were introduced in his Thesis for code division based cellular spread spectrum systems. This algorithm combines the dynamic optimization of Chernoff bound instead the well-known static effective bandwidth concept.

The most substantial advantage of the new method lies in its dynamic behavior that allows resilient adaptation to the continuously changing network parameters, which is one of the main drawbacks of the traditional static solutions. The proposed algorithm is able to adapt dynamically to an ever-changing radio environment and provides trade-off between decision efficiency and complexity.

LMGFs for general fading and traffic models were derived and as practical applications particular results for lognormal/Rayleigh fadings and/or ON/OFF traffic were calculated.

Simulation based investigations shored up performance and complexity efficiency of the new method.

Further research plans cover application of other typical channel models and intelligent handling of handover events in terms of capacity reservation. Another potential research direction extends the model with randomly changing minimum SIDR requirement because of the slow power control mechanism. The efficiency of the proposed solution can be improved if it is extended by measurement feedback. This Thesis did not distinguished priorities of incoming and handovered calls, therefore it is worth extending the CAC method

with capacity reservation schemes for handovers. The introduced soft handover model is simple and fits to the CAC, however, applying more sophisticated power control with more power controlled handover (main) legs would improve spectral efficiency.

Concerning the application of quantum computing to solve computationally complex infocom problems we discussed the generalized Grover search algorithm accepting arbitrary pure initial state of the index register. This extension allows the efficient application of quantum searching within a larger data base or even in a function. Furthermore it was showed that the generalization does not influence the computational complexity that is the optimal number of iterations remains the same.

As the next step ahead we introduced the quantum existence testing algorithm which can be regarded as a special case of quantum counting, however, because of the special problem we managed to decrease the corresponding computational complexity. Furthermore we presented how to combine classical binary search with quantum existence testing to design an efficient extreme value searching algorithm for unsorted databases/functions that performs significantly better than the currently available best solution. We emphasize that although minimum search is considered here, the proposed technique can be trivially modified to find the largest entry of a database.

In order to demonstrate how to involve quantum based techniques into solving a concrete classical infocom problem multi-user detection was considered.

Of course the quantum computing related results of this Thesis are the very first steps towards introducing quantum-assisted problem-solving in the infocom world. Many problems remained still open such as routing, medium access control etc.

Part III

Appendices

14
Summary of Theses

1. téziscsoport: Kvantum alapú adatbázis-keresés általánosítása

1.1. tézis: A Grover-operátor általánosítása (3. fejezet)
Definiáltam az általánosított Grover-operátort (Q), mely az indexek terén működik. Definiáltam az általános esetre a megoldások-nem megoldások kétdimenziós V terét. Megmutattam, hogy az általánosított Grover-operátor milyen feltételek mellett őrzi meg a V teret, valamint meghatároztam Q V-beli mátrixát.

1.2. tézis: A biztos találatot eredményező iterációs lépésszám meghatározása (3. fejezet)
Meghatároztam az általánosított kvantum alapú keresés hibamentes működéséhez szükséges iterációs lépésszámot. Ennek során megadtam a keresés θ és ϕ paramétere közötti fennálló ún. illesztési feltételt.

1.3. tézis: Az optimális iterációs lépésszám meghatározása (3. fejezet)
Megmutattam, hogy az általánosított algoritmus, miként vezethető vissza az alap megoldásra. Beláttam, hogy az általános keresés komplexitása megegyezik az alap Grover-algoritmus komplexitásával. Megadtam az általánosított algoritmus paraméterei kezdeti beállításának módját.

2. téziscsoport: Kvantum alapú szélsőérték keresés

2.1. tézis: Kvantum egzisztencia-tesztelés (4. fejezet)
Bevezettem a kvantum egzisztencia-tesztelés fogalmát. Megmutattam, hogy miként származtatható a kvantum egzisztencia-tesztelés a kvantum fázisbecslés módosításával. Megadtam a hibavalószínűség egzakt értékének képletét. Összefüggést adtam az algoritmus komplexitását meghatározó bitszám és a hibavalószínűség között. Elvégeztem az eljárás hibaanalízisét és megadtam az algoritmus komplexitását.

2.2. tézis: Kvantum szélsőérték keresés (4. fejezet)
Megmutattam, hogy a rendezetlen adatbázisban történő szélsőérték keresés miként vezethető vissza a kvantum egzisztencia-tesztelésre. Megadtam az algoritmus bonyolultságát.

2.3. tézis: Kvantum alapú többfelhasználós detekció DS-CDMA rendszerekben (5. fejezet)
Megmutattam, hogy az optimális többfelhasználós detekciós eljárás – mely klasszikusan nagy számításigényű feladat – miként vezethető vissza kvantum fázisbecslésre, jelentősen csökkentve a számítási komplexitást. Megadtam a vonatkozó kvantum architektúrat is.

3. téziscsoport: Hívásengedélyezés szórt spektrumú rendszerekben

3.1. tézis: Logaritmusos keresésre támaszkodó hívásengedélyezés (9. fejezet)
Beláttam, hogy a Chernoff-korlát alkalmazható az engedélyezési egyenlőtlenség hatékony végrehajtására, amennyiben az optimalizálási s paraméter értéke ismert. Megmutattam, hogy s optimális értéke miként változik a belépő, illetve kilépő hívások esetén. Bebizonyítottam, hogy logaritmikus kereséssel meghatározható s optimális értéke, megadtam a keresési tartomány határait.

3.2. tézis: Logaritmusos momentumgeneráló függvények általános alakja (10. fejezet)
Meghatároztam a felhasználói forgalmi modellt és a rádiócsatorna hatásait is tartalmazó logaritmikus momentumgeneráló függvényeket és azok deriváltjait kétutas hullámterjedéssel, multiplikatív fadinggel jellemzett, szimbólumidő tekintetében időinvariáns, korrelálatlan szimbólum mintákat generáló rádiócsatornát és memóriamentes teszőleges felhasználói forgalmat figyelembe véve. A rendszerben tökéletes teljesítményszabályozást feltételeztem. A felhasználói mozgást mobilitás-modellel vettem figyelembe, a mozgásból eredő Dopplerhatást elhanyagolhatónak tekintettem.

3.3. tézis: Logaritmusos momentumgeneráló függvények speciális alakja (10. fejezet)

Meghatároztam zárt alakban a logaritmikus momentumgeneráló függvényeket és azok deriváltjait ON/OFF felhasználói források, lognormál és Rayleigh-fading esetében, a 3.2. tézisben ismertetett feltételek figyelembe vételével.

15
Definitions

$F_Q(Q_0) \triangleq P(Q < Q_0)$: probability distribution function of r.v. Q.

$U_Q(Q_0) \triangleq 1 - F_Q(Q_0) = 1 - P(Q < Q_0) = P(Q \geq Q_0)$.

$\mathbb{E}(Q) \equiv m_Q \triangleq \int_{-\infty}^{\infty} q f_Q(q) dq$: Expected value of r. v. x, where the distinguished notation emphasizes that m_Q is constant.

$\mathbb{E}(g(Q,s)) \triangleq \int_{-\infty}^{\infty} g(q,s) f_Q(q) dq$: mean value function of r.v. $g(Q,s)$, where Q is a r.v. with pdf $f_Q(q)$ and s is deterministic.

$\sigma_Q \triangleq \mathbb{E}\left((Q - \mathbb{E}(Q))^2\right)$: variation of r.v. Q.

$M_Q(s) \triangleq \ln(\mathbb{E}(e^{sq}))$: Logarithmic moment generator function of r.v. Q.

$\delta(x - x_0) \equiv \delta(x_o)$: Dirac function, it is 1 if its argument equals zero i.e. $x = x_0$ else it is zero everywhere

$$\int_{-\infty}^{\infty} \delta(x) dx = 1,$$

for $f(x)$

$$\int_{-\infty}^{\infty} f(x)\delta(x - x_0) dx = f(x_0).$$

Moreover if $A \geq 0$ then

$$\delta\left(\frac{q}{A} - 0\right) = A\delta(q)$$

and for $A, B \geq 0$

$$\delta\left(\frac{q}{A} - B\right) = A\delta(q - AB).$$

Furthermore

$$\int_{-\infty}^{\infty} \delta(x - A)\delta\left(\frac{z}{x} - B\right)\frac{1}{x}dx = \delta(z - AB).$$

$\vartheta(x - x_0) \equiv \vartheta(x_o)$: Modified Heaviside step function, that is defined as 1 for $x < x_0$ and zero for $x > x_0$. It is related to the Dirac function as

$$\delta(x_0) \triangleq \frac{d\varepsilon(x - x_0)}{dx},$$

where $\varepsilon(x - x_0) \equiv \varepsilon(x_0)$ denotes the Heaviside function and for $f(x)$

$$\int_{-\infty}^{\infty} f(x)\vartheta(x_0)dx = \int_{-\infty}^{x_0} f(x)dx.$$

Moreover

$$\vartheta\left(\frac{p}{x} - \frac{q}{x}\right) = \vartheta(p - q).$$

The exponential integrals $\mathrm{Ei}(n, x)$ - where n is non-negative integer - are defined for $\mathbb{R}(x) > 0$ by

$$\mathrm{Ei}(n, x) \triangleq \int_{1}^{\infty} \frac{e^{xt}}{t^n}dt.$$

Error function for $x \in \mathbb{C}$

$$\mathrm{erf}(x) \triangleq \frac{2}{\sqrt{\pi}}\int_{0}^{x} e^{-t^2}dt.$$

Complementary error function

$$\mathrm{erfc}(x) \triangleq 1 - \mathrm{erf}(x).$$

D always stands for a constant

$$D_{hk} \triangleq \left(\frac{E_b}{I_0}\right)_k \cdot \frac{1}{A(d_{kk})},$$

$$D_{hkk\#} \triangleq A(d_{kk\#}) \cdot D_{hk} = \left(\frac{E_b}{I_0}\right)_h \cdot \frac{A(d_{kk\#})}{A(d_{kk})},$$

$$D_{lhkk^{\#}} \triangleq \frac{c}{P_{lh}^{max} A(d_{kk^{\#}})},$$

$$D_C \triangleq \frac{5}{2\sigma_C \ln(10)}.$$

V is called an n-dimensional vector space over complex numbers if the following criteria are satisfied:

1. Elements of V called vectors which are n-tuples of complex numbers $|v\rangle = [v_1, v_2, ...v_n]^T$, $v_i \in \mathbb{C}$.

2. There is an operation called *addition* defined as $|a\rangle = |v\rangle + |b\rangle, a_i = v_i + b_i$. Addition does not lead out from the vector space i.e. $|a\rangle \in V$.

3. Addition is *associative* and *commutative* and a so called zero vector exists $\mathbf{0}$ for which $\forall |v\rangle \in V, |v\rangle + \mathbf{0} = |v\rangle$.

4. A so called *additive inverse* $-|v\rangle$ belongs to each element of V such that $|v\rangle + (-|v\rangle) = \mathbf{0}$.

5. There is another operation called *scalar multiplication* between complex numbers c and vectors, $|a\rangle = c \cdot |v\rangle, a_i = c \cdot v_i$. Multiplication keeps the vector space, it is *associative* and *commutative* furthermore $1 \cdot |v\rangle = |v\rangle$.

Bases and linear independency:

- $|v_1\rangle, ..., |v_m\rangle$ are *spanning vectors* of m-dimensional space V if $\forall |v\rangle \in V, |v\rangle = \sum_i c_i |v_i\rangle, c_i \in \mathbb{C}$. A certain V has several spanning vector sets.

- $|v_1\rangle, ..., |v_m\rangle$ are *linearly dependent* if $\exists c_1, ..., c_m \in \mathbb{C}, c_i \neq 0$ such that $\sum_i c_i |v_i\rangle = \mathbf{0}$ else $\{|v_i\rangle\}$ are *linearly independent*.

- A spanning set of space V consisting of linearly independent vectors are called a *basis* of this space. *Dimension* of a certain space V equals the number of its basis vectors.

Basic operations on vectors:

- *Transpose (T)* of vector $|v\rangle$ produces a column vector and vice versa.

- *Complex conjugate (*)* of vector $|v\rangle$ conjugates each coordinates of the vector.

- *Adjoint (†)* of vector $|v\rangle$ is defined as $|v\rangle^{\dagger} \triangleq (|v\rangle^T)^*$ and denoted by $\langle v|$.

- *Scalar product* or *inner product* of two vectors $|v\rangle$ and $|w\rangle$ is a scalar quantity defined as $\langle v|w\rangle \triangleq \sum_i v_i^* \cdot w_i$ i.e.

$$\langle v|w\rangle = \begin{bmatrix} v_1^* & v_2^* & \cdots & v_m^* \end{bmatrix} \begin{bmatrix} w_1 \\ w_2 \\ \vdots \\ w_m \end{bmatrix} \sum_i v_i^* w_i.$$

  Furthermore in case of unit vectors $\langle v|w\rangle = 1$ if and only if $|w\rangle \equiv |v\rangle$ and $\langle v|w\rangle = 0$ if and only if $|v\rangle$ and $|w\rangle$ are *orthogonal*. Finally $\langle v|a\rangle \equiv (\langle a|v\rangle)^*$.

Norm:

- *Norm* can be interpreted as the generalization of notion of *absolute value* assigning to each $|v\rangle \in V$ a scalar and it is denoted by $\||v\rangle\|$. Norm has to fulfil the following constraints:

  1. $\||v\rangle\| \geq 0$ and $\||v\rangle\| = 0$ if and only if $|v\rangle = \mathbf{0}$ if $|v\rangle \in V$
  2. $\||v_1\rangle + |v_2\rangle\| \leq \||v_1\rangle\| + \||v_2\rangle\|$ if $|v_1\rangle, |v_2\rangle \in V$
  3. $\|c \cdot |v\rangle\| = |c| \cdot \||v\rangle\|$ if $|v\rangle \in V$ and $c \in \mathbb{C}$

- A vector space is *normalized* if a certain *norm* is defined for the space.

- A finite dimensional linear vector space is called *Hilbert space* if its vectors have complex coordinates and the norm is defined as $\||v\rangle\| = \sqrt{\langle v|v\rangle}$. In this case the norm represents the length of the vector.

- A vector $|v\rangle$ is *normalized* or we call it unit vector if the corresponding norm equals 1.

- Elements of a vector set $\{|v_i\rangle\}$ are *orthonormal* if they have unit length and they are mutually orthogonal i.e. $\langle v_i|v_j\rangle = \delta(i-j)$.

Linear operators:

Let V and W vector spaces over complex numbers. A transform U is called *linear operator* if it assigns to $\forall|v\rangle \in V$ a $|w\rangle = U|v\rangle \in W$ such that for arbitrary scalar $c \in \mathbb{C}$ and vectors $|v\rangle, |v_1\rangle, |v_2\rangle$

$$U(|v_1\rangle + |v_2\rangle) = U|v_1\rangle + U|v_2\rangle,$$

$$U(c \cdot |v\rangle) = c \cdot U|v\rangle.$$

The former constraint is called *superposition principle* and proves to be very useful when evaluating the operation of a certain quantum circuit. An identity operator I performs the following transformation $\forall|v\rangle \in V\ I|v\rangle = |v\rangle$ while the zero operator assigns the zero vector to each $|v\rangle \in V$ i.e $O|v\rangle = \mathbf{0}$.

Linear operator U connecting an m-dimensional space to an n-dimensional one is represented by means of its matrix form

$$\mathbf{U}_{nm} = \begin{bmatrix} U_{11} & U_{12} & \cdots & U_{1m} \\ U_{21} & U_{22} & \cdots & U_{2m} \\ \vdots & \vdots & \ddots & \vdots \\ U_{n1} & U_{n2} & \cdots & U_{nm} \end{bmatrix}.$$

The resulting vector $|w\rangle = U|v\rangle$ can be calculated as $w_i = \sum_j U_{ij} v_j$.

Outer product is a special linear operator with the following definition. Let $|v\rangle, |z\rangle \in V$ and $|w\rangle \in W$ be vectors in Hilbert spaces then outer product operator $|w\rangle\langle v|$ connects the two spaces as $|w\rangle\langle v||z\rangle \equiv |w\rangle\langle v|z\rangle = \langle v|z\rangle|w\rangle$. Matrix of $U = |w\rangle\langle v|$ can be computed as $U_{ij} = w_i \cdot v_j^*$ i.e.

$$\mathbf{U} = \begin{bmatrix} w_1 \\ w_2 \\ \vdots \\ w_n \end{bmatrix} \begin{bmatrix} v_1^* & v_2^* & \cdots & v_m^* \end{bmatrix} = \begin{bmatrix} w_1 v_1^* & w_1 v_2^* & \cdots & w_1 v_m^* \\ w_2 v_1^* & w_2 v_2^* & \cdots & w_2 v_m^* \\ \vdots & \vdots & \ddots & \vdots \\ w_n v_1^* & w_n v_2^* & \cdots & w_n v_m^* \end{bmatrix}.$$

If $\{|v_i\rangle\}$ form an orthonormal basis of space V then the following *completeness relation* holds

$$\sum_i |v_i\rangle\langle v_i| \equiv I.$$

Tensor product or *direct product* ($\otimes$) of vectors are used to unify separate vector spaces. If $\{|v_i\rangle \in V\}$ and $\{|w_j\rangle \in W\}$ are orthonormal bases then $\{|v_i\rangle \otimes |w_j\rangle\}$ form an orthonormal basis for vector space $V \otimes W$. Equivalent notations for tensor product are $|v\rangle \otimes |w\rangle$, $|v\rangle|w\rangle$, $|vw\rangle$. If operator A acts on space V while operator B on space W then $C = A \otimes B$ which operates on $V \otimes W$ can be calculated as

$$\mathbf{C} = \begin{bmatrix} A_{11}\mathbf{B} & A_{12}\mathbf{B} & \cdots & A_{1m}\mathbf{B} \\ A_{21}\mathbf{B} & A_{22}\mathbf{B} & \cdots & A_{2m}\mathbf{B} \\ \vdots & \vdots & \ddots & \vdots \\ A_{n1}\mathbf{B} & A_{n2}\mathbf{B} & \cdots & A_{nm}\mathbf{B} \end{bmatrix}.$$

16

Derivations Related to the Generalized Grover Algorithm

16.1 EIGENVALUES OF THE GENERALIZED GROVER OPERATOR

To find the eigenvalues of Q one should solve the characteristic equation $\det\{\mathbf{Q}-q\mathbf{I}\}=0$, which seems to be fairly hard task

$$\begin{aligned}(Q_{11}-q)(Q_{22}-q)-Q_{12}Q_{21}=0,\\ q_{1,2}=\frac{Q_{11}+Q_{22}\pm\sqrt{(Q_{11}+Q_{22})^2-4(Q_{11}Q_{22}-Q_{12}Q_{21})}}{2}.\end{aligned}\tag{16.1}$$

Therefore we follow a more pragmatic way. Applying the basis-independent product of eigenvalues in the form of $\det\{\mathbf{Q}\}=q_1q_2$ as well as exploiting the form of eigenvalues of unitary operators $e^{j\varepsilon}$,

$$\det(\mathbf{Q})=Q_{11}Q_{22}-Q_{12}Q_{21},\tag{16.2}$$

$$\begin{aligned}Q_{11}Q_{22} &= (-1)(-1)\left[1+\left(e^{j\theta}-1\right)\cos^2(\Omega)\right]e^{j\phi}\left[1+\left(e^{j\theta}-1\right)\sin^2(\Omega)\right]\\ &= e^{j\phi}\left[1+\left(e^{j\theta}-1\right)\underbrace{\left(\sin^2(\Omega)+\cos^2(\Omega)\right)}_{\equiv 1}+\left(e^{j\theta}-1\right)^2\sin^2(\Omega)\cos^2(\Omega)\right]\\ &= e^{j\phi}\left[e^{j\theta}+\left(e^{j\theta}-1\right)^2\sin^2(\Omega)\cos^2(\Omega)\right].\end{aligned}\tag{16.3}$$

$$\begin{aligned}Q_{12}Q_{21} &= (-1)(-1)e^{j\phi}\left(e^{j\theta}-1\right)\sin(\Omega)\cos(\Omega)\,e^{j\Lambda}\left(e^{j\theta}-1\right)\sin(\Omega)\cos(\Omega)\,e^{-j\Lambda}\\ &= e^{j\phi}\left[\left(e^{j\theta}-1\right)^2\sin^2(\Omega)\cos^2(\Omega)\right].\end{aligned}\tag{16.4}$$

Substituting (16.3) and (16.4) into (16.2) we get

$$\det(\mathbf{Q})=e^{j(\theta+\phi)}\tag{16.5}$$

since $q_i = e^{j\varepsilon_i}$, hence the eigenvalues of the generalized Grover operator become

$$q_{1,2} = -e^{j\left(\frac{\theta+\phi}{2} \pm \Upsilon\right)}. \tag{16.6}$$

Furthermore, it is known that the trace of $\mathbf{Q}$ can be expressed as

$$Q_{11} + Q_{22} = q_1 + q_2, \tag{16.7}$$

resulting in

$$\begin{aligned} Q_{11} + Q_{22} &= -\left[1 + \left(e^{j\theta} - 1\right)\cos^2(\Omega) + e^{j\phi}\left[1 + \left(e^{j\theta} - 1\right)\sin^2(\Omega)\right]\right] \\ &= -\left[\underbrace{1 - \cos^2(\Omega)}_{\sin^2(\Omega)} + e^{j\theta}\underbrace{\cos^2(\Omega)}_{1-\sin^2(\Omega)} + e^{j\phi} + e^{j(\phi+\theta)}\sin^2(\Omega) - e^{j\phi}\sin^2(\Omega)\right] \\ &= -\left[\sin^2(\Omega) + e^{j\theta} + e^{j\phi} - \sin^2(\Omega)\left(-e^{j\theta} - e^{j\phi} + e^{j(\phi+\theta)}\right)\right], \end{aligned} \tag{16.8}$$

where the equality stands if both the real and the imaginary parts of (16.8) holds separately. The imaginary one looks like

$$\begin{aligned} \Im\{Q_{11} + Q_{22}\} &= -\left[\sin(\theta) + \sin(\phi) + \sin^2(\Omega)\left(-\sin(\theta) - \sin(\phi) + \sin(\phi+\theta)\right)\right] = \\ = -\left\{2\sin\left(\frac{\phi+\theta}{2}\right)\cos\left(\frac{\phi-\theta}{2}\right) + \sin^2(\Omega)\left[\sin\left(\frac{\phi+\theta}{2}\right)\cos\left(\frac{\phi-\theta}{2}\right) + 2\sin\left(\frac{\phi+\theta}{2}\right)\cos\left(\frac{\phi+\theta}{2}\right)\right]\right\}, \end{aligned} \tag{16.9}$$

where the trigonometrical equivalence $\left[\sin x + \sin y = 2\sin\left(\frac{x+y}{2}\right)\cos\left(\frac{x-y}{2}\right)\right]$ is employed. Applying (16.6) on (16.7) and substituting them into (16.8) we get

$$\begin{aligned} \Im\{q_1 + q_2\} &= -\left\{\sin\left(\frac{\theta+\phi}{2} + \Upsilon\right) + \sin\left(\frac{\theta+\phi}{2} - \Upsilon\right)\right\} \\ &= -2\sin\left(\frac{\theta+\phi}{2}\right)\cos(\Upsilon). \end{aligned} \tag{16.10}$$

From (16.9) and (16.10) follows that

$$\begin{aligned} \cos(\Upsilon) &= \cos\left(\frac{\phi-\theta}{2}\right) + \sin^2(\Omega)\left(\cos\left(\frac{\theta+\phi}{2}\right) - \cos\left(\frac{\phi-\theta}{2}\right)\right) \\ &= \cos\left(\frac{\phi-\theta}{2}\right) - 2\sin^2(\Omega)\sin\left(\frac{\phi}{2}\right)\sin\left(\frac{\theta}{2}\right) \\ &= \cos\left(\frac{\phi}{2}\right)\cos\left(\frac{\theta}{2}\right) + \sin\left(\frac{\phi}{2}\right)\sin\left(\frac{\theta}{2}\right)\left[1 - 2\sin^2(\Omega)\right] \\ &= \cos\left(\frac{\phi}{2}\right)\cos\left(\frac{\theta}{2}\right) + \sin\left(\frac{\phi}{2}\right)\sin\left(\frac{\theta}{2}\right)\cos(2\Omega). \end{aligned} \tag{16.11}$$

The derivation of the real part of (16.8) is straightforward, hence

$$\Re\{Q_{11} + Q_{22}\} = -\left[2\cos\left(\frac{\theta+\phi}{2}\right)\cos\left(\frac{\theta-\phi}{2}\right) + \sin^2(\Omega)\cdot 2\cos^2\left(\frac{\theta+\phi}{2}\right)\right], \tag{16.12}$$

thus

$$\Re\left\{q_1+q_2\right\} = -2\cos\left(\frac{\theta+\phi}{2}\right)\cos\left(\Upsilon\right), \tag{16.13}$$

whereas we reached the same result as in (16.11)

$$\cos(\Upsilon) = \cos\left(\frac{\theta-\phi}{2}\right) + \sin^2\left(\Omega\right)\left(\cos\left(\frac{\theta+\phi}{2}\right) - \cos\left(\frac{\theta-\phi}{2}\right)\right).$$

Consequently, only one restriction has to be remarked, namely $\cos(\Upsilon) = \cos\left(-\Upsilon\right)$. At the same time according to the special form of the eigenvalues in (16.6) the two Υ's are equivalent to each other, since both lead to the same eigenvalue pair.

16.2 EIGENVECTORS OF THE GENERALIZED GROVER OPERATOR

In possession of the eigenvalues $q_{1,2}$ derived above in (16.6) we turn to derive the eigenvectors of $\mathbf{Q}$.

Starting form (3.19) and using expression

$$|\psi_1\rangle = \psi_{1\alpha}|\alpha\rangle + \psi_{1\beta}|\beta\rangle, \tag{16.14}$$

a homogenous linear equation system is obtained

$$\begin{aligned} Q_{11}\psi_{1\alpha} + Q_{12}\psi_{1\beta} &= q_1\psi_{1\alpha}, \\ Q_{21}\psi_{1\alpha} + Q_{22}\psi_{1\beta} &= q_2\psi_{1\beta}, \end{aligned} \tag{16.15}$$

from which

$$\frac{\psi_{1\alpha}}{\psi_{1\beta}} = \frac{q_1 - Q_{22}}{Q_{21}}, \tag{16.16}$$

$$\frac{\psi_{1\beta}}{\psi_{1\alpha}} = \frac{q_1 - Q_{11}}{Q_{12}}. \tag{16.17}$$

Apparently, there are infinite many solutions of (16.15), differing only in a scalar factor. For our purposes we only need those ones having unit length in form

$$|\psi\rangle_{\text{norm}} = \cos(z)e^{jC}|\alpha\rangle + \sin(z)|\beta\rangle. \tag{16.18}$$

According to (16.16) let $\psi_{1\alpha} = q_1 - Q_{22}$ and $\psi_{1\beta} = Q_{22}$. From the possible solutions we focus our attention on those that have unit length, $\||\psi_1\rangle_{\text{norm}}\| = 1$, thus $\left|\cos(z)e^{jC}\right|^2 + \left|\sin(z)\right|^2 = 1$, where

$$\sin^2(z) = \frac{|\psi_{1\beta}|^2}{|\psi_{1\alpha}|^2 + |\psi_{1\beta}|^2}, \tag{16.19}$$

$$\cos^2(z) = \frac{|\psi_{1\alpha}|^2}{|\psi_{1\alpha}|^2 + |\psi_{1\beta}|^2}. \tag{16.20}$$

Following our antecedent establishments

$$
\begin{aligned}
|\psi_{1\alpha}|^2 &= |q_1 - Q_{22}|^2 = \\
&= \overbrace{\left(-\cos\left(\frac{\theta+\phi}{2}+\Upsilon\right)+\sin^2(\Omega)\cos\left(\frac{\theta+\phi}{2}\right)+\cos^2(\Omega)\cos(\phi)\right)^2}^{|\Re()|^2} + \\
&+ \underbrace{\left(-\sin\left(\frac{\theta+\phi}{2}+\Upsilon\right)+\sin^2(\Omega)\sin\left(\frac{\theta+\phi}{2}\right)+\cos^2(\Omega)\sin(\phi)\right)^2}_{|\Im()|^2},
\end{aligned}
\tag{16.21}
$$

and

$$
|\psi_{1\alpha}|^2 = \psi_{1\alpha}\psi_{1\alpha}^*, \tag{16.22}
$$

$$
|\psi_{1\beta}|^2 = \psi_{1\beta}\psi_{1\beta}^*, \tag{16.23}
$$

respectively. As the next step let us derive $|\psi_{1\alpha}/\psi_{1\beta}|^2$ as follows

$$
\begin{aligned}
\left|\frac{\psi_{1\alpha}}{\psi_{1\beta}}\right|^2 &= \frac{-e^{j\left(\frac{\theta+\phi}{2}+\Upsilon\right)}+e^{j\phi}\left[\left(e^{j\theta}-1\right)\sin^2(\Omega)+1\right]}{-e^{j\phi}\left(e^{j\theta}-1\right)\sin(\Omega)\cos(\Omega)\,e^{-j\Lambda}}\cdot \\
&\cdot \frac{-e^{-j\left(\frac{\theta+\phi}{2}+\Upsilon\right)}+e^{-j\phi}\left[\left(e^{-j\theta}-1\right)\sin^2(\Omega)+1\right]}{-e^{-j\phi}\left(e^{-j\theta}-1\right)\sin(\Omega)\cos(\Omega)\,e^{j\Lambda}} \\
&= \frac{\left(1-e^{j\left(\frac{\theta-\phi}{2}+\Upsilon\right)}+\left(e^{j\theta}-1\right)\sin^2(\Omega)\right)}{\left(e^{j\theta}-1\right)\left(e^{-j\theta}-1\right)\sin^2(\Omega)\cos^2(\Omega)}\cdot \\
&\cdot \frac{\left(1-e^{-j\left(\frac{\theta-\phi}{2}+\Upsilon\right)}+\left(e^{-j\theta}-1\right)\sin^2(\Omega)\right)}{\left(e^{j\theta}-1\right)\left(e^{-j\theta}-1\right)\sin^2(\Omega)\cos^2(\Omega)} \\
&= \frac{\left[1-e^{j\left(\frac{\theta-\phi}{2}+\Upsilon\right)}-e^{-j\left(\frac{\theta-\phi}{2}+\Upsilon\right)}+1\right]+\left[1-e^{-j\theta}-e^{j\theta}+1\right]\sin^4(\Omega)}{\sin^2(\Omega)\cos^2(\Omega)\left[1-e^{-j\theta}-e^{j\theta}+1\right]}+ \\
&+ \frac{\sin^2(\Omega)\left[e^{j\theta}-1-e^{j\left(\frac{\theta+\phi}{2}-\Upsilon\right)}+e^{-j\left(\frac{\theta-\phi}{2}+\Upsilon\right)}+e^{-j\theta}-1-e^{-j\left(\frac{\theta+\phi}{2}-\Upsilon\right)}+e^{j\left(\frac{\theta-\phi}{2}+\Upsilon\right)}\right]}{\sin^2(\Omega)\cos^2(\Omega)\left[1-e^{-j\theta}-e^{j\theta}+1\right]} = \\
&= \frac{2-2\cos\left(\frac{\theta-\phi}{2}+\Upsilon\right)-\sin^2(\Omega)\cos^2(\Omega)\left[2-2\cos(\theta)\right]}{\sin^2(\Omega)\cos^2(\Omega)\left[2-2\cos(\theta)\right]}+ \\
&+ \frac{\sin^2(\Omega)\left[2-2\cos(\theta)-2+2\cos(\theta)-2\cos\left(\frac{\theta+\phi}{2}-\Upsilon\right)+2\cos\left(\frac{\theta-\phi}{2}+\Upsilon\right)\right]}{\sin^2(\Omega)\cos^2(\Omega)\left[2-2\cos(\theta)\right]} = \\
&= \frac{2-2\cos\left(\frac{\theta-\phi}{2}+\Upsilon\right)-\overbrace{\sin^2(\Omega)\cos^2(\Omega)4}^{\sin^2(2\Omega)}\sin^2\left(\frac{\theta}{2}\right)}{\sin^2(2\Omega)\sin^2\left(\frac{\theta}{2}\right)}+ \\
&+ \frac{\sin^2(\Omega)\left[2\cos\left(\frac{\theta-\phi}{2}+\Upsilon\right)-2\cos\left(\frac{\theta+\phi}{2}-\Upsilon\right)\right]}{\sin^2(2\Omega)\sin^2\left(\frac{\theta}{2}\right)}.
\end{aligned}
\tag{16.24}
$$

Keeping in mind expression (16.19) in which $|\psi_{1\alpha}/\psi_{1\beta}|^2$ can be substituted from (16.24),

$$\begin{aligned}
\frac{|\psi_{1\beta}|^2}{|\psi_{1\alpha}|^2+|\psi_{1\beta}|^2} &= \frac{\sin^2(2\Omega)\sin^2\left(\frac{\theta}{2}\right)}{2-2\cos\left(\frac{\theta-\phi}{2}+\Upsilon\right)\sin^2(\Omega)\left[2\cos\left(\frac{\theta-\phi}{2}+\Upsilon\right)-2\cos\left(\frac{\theta+\phi}{2}-\Upsilon\right)\right]} \\
&= \frac{\sin^2(2\Omega)\sin^2\left(\frac{\theta}{2}\right)}{2-2\cos\left(\frac{\theta-\phi}{2}+\Upsilon\right)+4\sin^2(\Omega)\sin\left(\frac{\theta}{2}\right)\sin\left(\frac{\phi}{2}-\Upsilon\right)} \\
&= \frac{\sin^2(2\Omega)\sin^2\left(\frac{\theta}{2}\right)}{2-2\cos\left(\frac{\theta}{2}\right)\cos\left(\frac{\phi}{2}-\Upsilon\right)-\underbrace{2\sin\left(\frac{\theta}{2}\right)\sin\left(\frac{\phi}{2}-\Upsilon\right)+4\sin^2(\Omega)\sin\left(\frac{\theta}{2}\right)\sin\left(\frac{\phi}{2}-\Upsilon\right)}_{\sin\left(\frac{\theta}{2}\right)\sin\left(\frac{\phi}{2}-\Upsilon\right)\underbrace{\left(4\sin^2(\Omega)-2\right)}_{-2\cos(2\Omega)}}}
\end{aligned}$$

which leads to

$$\sin^2(z)=\frac{\sin^2(2\Omega)\sin^2\left(\frac{\theta}{2}\right)}{2\left(1-\cos\left(\frac{\theta}{2}\right)\cos\left(\frac{\phi}{2}-\Upsilon\right)-2\cos(2\Omega)\sin\left(\frac{\theta}{2}\right)\sin\left(\frac{\phi}{2}-\Upsilon\right)\right)} \tag{16.25}$$

and obviously

$$\cos^2(z)=1-\sin^2(z).$$

Finally, to determine the eigenvectors $|\psi_{1,2}\rangle$, only the e^{jC} factor is remaining in (16.18). Considering the relation

$$\frac{\psi_{1\alpha}}{\psi_{1\beta}}=\frac{\cos(z)}{\sin(z)}e^{jC_1},$$

and thus

$$\left(\frac{\psi_{1\alpha}}{\psi_{1\beta}}\right)^2=\cot^2(z)e^{j2C_1}=\frac{Q_{12}}{Q_{21}}\cdot\frac{q_1-Q_{22}}{q_1-Q_{11}},$$

where equations (16.16), (16.17) were employed. It can be proven easily that

$$\frac{q_1-Q_{22}}{q_1-Q_{11}}$$

is a real number, which implies that

$$\frac{Q_{12}}{Q_{21}}=\frac{e^{-j\Lambda}e^{j\phi}}{e^{-j\Lambda}}=e^{j(\phi-2\Lambda)},$$

thus

$$\left(e^{jC_1}\right)^2=\frac{Q_{12}}{Q_{21}}=e^{j(\phi-2\Lambda)},$$

from which follows

$$e^{jC_1}=\pm e^{j\left(\frac{\phi}{2}-\Lambda\right)}. \tag{16.26}$$

Based on (16.26) the normalized eigenvector is

$$|\psi_1\rangle=\cos(z)\,e^{j\left(\frac{\phi}{2}-\Lambda\right)}|\alpha\rangle+\sin(z)\,|\beta\rangle. \tag{16.27}$$

Eigenvector $|\psi_2\rangle$ has to be calculated in a similar way, where the other eigenvalue q_2 should be taken into account, which results in a simple sign change of Υ. Due to the definition

of C_2 in (16.18), it does not depend on the sign of Υ, thus $e^{jC_2} = \pm e^{jC_1}$. To ensure the orthogonality the eigenvectors $|\psi_1\rangle$ and $|\psi_2\rangle$, e^{jC_2} must be equal to $-e^{jC_1}$, whereas the second eigenvector will be

$$|\psi_2\rangle = -\sin(z)\, e^{j\left(\frac{\phi}{2}-\Lambda\right)}|\alpha\rangle + \cos(z)\,|\beta\rangle. \tag{16.28}$$

17

Derivations Related to CAC in WCDMA Environment

17.1 THEOREMS

Theorem 9.1 *Let Q≥0 be a random variable with expected value m_Q . If $B^* > m_Q$ and s>0 then there exist one and only one s^* for which $\min_s \Psi(s) = \Psi(s = s^*)$ and $s^* \in (0, \infty]$.*

Proof. Since exp(.) is strictly increasing function, therefore

$$s^* = \arg\min_s \Psi(s) = \arg\min_s e^{\Psi(s)},$$

hence it is enough to search minimum places for

$$\Omega(s) := e^{\Psi(s)} = \frac{\mathbb{E}(e^{s \cdot Q})}{e^{s \cdot B^* - \gamma}} = \int_0^{+\infty} e^{s \cdot (q - B^*) + \gamma} f_Q(q) dq. \tag{17.1}$$

$\Omega(s)$ crosses the vertical axis at e^γ independently from B^* because

$$\Omega(s = 0) = e^\gamma \int_0^{+\infty} f_Q(q) dq = e^\gamma. \tag{17.2}$$

Next the first derivative of $\Omega(s)$ is calculated

$$\frac{d\Omega(s)}{ds} = \int_0^{+\infty} (q - B^*) e^{s \cdot (q - B^*) + \gamma} f_Q(q) dq, \tag{17.3}$$

whose zero points may refer to the minimum places depending on the second derivative. It is easy to see that the first derivative at s=0 is always negative since

$$\frac{d\Omega(s=0)}{ds} = e^{\gamma} \underbrace{\int_0^{+\infty} q f_Q(q) dq}_{m_Q} - e^{\gamma} B^* \underbrace{\int_0^{+\infty} f_Q(q) dq}_{1} = e^{\gamma}(m_Q - B^*) \tag{17.4}$$

and $e^{\gamma}(m_Q - B^*) < 0$ because of the initial condition $B^* > m_Q$.

Properties of the second derivatives determines the final claims for

$$\frac{d^2\Omega(s)}{ds^2} = \int_0^{+\infty} \underbrace{(q - B^*)^2}_{\geq 0} \underbrace{e^{s\cdot(q-B*)+\gamma}}_{>0} \underbrace{f_Q(q)}_{\geq 0} dq > 0. \tag{17.5}$$

Taking into account that $s = -\infty$ is the only case when any of the three terms equals to 0 independently of q, therefore the second derivative is always positive, which results in a strictly increasing first derivative. Considering furthermore that the first derivative at s=0 is always negative there exists one and only one point $s*$ where the first derivative crosses axis s and s^*>0 .

Finally we emphasize for later use that in case $B^* = m_Q$

$$\frac{d\Omega(s=0)}{ds} = 0 \quad \Rightarrow \quad s^* = 0. \tag{17.6}$$

□

Theorem 9.2 *Let $Q_{ij} \geq 0$ be random variables with expected values $m_{Q_{ij}}$ and $Q = \sum_{j=1}^{J} \sum_{i=1}^{N_j} Q_{ij}$. Let t denote the system time measured in number of call events (call arrival or call termination). If event t is a new call arrival then $s^*(t) < s^*(t-1)$ and in case of event t refers to a finished call then $s^*(t) > s^*(t-1)$.*

Proof. Because from s^* point of view $\Omega(s)$ and $\Psi(s)$ are equivalent this time we use the first derivative of $\Psi(s)$ to investigate $s^*(t)$. Combining (9.6) and (9.8) we get

$$\Psi(s) = \sum_{j=1}^{J} N_j M_{Q_j}(s) - s \cdot B^* + \gamma \tag{17.7}$$

and its first derivative is

$$\frac{d\Psi(s)}{ds} = \sum_{j=1}^{J} N_j \frac{dM_{Q_j}(s)}{ds} - B^*, \tag{17.8}$$

from which s^* can be calculated evaluating the following equation

$$\frac{d\Psi(s)}{ds} = 0 \;\Rightarrow\; \sum_{j=1}^{J} N_j \frac{dM_{Q_j}(s)}{ds} = B^*. \tag{17.9}$$

Let us assume that we already know $s^*(t-1)$ and taking into consideration the time-dependency of (17.9)

$$\sum_{j=1}^{J} N_j(t-1) \frac{dM_{Q_j}(s = s^*(t-1))}{ds} = B^*. \tag{17.10}$$

Based on (17.10), we can divide up B^* into smaller parts in the following way

$$B_j^*(t-1) = \frac{dM_{Q_j}(s = s^*(t-1))}{ds} \;\Rightarrow \sum_{j=1}^{J} N_j(t-1) \cdot B_j^*(t-1) = B^*. \tag{17.11}$$

We can interpret (17.11) as the total amount of system capacity is distributed among the sources according to the first derivatives of their LMGFs at $s^*(t-1)$

$$\frac{dM_{Q_j}(s = s^*(t-1))}{ds} = B_j^*(t-1) \; for \, \forall j. \tag{17.12}$$

Now, if a new source enters into the class j that is $N_j(t) = N_j(t-1)+1$ then the same amount of overall system capacity B^* should be partitioned virtually among the increased number of sources. Since $B_j^*(t) > 0$ therefore $B_j^*(t-1) > B_j^*(t)$.

Let us update (17.12)

$$\frac{dM_{Q_j}(s = s^*(t))}{ds} = B_j^*(t) \; for \, \forall j, \tag{17.13}$$

which results in a quiet large equation system. Fortunately solving any of the equations would give back the same $s^*(t)$. Therefore it is enough to concentrate on one of the equations. Comparing (17.12) and (17.13) we can conclude that we have in both cases the same function $\frac{dM_{Q_j}(s)}{ds}$ on the left hand side. Hence the shape of this function determines the relationship between $s^*(t-1)$ and $s^*(t)$ the intersection points with constant functions $y = B_j^*(t-1)$ or $y = B_j^*(t)$.

Next we introduce a much compact form for the first derivative of LMGFs

$$\frac{dM_{Q_j}(s)}{ds} = \frac{1}{\mathbb{E}(e^{s \cdot Q_j})} \int_0^{+\infty} q e^{sq} f_{Q_j}(q) dq = \frac{\mathbb{E}(Q_j e^{s \cdot Q_j})}{\mathbb{E}(e^{s \cdot Q_j})}, \tag{17.14}$$

that has the following values at s=0 and s=+∞

$$\frac{dM_{Q_j}(s=0)}{ds} = m_{Q_j}; \;\; \frac{dM_{Q_j}(s=+\infty)}{ds} = +\infty. \tag{17.15}$$

Taking into account that $B_j^*(t-1) > B_j^*(t) > m_{Q_j} > 0$ if we were able to prove that $\frac{d^2 M_{Q_j}(s)}{ds^2} > 0$ for s>0 i.e. $\frac{dM_{Q_j}(s)}{ds}$ has strictly increasing nature then the proof of Theorem 9.2 would be accomplished.

Unfortunately calculating

$$\frac{d^2 M_{Q_j}(s)}{ds^2} = \frac{\mathbb{E}(Q_j^2 e^{s \cdot Q_j})\mathbb{E}(e^{s \cdot Q_j}) - \mathbb{E}^2(Q_j e^{s \cdot Q_j})}{\mathbb{E}^2(e^{s \cdot Q_j})}. \tag{17.16}$$

does not lead to an obvious result. However taking into account Lemma 17.1 numerator of (17.16) is always greater than zero. So Theorem 9.1 has been proven.

□

Lemma 17.1. *For random variables q and p with the same probability density function $f(q)$ and for nonnegative functions $h(.), l(.)$ and $t(.)$ where $h^2(.) = t(.)l(.)$ the following inequality always holds:*

$$\mathbb{E}(t(q)l(p)) \geq \mathbb{E}^2(h(q)), \tag{17.17}$$

Proof.

$$\mathbb{E}(t(q)l(p)) = \left(\int_{-\infty}^{+\infty} t(q)f(p)dp\right)\left(\int_{-\infty}^{+\infty} l(p)f(p)dp\right) = \int_{-\infty}^{+\infty}\int_{-\infty}^{+\infty} \overbrace{t(q)l(p)\underbrace{f(q)f(p)}_{D(q,p)}}^{A(q,p)} dqdp$$

$$\mathbb{E}^2(h(q)) = \left(\int_{-\infty}^{+\infty} h(q)f(p)dp\right)\left(\int_{-\infty}^{+\infty} h(p)f(p)dp\right) = \int_{-\infty}^{+\infty}\int_{-\infty}^{+\infty} \overbrace{h(q)h(p)f(q)f(p)}^{B(q,p)} dqdp$$

Calculation of both sides of inequality (17.17) requires integration of $A(q,p) \cdot B(q,p)$ above the $(q-p)$ plane i.e. we have to determine the space below these functions.

One way to prove inequality (17.17) if we are able to guarantee for all $(q_0, p_0) \in plane(q,p)$ that $A(q_0,p_0) \geq B(p_0,q_0)$. Unfortunately it is not possible to shore up this claim. Instead we trace back these integrations to summations of function value pairs $A(q_0,p_0) + A(p_0,q_0)$ and $B(q_0,p_0) + B(p_0,q_0)$ respectively, that is we prove

$$A(q_0,p_0) + A(p_0,q_0) \geq B(q_0,p_0) + B(p_0,q_0) \tag{17.18}$$

Since $D(q,p)$ is symmetric on the $p = q$ axis i.e. $D(q_0,p_0) = D(p_0,q_0)$, therefore (17.18) leads to

$$t(q_0)l(p_0) + t(p_0)l(q_0) \geq 2h(q_0)h(p_0) \tag{17.19}$$

Applying condition $h^2(.) = t(.)l(.)$ we get the following constrains

$$
\begin{aligned}
h(q_0) &= t(q_0)\Delta(q_0),\\
h(p_0) &= l(p_0)\Delta(p_0),\\
h(p_0) &= \tfrac{t(p_0)}{\Delta(p_0)},\\
h(q_0) &= \tfrac{l(q_0)}{\Delta(q_0)},
\end{aligned}
$$

where $\Delta(.) > 0$.

Substituting these parameters into the left hand side of (17.19) we find that it is greater or equal to the right hand side

$$
\begin{aligned}
&\frac{h(q_0)}{\Delta(q_0)}\frac{h(p_0)}{\Delta(p_0)} + h(p_0)\Delta(p_0)h(q_0)\Delta(q_0)\\
&= h(q_0)h(p_0)\left(\underbrace{\Delta(p_0)\Delta(q_0) + \frac{1}{\Delta(q_0)\Delta(p_0)}}_{\geq 2}\right) \geq 2h(q_0)h(p_0).
\end{aligned}
$$

□

17.2 DERIVATION OF $F_{Q_{HKK\#}}(Q)$

Pdf of $L' = T' \cdot R'$ can be calculated as

$$
\begin{aligned}
&f_{L'}(l\,|x) = \delta(l-0)\cdot \int\limits_{L^{\max}_{hkk\#}(x)}^{+\infty} f_L(l)dl + \vartheta(L^{\max})\cdot f_L(l) =\\
&\delta(l-0)\int\limits_{L^{\max}_{hkk\#}(x)}^{+\infty} f_L(l)dl + \vartheta(L^{\max}_{hkk\#})\cdot \int\limits_{0}^{+\infty} \tfrac{1}{4\sqrt{l}} f_W(\sqrt{r}) f_Y\left(\sqrt{lr}\right)dr =\\
&\delta(l-0)\cdot U_L(L^{\max}_{hkk\#}(x)) + \int\limits_{0}^{L^{\max}_{hkk\#}(x)} \tfrac{1}{4\sqrt{l}} f_W(\sqrt{r}) f_Y\left(\sqrt{lr}\right)dr,
\end{aligned}
$$

where

$$
L^{\max}_{hkk\#}(x) = T^{\max}_{kk\#}\cdot R^{\max}_{hk} = \frac{1}{A(d_{kk\#})}\frac{P^{\max}_h A(d_{kk})}{\lambda\cdot(X_h = x)}\left(\frac{I_0}{E_b}\right)_h = \frac{P^{\max}_h}{\lambda D_{hkk\#}\cdot(X_h = x)} \tag{17.20}
$$

and $U_L(L_0) = 1 - F_L(L_0) = P(L \geq L_0)$, hence

$$
U_L(L^{\max}_{hkk\#}(x)) = \int\limits_{L^{\max}_{hkk\#}(x)}^{+\infty} f_L(l)dl = \int\limits_{L^{\max}_{hkk\#}(x)}^{+\infty}\int\limits_{0}^{+\infty} \frac{1}{4\sqrt{l}} f_W(\sqrt{r}) f_Y\left(\sqrt{lr}\right)drdl.
$$

Using transformation $Z_{hkk\#} = D_{hkk\#}\cdot L'$

$$f_{Z_{hkk\#}}(z\,|x) = f_{L'}\left(\frac{z}{D_{hkk\#}}\middle|\, x\right)\frac{1}{D_{hkk\#}} =$$
$$\delta(z-0)\cdot U_L(L^{\max}_{hkk\#}(x)) + \int_0^{Z^{\max}_{hkk\#}(x)} \frac{1}{4\sqrt{zD_{hkk\#}}} f_W(\sqrt{r}) f_Y\left(\sqrt{\frac{zr}{D_{hkk\#}}}\right)dr =$$
$$\delta(z-0)\cdot U_L(L^{\max}_{hkk\#}(x)) + \vartheta(z - Z^{\max}_{hkk\#}(x)) \int_0^{+\infty} \frac{1}{4\sqrt{zD_{hkk\#}}} f_W(\sqrt{r}) f_Y\left(\sqrt{\frac{zr}{D_{hkk\#}}}\right)dr,$$

where

$$Z^{\max}_{hkk\#}(x) = D_{hkk\#}\cdot L^{\max}_{hkk\#}(x) = \frac{P^{\max}_h}{\lambda\cdot(X_h = x)}. \tag{17.21}$$

Finally considering that X_h and $Z_{hkk\#}$ are not independent random variables, first we calculate

$$f_{Z_{hkk\#},X_h}(z,x) = f_{Z_{hkk\#}}(z\,|x)\cdot f_{X_h}(x) =$$
$$\delta(z-0)\cdot U_L(L^{\max}_{hkk\#}(x))\cdot f_{X_h}(x) +$$
$$f_{X_h}(x)\cdot\vartheta(z - Z^{\max}_{hkk\#}(x)) \int_0^{+\infty} \frac{1}{4\sqrt{zD_{hkk\#}}} f_W(\sqrt{r}) f_Y\left(\sqrt{\frac{zr}{D_{hkk\#}}}\right)dr$$

from which one obtains for $Q_{hkk\#} = X_h Z_{hkk\#}$

$$f_{Q_{hkk\#}}(q) = \int_0^{+\infty} f_{Z_{hkk\#},X_h}\left(\tfrac{q}{x},x\right)\tfrac{1}{x}dx =$$
$$\int_0^{+\infty}\delta\left(\tfrac{q}{x}-0\right)\cdot U_L(L^{\max}_{hkk\#}(x))\cdot f_{X_h}(x)\tfrac{1}{x}dx +$$
$$\int_0^{+\infty}\vartheta\left(\tfrac{q}{x} - Z^{\max}_{hkk\#}(x)\right)\int_0^{+\infty}\frac{1}{4\sqrt{qxD_{hkk\#}}} f_W(\sqrt{r}) f_Y\left(\sqrt{\frac{qr}{xD_{hkk\#}}}\right)dr\cdot f_{X_h}(x)dx =$$
$$\int_0^{+\infty}\delta\left(\tfrac{q}{x}-0\right)\cdot U_L(L^{\max}_{hkk\#}(x))\cdot f_{X_h}(x)\tfrac{1}{x}dx +$$
$$\int_0^{+\infty}\vartheta\left(\tfrac{q}{x} - \tfrac{P^{\max}_h}{\lambda x}\right)\int_0^{+\infty}\frac{1}{4\sqrt{qxD_{hkk\#}}} f_W(\sqrt{r}) f_Y\left(\sqrt{\frac{qr}{xD_{hkk\#}}}\right)dr\cdot f_{X_h}(x)dx.$$

Since $\delta\left(\frac{q}{A}-0\right) = A\cdot\delta(q)$, $\vartheta\left(\frac{p}{x}-\frac{q}{x}\right) = \vartheta(p-q)$ and Y and W have the same pdf, moreover we defined $Q^{\max}_{hkk\#} \triangleq \frac{P^{\max}_h}{\lambda}$, hence

$$\begin{aligned} f_{Q_{hkk\#}}(q) &= \delta(q)\int_0^{+\infty} U_L(L^{\max}_{hkk\#}(x))\cdot f_{X_h}(x)dx \\ &+ \vartheta(q - Q^{\max}_{hkk\#})\int_0^{+\infty}\int_0^{+\infty}\frac{1}{4\sqrt{qxD_{hkk\#}}} f_Y(\sqrt{r}) f_Y\left(\sqrt{\frac{qr}{xD_{hkk\#}}}\right)dr\cdot f_{X_h}(x)dx. \end{aligned} \tag{17.22}$$

(17.22) can be summarized in a much concentrated form if one recognizes that $f_{Q_{hkk\#}}(q)$ is a pdf and therefore

$$\int_0^{+\infty} U_L(L_{hkk\#}^{\max}(x)) f_{X_h}(x)dx =$$
$$1 - \underbrace{\int_0^{Q_{hkk\#}^{\max}} \vartheta(q - Q_{hkk\#}^{\max}) \int_0^{+\infty}\int_0^{+\infty} \frac{1}{4\sqrt{qxD_{hkk\#}}} f_Y(\sqrt{r}) f_Y\left(\sqrt{\frac{qr}{xD_{hkk\#}}}\right) dr f_{X_h}(x)dxdq}_{G_{hkk\#}(q)} =$$
$$1 - \int_0^{Q_{hkk\#}^{\max}} G_{hkk\#}(q)dq,$$

which leads to

$$f_{Q_{hkk\#}}(q) = \delta(q)\left(1 - \int_0^{Q_{hkk\#}^{\max}} G_{hkk\#}(q)dq\right) + G_{hkk\#}(q). \tag{17.23}$$

Remark: (17.22) was derived considering realistic power control and channel gain and it represents the pdf of $Q_{hkk\#} = D_{hkk\#} X_h (Y')^2 \frac{1}{(W')^2}$. It is interesting to highlight that if we calculated the pdf of $Q_{hkk\#}^* = D_{hkk\#} X_h Y^2 \frac{1}{W^2}$ which refers to the case when the previously mentioned effects were omitted then following relationship $G_{hkk\#}(q) = \vartheta(q - Q_{hkk\#}^{\max}) f_{Q_{hkk\#}^*}(q)$ could be recognized.

References

[1]. Omnet++ simulation environment webpage. http://whale.hit.bme.hu/omnetpp/.

[2]. A. Ahuja, S. Kapoor. A quantum algorithm for finding the maximum. 1999. e-print quant-ph/9911082.

[3]. A. Bell, T.J. Sejnowski. An information-maximisation approach to blind separation and blind deconvolution. *Neural Computation*, 7:1129–1159, 1995.

[4]. A. Engelhart, W. Teich, J. Lindner, G. Jeney, S. Imre, L. Pap. A survey of multiuser/multisubchannel detection schemes based on recurrent neural networks. *Wireless Communications and Mobile Computing*, 2(3):269–284, 2002. Special issue on Advances in 3G Wireless Networks.

[5]. A. Hyvärinen, J. Karhunen, E. Oja. *Independent Component Analysis*. Adaptive and Learning Systems for Signal Processing, Communication and Control. Wiley & Sons, New York, 2001.

[6]. A. I. Elwalid and D. Mitra. Effective bandwidth of general markovian traffic sources and admission control of high speed networks. *IEEE/ACM Trans. Netw.*, 1(6):329–343, 1993.

[7]. A. I. Zreikat and K. Begain. Soft handover-based cac in umts systems. *International Conference in Telecommunication, ICT'2003 Conference, Feb.23 - Mar.01, Tahiti, French Polynesia*, 2003.

[8]. A. Stefanov, O. Guinnard, L. Guinnard, H. Zbinden and N. Gisin. Optical quantum random number generator. *J. Modern Optics*, 47:595–598, 2000. e-print quant-ph/9907006.

[9]. A. Zeilinger. Quantum teleportation. *Scientific American*, 285(4):32–41, 2000. e-print $http://www.quantum.univie.ac.at/links/sci_am/teleportation.pdf$.

[10]. B. Aazhang, B.-P. Paris, G.C. Orsak. Neural networks for multiuser detection in code-division multiple-access communications. *IEEE Trans. on Communications*, 40(7):1212–1222, July 1992.

[11]. J. A. Bucklew. *TLarge Deviations Techniques in Decision, Simulation and Estimation*. John Wiley and Sons, New York, USA, 1990.

[12]. C. Chang, C. J. Chang, and K. R. Lo. Analysis of a hierarchical cellular system with reneging and dropping for waiting new calls and handoff calls. *IEEE Trans. Veh. Technol.*, 48(4):1080–1091, 1999.

[13]. C. Dürr, P. Hoyer. A quantum algorithm for finding the minimum. 1996. e-print quant-ph/9607014.

[14]. C. H. Bennett, E. Bernstein, G. Brassard, U. Vazirani. Strengths and weakness of quantum computing. *SIAM Journal on Computing*, 26(5):1510–1523, 1997. e-print quant-ph/9701001.

[15]. C. H. Bennett, G. Brassard and A. Ekert. Quantum cryptography. *Scientific American*, 267(4):50–57, 1992.

[16]. C. H. Yoon and C. K. Un. Performance of personal portable radio telephone systems with and without guard channels. *IEEE J. Select. Areas Commun.*, 11(6):911–917, 1993.

[17]. C.-J. Ho, J.A. Copeland, C.-T. Lea, and G.L. Stuber. On call admission control in ds/cdma cellular networks. *IEEE Trans. Veh. Technol.*, 50(11):1328–1343, 2001.

[18]. J. P. Castro. *The UMTS Network and Radio Access Technology: Air Interface for Future Mobile Systems*. John Wiley and Sons, Chichester, England, 2001.

[19]. J. K. Cavers. *Mobile Channel Characteristics*. Kluver Academic Publishers, 2000.

[20]. L. M. Correia, editor. *Wireless Flexible Personalised Communications*. Wiley & Sons, 2001.

[21]. D. Biron, O. Biham, E. Biham, M. Grassl, D.A. Lidar. *Generalized Grover Search Algorithm for Arbitrary Initial Amplitude Distribution*, volume 1509 of *Lecture Notes in Computer Science*, pages 140–147. Springer, 1998. e-print quant-ph/9801066.

[22]. D. Hong and S. S. Rappaport. Traffic model and performance analysis for cellular mobile radio telephone systems with prioritized and nonprioritized handoff procedures. *IEEE Trans. Veh. Technol.*, 35(3):77–92, 1986.

[23]. D. Ramakrishna, N. Mandayam, and R. Yates. Subspace based estimation of the signal-to-interference ratio for cdma cellular systems. *IEEE Trans. Veh. Technol.*, 49(9):1732–1742, 2000.

[24]. D. Shen, C. Ji. Admission control of multimedia traffic for third generation cdma network. *Proceedings of IEEE INFOCOM 2000*, pages 1077–1086, 2000.

[25]. D. Staehle, K. Leibnitz, K. Heck. A fast prediction of coverage area in umts networks. *Proceedings of IEEE Globecom, Taiwan, November, 2002*, pages 1077–1086, 2002.

[26]. D. Staehle, K. Leibnitz, K. Heck, B. Schroder, A. Wellner, P. Tran-Gia. Approximating the othercell interference distribution in inhomogeneous umts network. *Proceedings of IEEE VTC Spring (Birmingham, AL), May, 2002*, pages 1077–1086, 2002.

[27]. E. Biham, O. Biham, D. Biron , M. Grassl, D.A. Lidar. *Grover's Search Algorithm for an Arbitrary Initial Amplitude Distribution*, volume 60, pages 2742–2745. 1999. e-print quant-ph/9807027.

[28]. E. Biham, O. Biham, D. Biron , M. Grassl, D.A. Lidar, D. Shapira. Analysis of generalized grover's search algoritms using recursion equations. *Phys. Rev. A*, 63, 2001. e-print quant-ph/0010077.

[29]. E. D. Re, R. Fantacci, and G. Giambene. Handover queueing strategies with dynamic and fixed channel allocation techniques in low earth orbit mobile satellite systems. *IEEE Trans. Commun.*, 47(1):89–102, 1999.

[30]. E. Geijer Lundin, F. Gunnarsson, F. Gustafsson. Uplink load estimates in wcdma with different availability of measurements. *IEEE Veh. Technol. Conf*, 2003.

[31]. Jerry D. Gibson ed. *The Mobile Communications Handbook*. Springer Gmbh Germany, 1999. Second Ed.

[32]. F. Balázs, S. Imre. Quantum computation based probability density function estimation. *International Journal of Quantum Information*, 3(1):93–98, 2005.

[33]. F. Chiti, R. Fantacci, G. Mennuti, D. Tarchi. Dynamic sir based admission control algorithm for 3g wireless networks. *IEEE International Conference on Communications*, 26:1907–1911, 2003.

[34]. F. Gunnarsson, E. Geijer Lundin, G. Bark, N. Wiberg. Uplink admission control in wcdma based on relative load estimates. *IEEE International Conference on Communications*, 2002.

[35]. G. Brassard, P. Hoyer, A. Tapp. *Quantum Counting*, volume 1443 of *Lecture Notes in Computer Science*, pages 820–831. Springer, July 1998. Proceedings of the 25th

International Colloquium on Automata, Languages, and Programming, e-print quant-ph/9805082.

[36]. G. Brassard, P. Hoyer, M. Mosca, A. Tapp. Quantum amplitude amplification and estimation. *Quantum Computation & Quantum Information Science, AMS Contemporary Math Series*, 2000. e-print quant-ph/0005055.

[37]. G. Jeney, S. Imre, L. Pap, A. Engelhart, T. Dogan, W.G. Teich. Comparison of different multiuser detectors based on recurrent neural networks. *COST 262 Workshop on Multiuser Detection in Spread Spectrum Communication, Schloss Reisensburg, Germany*, pages 61–70, January 2001.

[38]. G. L. Long, C. C. Tu, Y. S. Li, W. L. Zang and L. Niu. A novel so(3) picture for quantum searching. 1999. e-print quant-ph/9911004.

[39]. G. L. Long, L. Xiao, Y. Sun. General phase matching condition for quantum searching. 2001. e-print quant-ph/0107013.

[40]. G. L. Long, Y. S. Li, W. L. Zang and L. Niu. Phase matching in quantum searching. *Phys. Lett. A*, 262:27–34, 1999. e-print quant-ph/9906020.

[41]. G. Seres, Szlávik, J. Zátonyi, J. Bíró. Quantifying resource usage - a large deviation-based approach. *IEICE Transactions on Communications, Special Issue on Internet Technology II -Traffic Control and Performance, Evaluation in the Internet, Vol.E85-B No.1*, 2002.

[42]. R. G. Gallager. *Information Theory and Reliable Communication*. John Wiley and Sons, 1968.

[43]. L. K. Grover. Quantum mechanics helps in searching for a needle in a haystack. *Phys. Rev. Lett.*, 79(2):325–328, July 1997. e-print quant-ph/9706033.

[44]. L. K. Grover. Quantum computers can search rapidly by using almost any transformation. *Phys. Rev. Lett*, 80(19):4329–4332, 1998. e-print quant-ph/9712011.

[45]. L.K. Grover. A fast quantum mechanical algorithm for database search. *Proceedings, 28th Annual ACM Symposium on the Theory of Computing*, pages 212–219, May 1996. e-print quant-ph/9605043.

[46]. L.K. Grover. Tradeoffs in the quantum search algorithm. 2002. e-print quant-ph/0201152.

[47]. R. A. Guerin. Queueing-blocking system with two arrival streams and guard channels. *IEEE Trans. Commun.*, 36(2):153–163, 1988.

[48]. F. Hillebrand, editor. *GSM and UMTS: The Creation of Global Mobile Communication*. Wiley & Sons, 2002.

[49]. P. Hoyer. Arbitrary phases in quantum amplitude amplification. *Phys. Lett. A*, 62(052304), 2000. e-print quant-ph/0006031.

[50]. I. Kim, B. Shin, and D. Lee. Sir-based call admission control by intercell interference prediction for ds-cdma systems. *IEEE Comm. Let.*, 4(1):29–31, 2000.

[51]. I. Koo, A. Furuskar, J. Zander and K. Kim. Erlang capacity of multiaccess systems with service-based access selection. *IEEE Comm. Let.*, 8(11):662–664, 2004.

[52]. I.L. Chuang, N. Gershenfeld and M. Kubinec. Experimental implementation of fast quantum searching. *Phys. Rev. Lett.*, 18(15):3408–3411, 1998. e-print http://feynman.media.mit.edu/ike/homepage/papers/QC-chuang-gershenfeld-kubinec-nmrqc-grover-alg-prl-13apr98.pdf.

[53]. S. Imre. Extreme value searching in unsorted databases based on quantum computing. *International Journal of Quantum Information*, 3(1):171–176, 2005.

[54]. J. Evans and D. Everitt. Effective bandwidth-based admission control for multi-service cdma cellular networks. *IEEE Trans. Veh. Technol.*, 48(1):36–46, 1999.

[55]. J. Evans and D. Everitt. On the teletraffic capacity of cdma cellular networks. *IEEE Trans. Veh. Technol.*, 48(1):153–165, 1999.

[56]. J-Y. Hsieh, C-M. Li. A general su(2) formulation for quantum searching with certainty. *Phys. Rev. A*, 65(052322), 2002. e-print quant-ph/0112035.

[57]. J.A. Jones, M. Mosca and R. H. Hansen. Implementation of a quantum search agorithm on a nuclear magnetic resonance quantum computer. *Nature*, (393):344–346, 1998. e-print quant-ph/9805069.

[58]. T. Novosad JJ. Laiho, A. Wacker. *Radio Network Planning and Optimisation for UMTS*. John Wiley and Sons Ltd., 2001.

[59]. F. P. Kelly. Effective bandwidth at multi-class queues. *Queuing Systems*, 9:968–981, 1991.

[60]. D. E. Knuth. *The Art of Computer Programming, Vol. 3. (Sorting and searching)*. Addison-Wesley, 1973.

[61]. G. L. Long. Grover algorithm with zero theoretical failure rate. *Phys. Rev. A*, 64(022307), 2001. e-print quant-ph/0106071.

[62]. W. W. Lu. *Broadband Wireless Mobile: 3G and Beyond*. Wiley & Sons, 2002.

[63]. M. Boyer, G. Brassard, P. Hoyer, A. Tapp. Tight bounds on quantum searching. *Proceedings 4th Workshop on Physics and Computation*, 46(4-5):36–43, 1996. Also in Fortschritte der Physik, Vol. 46, No. 4-5, 1998, pp. 493-505 quant-ph/9605034.

[64]. M. D. Kulavaratharasah and A. H. Aghvami. Teletraffic performance evaluation of microcellular personal communication networks (pcn's) with prioritized handoff procedures. *IEEE Trans. Veh. Technol.*, 48(1):137–152, 1999.

[65]. M. Varnashi, B. Aazhang. Multistage detection for asynchronous code-division multiple access communication. *IEEE Trans. on Communication*, 38(4):509–519, April 1990.

[66]. M. Mouly and M.-B. Pautet. *The GSM System for Mobile Communications*. published by the authors 49 Rue Louise Bruneau, Palaiseau, France, 1992.

[67]. J. Mullins. Making unbreakable code. *IEEE Spectrum*, 39(5):40–45, 2002.

[68]. N. Bhattacharya, H. B. van Linden van den Heuvell and R. J. C. Spreeuw. Implementation of quantum search algorithm using classical fourier optics. *Phys. Rev. Lett.*, 88(137901), 2002. e-print quant-ph/0110034v3.

[69]. M. A. Nielsen. Rules for a complex quantum world. *Scientific American*, 287(5):49–57, 2002.

[70]. O. Sallent, J. P. Romero, R. Agusti, F. Casadeval. Provisioning multimedia wireless networks for better qos: Rrm strategies for 3g w-cdma. *IEEE Communications Magazine*, pages 100–106, 2003.

[71]. J. D. Parsons. *The Mobile Radio Propagation Channel*. Wiley & Sons, 2nd edition, 2001.

[72]. R. Akl, M. V. Hegde and M. Naraghi-Pour. Mobility-based cac algorithm for arbitrary call-arrival rates in cdma cellular systems. *IEEE Trans. Veh. Technol.*, 54(2):639–651, 2001.

[73]. R. Ramjee, D. Towsley, and R. Nagarajan. On optimal call admission control in cellular networks. *Wireless Networks*, 3:29–41, 1997.

[74]. R.Nee, E. Prasad. *TOFDM for Wireless Multimedia Communications*. Artech House Publishers, London, England, 2000.

[75]. S.-I. Amari, A. Cichocki. Adaptive blind signal processing-neural network approaches. *Proc. IEEE*, 86(10), October 1998.

[76]. S. Imre. Dynamically optimised chernoff bound based cac for 3g/4g wcdma systems. *11th Microcoll Conference, September 10-11, 2003, Budapest, Hungary*, pages 27–30, 2003.

[77]. S. Imre, F. Balázs. Positiv operation valued measurement based multiuser detection in ds-cdma systems. *IX. Int' Conference on Software Telecommunications and Computer Networks (SoftCOM'01)*, 1:421–429, October 09-12 2001. e-print quant-ph/0201039.

[78]. S. Imre, F. Balázs. Non-coherent multi-user detection based on quantum search. *IEEE International Conference on Communication (ICC),New York, USA*, April 28 - May 2 2002.

[79]. S. Imre, F. Balázs. Performance evaluation of quantum based multi-user detector. *IEEE International Symposium on Spread Spectrum Techniques and Applications (ISSTA'02)*, pages 722–725, September 2-5 2002.

[80]. S. Imre, F. Balázs. A tight bound for probability of error for quantum counting based multiuser detection. *IEEE International Symposium on Information Theory (ISIT'02)*, page 43, Juni 30- July 5 2002. e-print quant-ph/0205138.

[81]. S. Imre, F. Balázs. The generalized quantum database search algorithm. *Computing*, 73(3):245–269, 2004.

[82]. S. Imre, F. Balázs. *Quantum Computing and Communications - An Engineering Approach*. John Wiley and Sons Ltd, 2005.

[83]. S. Imre, K. Hankó, P. Petrás, R. Tancsics. Optimized effective bandwidth based admission control for multi-service cdma cellular networks. *10th SoftCOM2002, October 08-11, 2002*, pages 299–304, 2002.

[84]. S. Imre, K. Hankó, P. Petrás, R. Tancsics. Efficient call admission control method for 3g/4g wcdma networks. *7th International Conference on Telecommunications, CONTEL2003, June 13-15, 2003, Zagreb, Croatia*, pages 93–98, 2003.

[85]. S. Imre, L. Pap. Neuron based call admission control method for transport network of 3rd generation mobile systems. *IEEE Symposium on Communications and Vehicular Technology, SCVT-2000, Leuven, The Netherlands*, October 09-12 20010. e-print quant-ph/0201039.

[86]. S. Imre, P. Petrás, R. Táncsics. Efficiency validation of 3g/4g wcdma air interface call admission control in omnet++ environments. *SoftCOM2003, October 07-10, 2003, Split, Dubrovnik (Croatia), Ancona, Venice (Italy)*, pages 852–858, 2003.

[87]. P.W. Shor. Introduction to quantum algorithms. *AMS PSAPM*, 58:143–159, May 2002. e-print quant-ph/0005003.

[88]. T. H. Cormen, C. E. LeisersonR. L. Rivest, C. Stein. *Introduction to Algorithms*. The MIT Press/McGraw Hill, 4th edition, 2003.

[89]. K. Tachikawa, editor. *W-CDMA Mobile Communications System*. Wiley & Sons, 2002.

[90]. V. K. N. Lau and S. V. Maric. Mobility of queued call requests of a new call-queueing technique for cellular systems. *IEEE Trans. Veh. Technol.*, 47(2):480–488, 1998.

[91]. S. Verdu. *Multiuser Detection*. Cambridge University Press, 1998.

[92]. A. J. Viterbi. *CDMA-Principles of Sperad Spectrum Communication*. Addison-Wesley, 1995.

[93]. W.-B. Yang and E. Geraniotis. Admission policies for integrated voice and data trffc in cdma packet radio networks. *IEEE JSAC*, 12:654–664, 2003.

[94]. W. Ying, Z. Jingmei,W. Weidong, and Z. Ping. Call admission control in hierarchical cell structure. *IEEE Veh. Technol. Conf*, pages 1955–1959, 2002.

[95]. Y. B. Lin, S. Mohan, and A. Noerpel. Queueing priority channel assignment strategies for handoff and initial access for a pcs network. *IEEE Trans. Veh. Technol.*, 43(3):704–712, 1994.

[96]. Y. Fang, Y. Zhang. Call admission control schemes and performance analysis in wireless mobile networks. *IEEE Trans. Veh. Technol.*, 51(2):371–382, 1999.

[97]. Y. Gou, H. Chaskar. Class-based quality of service over air interfaces in 4g mobile networks. *IEEE Communications Magazine*, pages 132–137, 2002.

[98]. Y. Ishikawa and N. Umeda. Capacity design and performance of call admission control in cellular cdma systems. *IEEE J. Sel. Areas Commun.*, 15(8):1627–1635, 1997.

[99]. Y. Ma, J.J. Han and K.S. Trivedi. Call admission control for reducing dropped calls in code division multiple access (cdma) cellular systems. *Computer Communications*, 25:689–699, 2002.

[100]. Z. Heszberger, J. Zátonyi, J Bíró. Performance bounds for rate envelope multiplexing. *Performance Evaluation*, 48:87–101, 2002.

[101]. Z. Liu and M. El Zarki. Sir-based call admission control for ds-cdma cellular systems. *IEEE J. Select. Areas Commun.*, 12(5):638–644, 1994.

[102]. C. Zalka. Simulating quantum systems on a quantum computer. *Phys. Rev. A.*, 454:313–322, 1998.

[103]. C. Zalka. Grover's quantum searching algorithm is optimal. e-print quant-ph/9711070v2, 1999.

Index